Effect of alternate stopbank alignments on the Waiho River, Westland, New Zealand:

A microscale modelling investigation

by

Rosemary Patricia Jane Beagley

B.Sc., The University of Melbourne, 2014

A THESIS SUBMITTED IN PARTIAL FULFILLMENT OF
THE REQUIREMENTS FOR THE DEGREE OF

MASTER OF SCIENCE

in

The Faculty of Graduate and Postdoctoral Studies

(Geography)

THE UNIVERSITY OF BRITISH COLUMBIA

(Vancouver)

November 2017

Abstract

The Waiho River in Westland, New Zealand has been rapidly aggrading its bed as a result of lateral confinement by a stopbank network which restricts the river to 30% of its natural fan accommodation space. The ongoing aggradation has prompted the need to repeatedly raise the crest level of the stopbanks. This had led to the bed and stopbank elevation reaching unpreceded and dangerously high levels, putting the surrounding land, infrastructure and Franz Josef community at even greater risk than before should the stopbanks fail. This thesis investigates an alternative solution to the current management practice. Using a microscale model it tests the response of an experimental Waiho River and fan to the removal of the Southern stopbank and replacement with two alternatives which allow the river greater access to its Southern fan surface. In addition, the study allowed for an exploration of several microscale modelling techniques.

The results found that an experimental fan in a state of dynamic equilibrium would not aggrade when confined as previously thought. Only when the fan was already aggrading did it continue to aggrade when confined. In this instance, when the confinement was removed it did not result in degradation to lower elevations. Aggradation continued, albeit at a reduced rate. This suggests that the Waiho was already in a state of aggradation prior to human interference, and that confinement exacerbated the rate. This result has implications for the future management of the Waiho. If the current aggradation trend is to continue, then increasing stopbank crest height is not a viable solution, however releasing the river to the South will reduce the rate of aggradation as well as the pressures on the Northern stopbanks which protect the Franz Josef township. Effectively, this buys time for more drastic action (i.e. relocation of the township) to be taken. In addition to these results, the experiments found that measurement tools and model materials used previously in other microscale models produced unreliable fan behaviour and results. That they have failed in this study, motivates the need for further investigation into the underlying principles of microscale modelling and its practice.

Lay summary

Since the 1980s the Waiho River in Westland, New Zealand has been rapidly increasing its bed elevation in response to confinement by stopbanks. These stopbanks are repeatedly built up to ensure the river does not overtop them. Both river bed and stopbank height have now reached unpreceded and dangerously high levels which puts the surrounding land, infrastructure and Franz Josef community at even greater risk than before should the stopbanks fail. This thesis investigates an alternate solution, using a microscale model to test the response of an experimental river to reduced confinement. The results indicate that reduced confinement does not prevent the bed elevation from increasing, however it does slow the rate, as well as reducing the pressures on the other remaining stopbanks. Effectively, this alternate solution buys time for the planning and undertaking of more drastic action such as town, highway, and farmland relocation, out of the Waiho's way.

Preface

This thesis was completed by the author, under the guidance of a supervisory committee that included Brett Eaton (University of British Columbia) and Tim Davies (University of Canterbury). The microscale model was designed based off previous modelling experiments (Davies et al., 2003a, 2013), and constructed with the support of Warwick Hill (Lincoln University) in the Soil and Water Laboratory at Lincoln University. All data collection and processing was completed by the author, with technical (ArcGIS) support from Crile Doscher (Lincoln University). Both Brett Eaton and Tim Davies contributed to edits in the thesis, however the author was solely responsible for its composition.

Table of Contents

List of Tables

List of Figures

Acknowledgements

First and foremost, a huge thank you to Brett Eaton and Tim Davies for giving me the opportunity to work on a project I was so interested in, and providing endless support and thoughts to my endeavour. Brett has encouraged and pushed me to pursue my ideas throughout the last few years without which I doubt I would have developed the knowledge and skills I have today. Tim's knowledge of the Waiho, alluvial fans and microscale modelling, and pursuit of a topic he's obviously passionate about has been motivational. I feel like I always come away from our chats having learnt something new, and with plenty to ponder. It has been amazing getting to work with both Brett and Tim as I've delved into the realms of microscale modelling, alluvial fans, and the problem of the rapidly aggrading Waiho.

To Crile and Warwick. Thank you so much for all the help you gave me whilst I was working in the Soil and Water Laboratory at Lincoln University. I don't know what I would have done without Warwick's expertise in model construction and problem solving (for the many hiccups and ideas that turned up throughout the four months), it was an absolute pleasure working in the lab with him. Also, I would have been lost in the GIS world without Crile. He re-opened my eyes to working in ArcGIS.

I have also felt so supported and encouraged this past year by both family and friends. It would be hard to thank everyone individually, however I would like to make special mention to a particular few.

To Tegan and Jessie, their bubbling enthusiasm both in Canada and NZ has been incredible. They've been there every step of the way, for outdoor adventures when I could spare the time, delicious dinners or vegan treats and coffee to give me a break from modelling or writing, and motivational texts or phone conversations when I needed them. I couldn't have asked for two better friends. Thank you.

Col. For for all the little things she has done unasked (and continues to do) to help make these past few years easier. It has all been so appreciated.

And of course my parents, who not only helped proof read this thesis but were (and are) always only a phone call or text message away when I've needed to talk or hear words of encouragement. (Sorry I don't make it back to Australia as often as we'd all like).

Finally, Linden. I'm so grateful to have had your suport from the opposite side of the world (and island) for the last two and a half years. Thank you too for the reminders to put down the books, tuck away the thoughts and get outside for a break - it's undoubtedly the best medicine to clear ones mind and refresh. I'm looking forward to all the adventures we can have now that I'm finished and can come back home to the best West Coast.

Dedication

This thesis is dedicated to future microscale modellers, in the hope that beyond the practical reasons, they too may enjoy the "*irresistible fascination in watching a small, controlled landscape evolve, creating dynamic patterns that seem to come from out of nowhere*" (Paola et al., 2009).

Chapter 1

Introduction

Stopbanks, also known as flood control banks, levees, or longitudinal training banks, are anthropogenically constructed walls which confine a river to a restricted width, and prevent it from utilizing the surrounding area (Davies and McSaveney, 2006; Warburton, 1996). Not only do they act as a barrier between a river and surrounding land, they are also designed to increase the mean flow depth, and therefore mean bed shear stress (Davies and McSaveney, 2006; Warburton, 1996). This theoretically serves to increase the transport capacity of the river and therefore prevent aggradation of the river bed (Warburton, 1996; Acheson, 1968; Henderson, 1966).

Stopbanks have been a common management practice for braided gravel-bed rivers in New Zealand (Grant, 1948; Acheson, 1968; Nevins, 1969; Davies and McSaveney, 2006). This type of river is known for its highly dynamic nature which results in an everchanging network of intertwining channels around bars and islands (Mètivier and Barrier, 2012; Bristow and Best, 1993). The ability of these rivers to continually alter their channel morphology presents problems where humans and rivers interact (Piegay et al., 2006). Infrastructure and land use within and around the channel are at risk from any changes in the river pattern. This has led to the use of stopbanks as a means of restricting rivers to a set path, and protecting the surrounding land and infrastructure from changes in channel location and pattern, as well as from high flow events (Davies and Lee, 1988; Davies and McSaveney, 2001; Fleming, 2002).

However, there are a growing number of cases in New Zealand where the use of stopbanks has had the opposite effect to that intended (Davies and McSaveney, 2006; Davies and Lee, 1988). Rather than reduce the risk posed by this type of river, the stopbanks have led to increased aggradation within the confined reach (Davies and McSaveney, 2006). Subsequently, stopbanks are then built up to restore the designed flood cross-sectional area and prevent overtopping, which would put the surrounding area at risk from the flooding and/or avulsion (dramatic channel course change)

hazards which they had originally been installed to mitigate and control (Davies and Lee, 1988). In these cases, the original management strategy has not eliminated the problem, and the ongoing addition to stopbank crest height is only delaying its inevitable failure.

A prominent example of this, and one which this study will be focussing on, is the Waiho River Franz Josef situation.

1.1 Waiho River and Franz Josef township context

The Waiho River flows out of the steep mountains west of the main divide of the Southern Alps onto and across the foreland plains of the West Coast region of the South Island to the Tasman Sea some 15km away (Davies et al., 2003a) (Figure 1.1). At the point of emergence from the mountains, an alluvial fan has formed that extends as a valley train to the coast (Davies et al., 2003a). Alluvial fans are formed by the deposition of sediment by a river as it exits a confined valley onto open plains (Whitehouse and McSaveney, 1990; Thornbury, 1954). Sediment is distributed across the fan surface via a network of channels that take on the characteristic of braided gravel-bed rivers (Rachocki, 1981). This is the case for the Waiho River and Fan.

At present, the upper few km of the Waiho River is restricted to about a third of its original fan surface (Davies and McSaveney, 2006). In the early 1900s, stopbanks were installed along the Waiho River to protect the surrounding land and infrastructure from flooding and minor aggradation (Davies et al., 2003a). However, over the last few decades, the upper fan where the Waiho River is confined has experienced rapid rates of aggradation (currently 300 mm a^{-1}), which has prompted the need to repeatedly increase the crest level of the stopbanks (Davies et al., 2003a; Davies and McSaveney, 2006). This had led to the bed and stopbank elevation reaching unpreceded and dangerously high levels, putting the surrounding land, infrastructure and Franz Josef community at even greater risk than before should the stopbanks fail (Figure 1.2) (Davies, 1997; Davies and McSaveney, 2001).

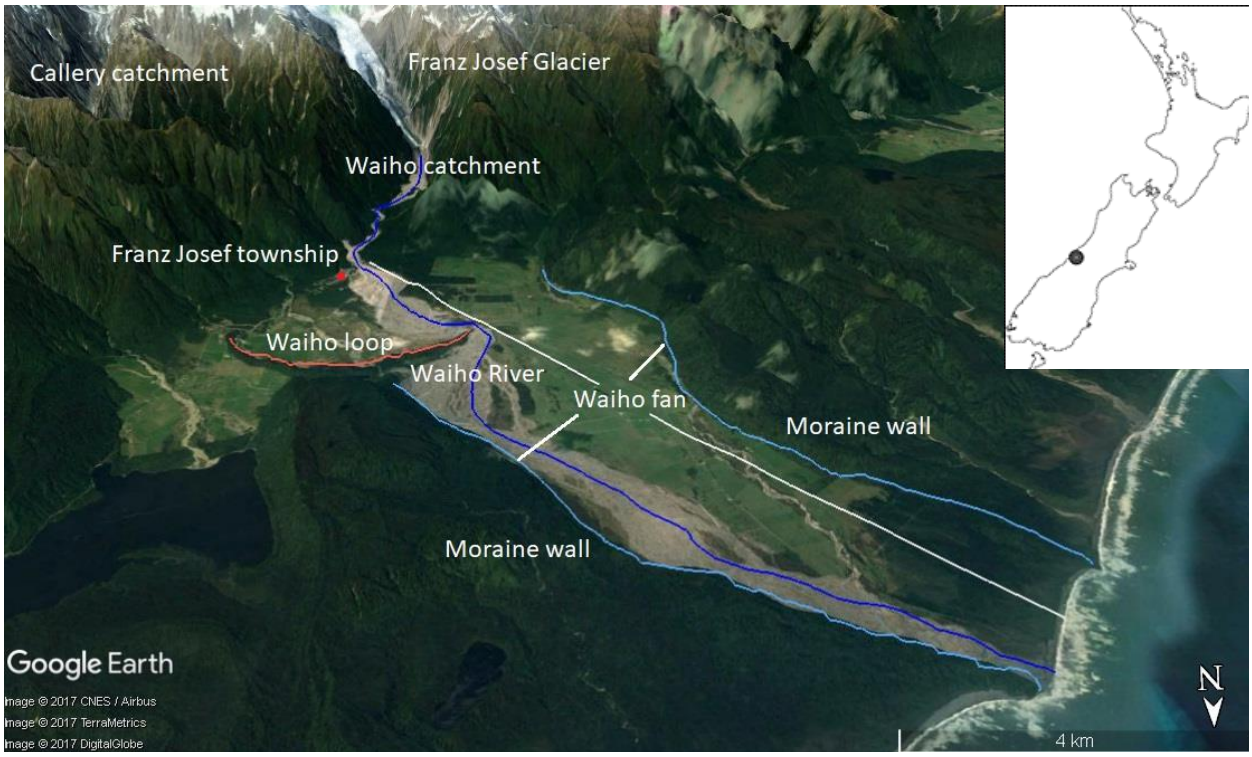

Figure 1.1: Google Earth image of the Waiho River and fan from source to sea. Insert shows location in New Zealand.

As the mean rate of sediment supply is believed to have changed little in the last few thousand years (Davies et al., 2003a), and the position of the fan toe has been fixed in position at a constant base level as a result of the stabilization of sea level 6000 years (Davies and McSaveney, 2001), it is believed that the basic cause of the aggradation is the confinement of the fan width (Davies and McSaveney, 2001). Using a 1:2000 microscale model Davies et al (2003a) replicated this situation; and with no change to sediment supply, discharge or base level, the installation of the current stopbank alignment resulted in rapid aggradation of the river bed in the confined reach; with a spatial distribution of relative aggradation rates that corresponded to field data.

Since the 1990s, corresponding to the increasing elevation of the river bed, the severity of flood events has increased (Davies et al., 2003a). The

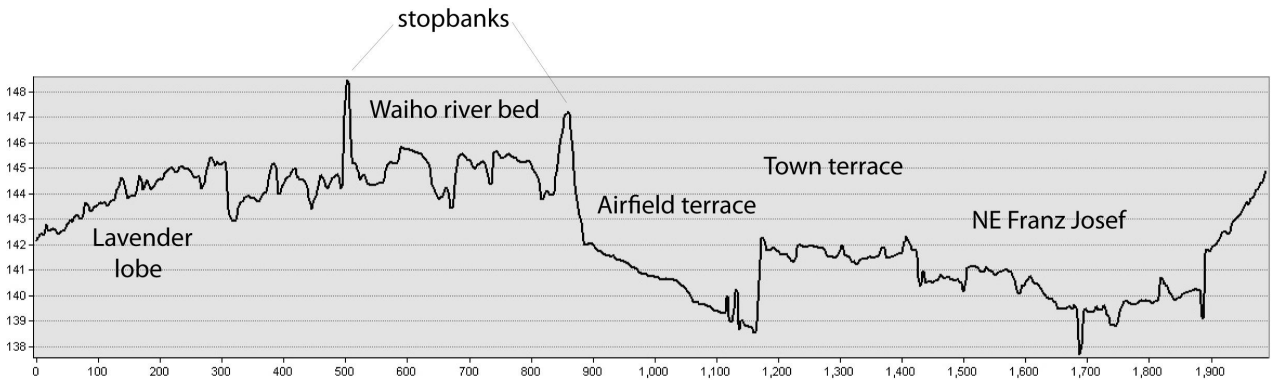

Figure 1.2: A topographic cross sectional profile drawn across the Waiho fan from the Lavender lobe in the SW to the edge of the Tartare fan, NE of Franz Josef town using LiDAR data. The Waiho River bed is considerably higher than the land to either side of it. Figure taken from Langridge et al., 2016

increasing bed elevation means that not only has the size of flood required to overtop the stopbanks been reduced, but the river bed elevation is now significantly higher than that of the surrounding land, as is the height of flood peaks (Davies, 1997). Also, despite the increased height of the stopbanks, it would appear that during high flow events the Waiho River is still able to overtop its banks and inundate the surrounding low lying land including the lower township area of Franz Josef (Davies, 1997). An example of this is the flooding of the Heartland hotel The Mueller during a 2016 flood event (Aulakh and Mills, 2016) (Figure 1.3).

In addition to this increasing river bed elevation and flood risk, recent river behaviour during flood stages has begun to indicate an avulsion into the Tatare River. Building upon the previous modelling done by Davies et al (2003a), a second microscale model was constructed to investigate if the increasing rates of aggradation would result in such an avulsion, and the effect on the township (Davies et al., 2013). Replicating the methodology of Davies et al (2003a), ongoing aggradation resulted in an avulsion from the Waiho River into the Tatare River. This was followed by knickpoint recession of the junction between the two rivers upstream towards the Franz Josef township, placing it at greater risk (Davies et al., 2013).

Figure 1.3: Gravel deposits around the Heartland hotel (the Mueller) left behind by the 2016 flood. Photo by Rob Pieper

The consequences of an avulsion and the upstream knickpoint recession, the increasing flood risks, and the rising potential of stopbank failures have prompted the need to find a solution to the rapidly aggrading river bed. However, this is not straightforward.

1.2 Method of research

The Waiho-Franz Josef situation presents a difficult scenario to study for a number of reasons

- Large spatial scale

  The area of confinement and aggradation is substantial. It extends from the junction of the Callery and Waiho rivers down to an ancient terminal moraine (ca. 11,000 years B.P) known as the Waiho Loop (Davies and McSaveney, 2001). This area is approximately 4 km long, with a width of 1.3 km at its widest. The width of the entire unconfined

fan in this section is 4 km (Davies and McSaveney, 2001). This is a large expanse of area to monitor regularly or model.

- Long temporal scale

  The Waiho River is a braided gravel bed river (Davies and McSaveney, 2001). It has a high sediment load made up by a significant fraction of bedload (Davies et al., 2003a). Bedload plays an important role in gravel-bed rivers. Comprising primarily the coarser particles, bedload has been found to account for a large fraction of the total mass transported in these rivers (Malverti et al., 2008). The evolution of a river bed through bedload transport operates at timescale from 10^{-1} to 10^{4} years (Malverti et al., 2008). Therefore, morphologic change cannot be measured over a period of days, it can take months, years, or even hundreds of years. This a considerable amount of time when considering the human lifespan, and too long for people to directly perceive and measure the river dynamics (Malverti et al., 2008).

- Difficulties associated with monitoring a highly dynamic and braided system

  Braided gravel bed rivers are highly dynamic systems, with a bed that is constantly evolving, as the network of channels, bars, and islands changes (Bertoldi et al., 2009; Schumm, 1985). These changes often occur rapidly during periods of high flow (Davies and McSaveney, 2006; Piegay et al., 2006). During these events, taking measurements and observation of the processes and changes is near impossible, not to mention dangerous (Mètivier and Barrier, 2012; Bristow and Best, 1993). In addition to this, braiding makes measurement of sediment transport and water flow difficult, as there are too many channels (that are regularly changing course) to measure (Ashmore, 1991; Davies, 1987).

- Lack of historical data available

  Due to the difficulties discussed above there is a severe lack of historical data for bedload transport and water flow rates of the Waiho River (Davies and McSaveney, 2001). Additionally, aerial photography only reaches back to 1948 (Davies and McSaveney, 2001). The only record of the river and fan behaviour prior to this are some sketches from the 1850s and photos from 1870 (Davies and McSaveney, 2001).

- Degree of urgency required for a solution

A solution is required urgently. The west coast of the South Island is subject to frequent periods of intense rainfall (Davies and McSaveney, 2001). The head waters of the Waiho catchment receive an average annual precipitation of 11,000 mm (McSaveney and Davies, 1998), with as high as 14,000 mm being recorded (Henderson and Thompson, 1999). 3-day rainfalls up to 750 mm have also been recorded. This means that the likelihood of large floods is high, as are the consequences of stopbank overtopping or failure for the neighbouring township of Franz Josef Glacier (Davies, 1997).

With these difficulties in mind, many of the common alternatives such as field and analytical studies appeared impractical (Davies and Lee, 1988), and/or beyond the scope of the present Masters thesis. Without these studies, real time (and historical) data on the sediment transport capacity, river channel pattern and location, and river hydrology are not available for the calibration of many types of numerical and physical models.

1.2.1 Field observations and analysis

Fieldwork has a long history in geomorphic research. It provides a direct way to access, visualize and understand natural systems. In addition, historical data are invaluable for showcasing morphological change over time, as well as for the calibration of both numerical and physical model techniques (Popescu, 2014; Peakall et al., 1996). However, limitations exist in terms of spatial and temporal scales that can be monitored and measured. These become apparent when considering field observation and analysis as a method of study for the Waiho River.

- The temporal scale over which the Waiho River and fan has been changing and will continue to change, is too long to observe. There is just not the time available to spend monitoring this system, especially under the timeline of a Master of Science program and the degree of urgency for a solution.
- The spatial extent of the aggrading area. The stopbanked area and total fan accommodation space is too large to be monitored regularly in detail. In addition to this, its highly dynamic nature and changes occurring during high flows makes taking measurements and making observations difficult and dangerous.
- There is lack of historical data. Current investigations would be starting from now without any detailed historical perspective.

1.2.2 Numerical modelling

Numerical modelling is the simulation of a system and/or component on a computer (Popescu, 2014). It involves the quantification of a system and its properties through mathematical equations that can be either empirical or derived from basic principles. These equations as well as the boundary conditions and any other input data necessary, are then translated into computer form using a range of numerical approaches (Popescu, 2014). This type of modelling requires a sound understanding of the system being modelled to ensure all the relevant physical processes and their mathematical representations, are included as well as real data from the prototype system (Popescu, 2014). Numerical modelling has proven to be an invaluable tool for scientists, promoting significant advances in the understanding of the interrelationships between sediment production, transport and deposition within dynamic fluvial environments (Peakall et al., 1996). Not limited to the geomorphic discipline, its use extends from climate and weather predictions and forecasts (McKendry, 1992; Trenberth et al., 1998) to understanding tectonics (Hoink et al., 2013; Lenardi et al., 2003). However, it presents some difficulties when considered for the Waiho-Franz Josef situation.

- Numerical simulation models need to be calibrated to ensure that they are representing what they're supposed to be. The lack of historical data and the difficulties surrounding present day data collection, mean that there is insufficient data to create an accurate numerical model of the Waiho River.
- In addition, the time, money and tools required to gather present-day data are beyond the scope of this project.

Whilst a numerically simulated model is a viable method for the Waiho-Franz Josef situation, without any data or means to collect data on water flow rates or sediment transport and supply, it is not a suitable method for this project.

1.2.3 Physical modelling

Physical modelling is the physical replication of components of a system, or in some cases the entire system, in a laboratory (Mosley and Zimpfer, 1978). Physical models allow for sediment-flow interactions and bed morphology to be reproduced and visualized under clear, safe and controlled conditions (Peakall et al., 1996). In addition to this they provide the option for different temporal and spatial scales, depending on the type of model chosen

(Peakall et al., 1996). There are three main types of models; one-to-one (unscaled reality; Chorley, 1967), scaled, and analogue (Peakall et al., 1996; Mosley and Zimpfer, 1978). All three have been used interchangeably by geomorphologists to study form, process and evolution in the geomorphic landscape (Peakall et al., 1996). In the case of the Waiho fan and river, where large time and spatial scales are required to represent the dynamics, behaviour and evolution of the system, and there is a lack of historical data, both one-to-one and scaled physical model types are impractical. However, analogue models provide a feasible option.

- A one-to-one model has not been scaled down, it is the same size as its prototype. These models focus on a particular component of a system, and therefore focus on the smallest scales of geomorphic interest (Peakall et al., 1996). For example, hydraulic flumes have long been used to study bedform generation in both sands and gravels (Peakall et al., 1996). Thus, there exists a limitation on the spatial extent of what a one-to-one model can replicate. Not only would it be impossible to build a one to one model of the Waiho Franz Josef situation in a laboratory, but there is a lack of sediment and water flow data available to calibrate it with.

- Scaled models are a scaled-down version of the prototype, with attempts made to replicate the flow and sediment conditions using dimensionless values (Peakall et al., 1996; Malverti et al., 2008). In the case of alluvial river systems dominated by bedload transport, these values include the Froude, Reynolds and Shields numbers, relative density, and ratio of flow depth to grain size (Malverti et al., 2008). There are several types, the main two being Froude and distorted scaled models (Mosley and Zimpfer, 1978). Whilst this type of modelling requires less space and time than a one-to-one model, the size of model required for the Waiho-Franz Josef situation with accurate replication of the flow and sediment conditions is too big for the scope of this thesis due to laboratory space and finances. Warburton (1996) estimated the required size of a Froude scaled model to be of the order of 50 m by 50 m. In addition, as with the other modelling types, there are no historical or current sediment or flow data to calibrate the model.

1.2.4 Analogue models: microscale modelling

Analogue models are physical models, in which no attempt to replicate flow and sediment conditions has been made, and there is some degree of vertical distortion (Mosley and Zimpfer, 1978; Malverti et al., 2008; Gaines and Maynord, 2001). They are often used to create scaled laboratory systems that are not based on a particular prototype (Peakall et al., 1996). Instead they are used to study form, process and evolution, as entities in themselves (Peakall et al., 1996).

However, microscale models, a sub-branch of analogue models, can be used for case studies as long as the model reproduces some known response or behaviour of the prototype (Gaines and Smith, 2002). This involves the replication of geometric boundaries and forms, but relaxation of dynamic similarity criteria (Gaines and Maynord, 2001; Gaines and Smith, 2002; Maynord, 2006).

- These models do not have a requirement for large of amounts of historical and present day data from the system they are replicating
- They can handle large temporal and spatial scales
- They are not affected by the difficulties associated with access and taking measurements to collect data
- They can provide a result within months.

With these advantages in mind, microscale modelling appears to be a viable method of investigation for finding a solution to the Waiho-Franz Josef situation, and falls within the scope of this thesis. The model can be built to include the entire fan area, without requiring large amounts of data, availability of which is limited. It will reduce the time required for fan evolution and response to a more manageable timeframe, which benefits this study, as a solution is required sooner rather than later; and it will provide a controlled platform where fan behaviour can be directly observed and monitored.

In addition, microscale models have been used previously to study the Waiho-Franz Josef situation. Davies et al. (2003a; 2013) constructed models of the area to investigate in the first instance, the cause of the aggradation, and in the second, the effect of ongoing aggradation and subsequent avulsion into the Tatare River. These models all utilized the sandtray at the Soil and

Water Laboratory at Lincoln University, therefore the equipment required is already in place.

1.3 Thesis aims, objectives and structure

The primary aim of this project is to investigate the effects of alternative stopbank alignments on the bed surface level of the Waiho River on the upper part of its fan using a microscale model (Figure 1.4). The effects of the two stopbank alignments investigated would then be used to determine the future viability of the surrounding roads and infrastructure, and could be incorporated into the management strategy for the river. In addition to this, it would provide the opportunity to build upon the investigations by Davies et al. (2003a; 2013), who showed that stopbanks induced both increased aggradation rates and an avulsion in their 1:2000 and 1:5000 microscale models of the Waiho River.

To achieve this aim within the scope of the thesis the following objectives were undertaken:

- Establish the long-term steady state of the fanhead bed level corresponding to alternative stopbank alignments.
- Determine which alignment provides the better outcome for the surrounding land and infrastructure, and community of the Franz Josef Township.

A secondary aim was developed during the research phase of this thesis. This involved the exploration of the techniques used in microscale modelling. Microscale modelling is a relatively new type of physical modelling, and as a result the methodology and techniques in the literature have had little experimental assessment and/or discussion. As the experiments in this study progressed, problems with boundary roughness, input conditions, and the tools used to measure change occurred. Solving these problems developed a better understanding of microscale modelling and what is required for a successful model and experiment.

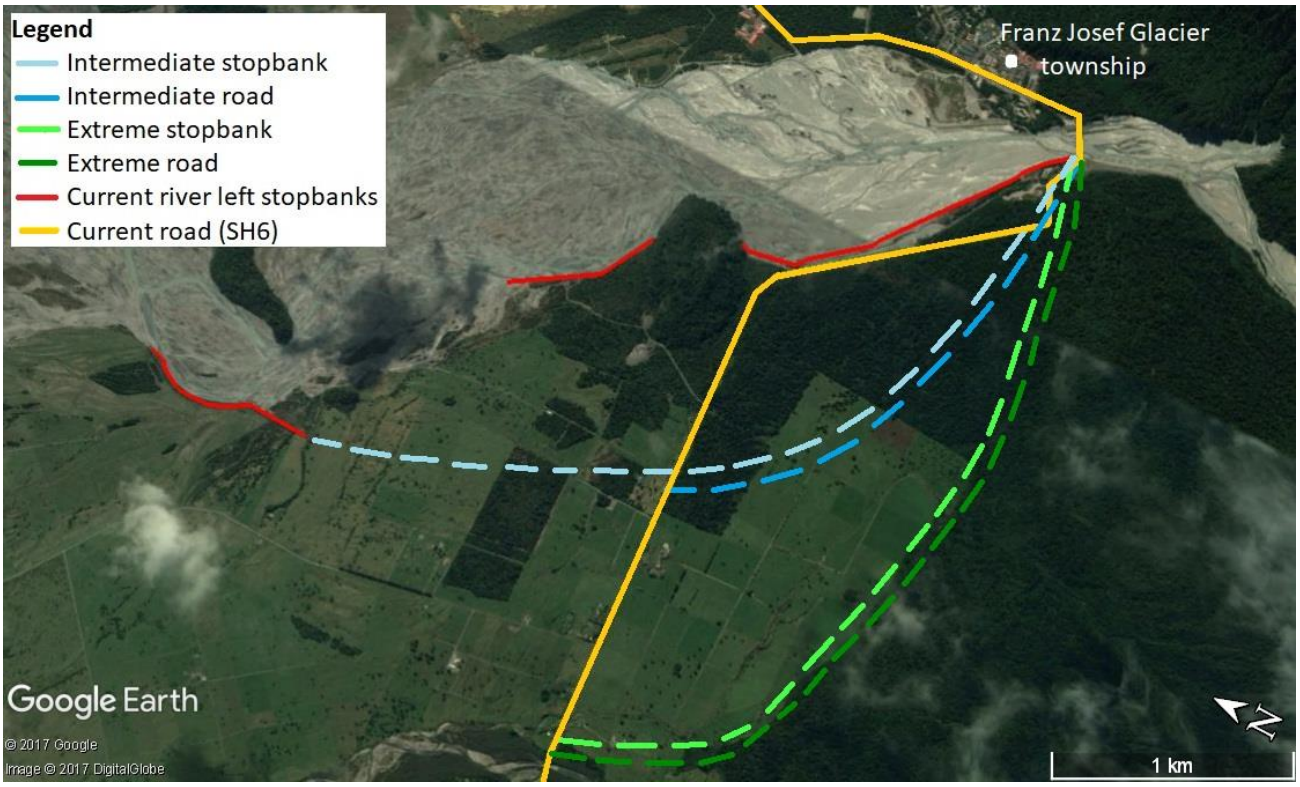

Figure 1.4: Google earth image of the Waiho River and fan with the 2 stopbank alignments to be tested drawn in.

This thesis is structured as follows.

- Chapter two will review the literature available on alluvial fan form, process and evolution, before discussing the Waiho River and fan system.
- Chapter three will then explore microscale modelling theory and practice, followed by an outline of the Waiho microscale model design and construction, as well as experimental design.
- Chapters four and five will discuss the experimental results and what they mean for microscale modelling. Chapter four will focus on the steady input experiments, whilst five will focus on the variable input experiments.

- Chapter six will apply the results to the Waiho-Franz Josef situation.
- Chapter seven is the conclusion. This will include implications and recommendations for the Waiho River and fan system, as well as opportunities for future research.

Chapter 2

Alluvial fans

For the purpose of clarity and understanding it is important to outline the underlying alluvial fan theory before discussing the study site itself. Therefore this chapter will first address what an alluvial fan is, the processes in play and its evolution, before discussing the Waiho River and fan system.

2.1 Alluvial fan theory

Alluvial fans are depositional landforms (Whitehouse and McSaveney, 1990) which are found in a diverse range of climatic and tectonic regimes (Clarke, 2015; Harvey et al., 2005). They occur where there is a high sediment supply, and a lowland area upon which the sediment can be deposited (Schumm, 1977) (Figure 2.1). Alluvial fans play an important role in fluvial systems by acting as storage sites that moderate the transfer of sediment from the upper, sediment-producing part of the catchment to the lower, transitionary and depositional region (Clarke, 2015).

There are two types of alluvial fans and these are differentiated by their dominant primary processes and resulting behaviour (Blair and McPherson, 1994a). The first of these is the debris-flow fan, which forms by the force of gravity acting directly on the sediment-water mixture in a stream and transporting it. The second of these is the fluvially-formed fan, formed by the transport of sediment by water (Blair and McPherson, 1994a,b). This study will focus on fluvial alluvial fans, and henceforth these will just be called alluvial fans.

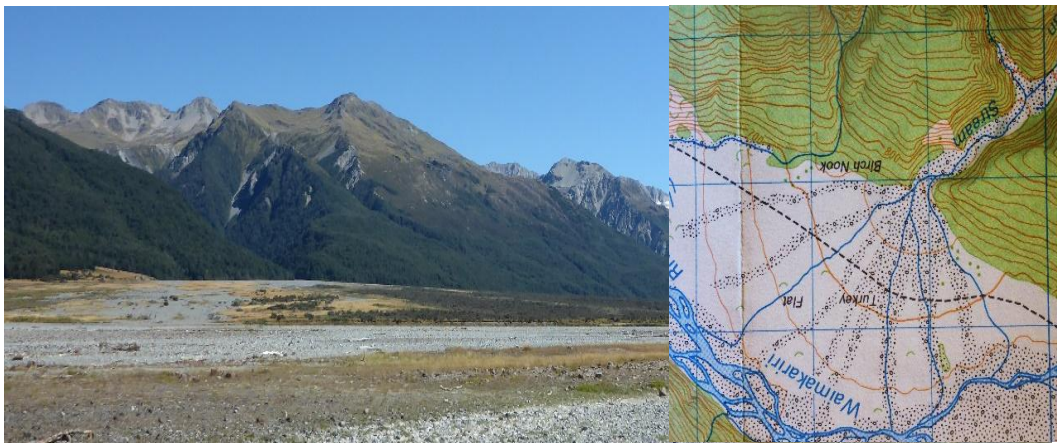

Figure 2.1: The Turkey flat alluvial fan formed by the Jordan Stream as it exits the Black mountain range into the Waimakariri River valley. Toe trimming by the Waimakariri River, braided channels, and depositional lobes on this beautiful fan specimen are clearly observable in the picture; whilst the topographic map (right) provides a birds eye view of the symmetrical radial shape.

Alluvial fans have been defined in different ways by geomorphologists using emphasis on form, process, and evolution to differentiate them (Rachocki, 1981). A simple definition may focus only on the form of the fan and surrounding landforms, describing it as:

A stream deposit whose surface forms a segment of cone that radiates downslope from the point where the stream channel emerges from a mountainous area (Bull, 1964).

In this case, the fan is described as a cone. In the literature, this term has been used interchangeably with fan to describe alluvial fans (Rachocki, 1981). Henceforth, this thesis will only use fan.

In a more complex definition which includes a more process-based focus, Whitehouse and McSaveney (1990) define alluvial fans by the exit of flow from a steep confined channel to a more gently sloping surface where the channel/s are no longer constrained to a fixed position and are free to spread out. The decrease in stream gradient and increase in channel width which

usually accompanies it, decrease the stream power per unit flow width available to transport sediment and the excess sediment is deposited (Whitehouse and McSaveney, 1990).

2.1.1 Form

An alluvial fan forms in a characteristic semicircular shape, which radiates from a singular upstream point (Rachocki, 1981). It consists of three main aspects:

1. A fan apex, which is the highest point of the fan where the river emerges from the mountains.
2. A distributional channel network across the surface, and
3. Fan lobes in the lower section which indicate the laterally migrating phases of deposition that result in toe progradation (figure 2.2; Blair and Mcpherson, 1994b)

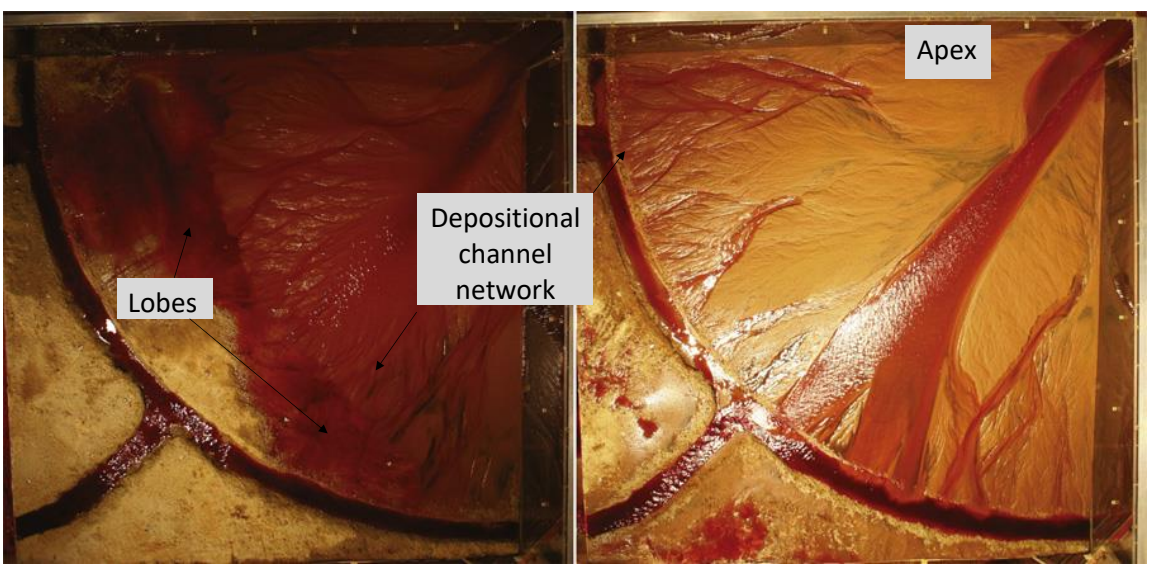

Figure 2.2: Sheet flow and channelized flows in an experimental fan (images are from alluvial fan experiments run by Lucy Clarke at the University of Exeter Sediment Research Facility (Clarke, 2015))

The overall size, shape and slope of the fan reflect the inputs of water and sediment, determined by the upper drainage basin relief, size and geology, as well as the available accommodation space (Harvey et al., 2005; Schumm et al., 1987; Kochel, 1990)

Fan size, shape and slope

Several studies have indicated that quantitative relations exist between the size, shape and slope of an alluvial fan and the relief, size and geology of its upper drainage basin (Eckis, 1928; Bull, 1964; Denny, 1965; Ryder, 1971).

Fan size can be related to the size of its drainage basin (Denny, 1965; Bull, 1964). The larger a drainage basin, the greater its supply of sediment in a given region. Therefore, there is more sediment to be deposited, producing a larger fan. Bull's (1964) studies of the alluvial fans in Fresno, California, indicated a strong relationship between these two elements. He also found that the geology of the drainage basin played an important role in fan size. Sediments from basins composed primarily of sandstone produced smaller fans, than those of mudstone and shale (Schumm, 1977). Mudstone and shale are highly erodible, and therefore produce more sediment than sandstone (Schumm, 1977).

Fan shape, in terms of its profile concavity, can also be related to fan size. The profile is the topographic profile of a line drawn down the fan surface from the apex to the toe (Bull, 1964). Alluvial fans have a slightly concave long profiles (and convex cross-profiles; Clarke, 2015). Eckis (1928) observed that larger fans which have a correspondingly gentler slope have a less concave profile, compared to smaller fans with a steeper slope.

Fan slope in a given region can be inversely related to the drainage basin size and sequently fan volume (Bull, 1964). As basin area and therefore fan volume increase, fan slope decreases. Thus, the larger a fan, the gentler its overall slope. Additionally Ryder (1971), in a study of fans located in British Columbia, found that steeper average relief of a drainage basin corresponded to a steeper fan gradient.

2.1.2 Processes

Alluvial fans are depositional landforms (Clarke, 2015). They are depositional because as the channel exits the mountainous terrain and flows out over open and often flat landscape, transport capacity declines, and sediment is deposited (Clarke, 2015). This process occurs via a distributional channel network which radiates out from the apex of the fan, with individual channels migrating laterally across the fan surface over time (Blair and McPherson, 1994a).

The distributional channel network has been found to share the characteristics of a braided river (Rachocki, 1981; Davies, 1997). Like a braided river, it is highly dynamic and characterised by a braided channel pattern (Bertoldi et al., 2009). This pattern is associated with wide and shallow channels dissected by bars and/or islands, as well as low channel stability which results in lateral channel migration and flow diversion processes such as bifurcation, crevasse splays and avulsion (Blair and McPherson, 1994a; Mètivier and Barrier, 2012; Kleinhans et al., 2013).

In addition, alluvial fans exhibit incisional, fan head trenching, and channel backfilling behaviours (Blair and McPherson, 1994a), as well as sheet flows, which occur where flow becomes unchannelized (Hooke, 1967; Blair and McPherson, 1994b). Zarn and Davies (1994) noted a tendency for alternate build-up of different sides of the fan and toe progradation, accompanied by channel migration which they termed the "windscreen-wiper effect".

At this point it is important to note that not all channels emerging from mountainous terrain will form alluvial fans (Blair and McPherson, 1994b). Bedload-dominated rivers may form instead. In these instances, the river is capable of maintaining its transport capacity and channel banks without forming a fan (Blair and McPherson, 1994b).

Flow diversion processes

The braided channel pattern on alluvial fans reflects three flow diversion processes: bifurcation, crevasse splays and avulsions (Bryant et al., 1995; Clarke et al., 2010). These three processes are the result of local deposition. Bifurcation refers to the points in the channel network where a single channel splits into two downstream branches (Kleinhans et al., 2013); whilst crevasse splays occur when small channels break their natural boundaries depositing sediment in the surrounding area (Bryant et al., 1995). These two processes

can also induce the gradual lateral migration of the channel network, which allows for the distribution of sediment across the whole of the fan surface over time (Blair and McPherson, 1994a).

A much larger shift in the network location can be induced by avulsion (Kleinhans et al., 2013). An avulsion is a major flow diversion process (Clarke et al., 2010). It involves the dramatic shift of the main channel to a new location (Clarke et al., 2010), and can be differentiated from the more minor processes by carrying over 50% of the old channels flow, and leading to the eventual abandonment of the previous channel (Bryant et al., 1995). Avulsions tend to occur in places where deposited sediment has aggraded the channel bed level to the point where neighbouring surfaces are at lower elevation (Jerolmack and Mohrig, 2007). The now elevated channel then abandons its current location and shifts course (Reitz and Jerolmack, 2012). The process of avulsion is typically associated with aggrading surfaces, such as a developing alluvial fan (Reitz and Jerolmack, 2012). However, it can also occur in systems in states of equilibrium and degradation, during episodic inputs of sediment or high periods of flow (Davies and McSaveney, 2008).

Incisional processes

Fanhead trenching is a type of incision that occurs in the main channel at the fan apex, with the depth of the incision declining as it progresses downslope (Schumm et al., 1987) (Figure 2.3). The trench tends to traverse the proximal region of the apex, and therefore can be described to be dissecting the fan (Schumm et al., 1987). The entrenched channel transfers the sediment away from the fanhead to the middle and lower reaches of the fan (Schumm et al., 1987). In the lower reaches, channel backfilling occurs, infilling the channel as the sediment is deposited from the toe upwards (Schumm et al., 1987).

What induces channel entrenching, is a question that has produced many responses (Rachocki, 1981; Schumm et al., 1987). Reasoning tends to fall under two categories relating to either changes in external influences or to internal processes (Hooke, 1967; Wasson, 1977); a detailed discussion and list of these can be found in Schumm et al (1987).

Figure 2.3: Fanhead trenching occurring in Lucy Clarke's (Clarke, 2015) experimental fan

However, in the last decade, the increasing use of physical modelling to study alluvial fans has brought about a different theory, related to the surface state of the fan (Davies and Korup, 2007). Studies have found that fan head trenching can also occur in experimental fan evolution, when it reaches a state of dynamic equilibrium (Davies and Korup, 2007; Clarke et al., 2010).

2.1.3 Evolution

Alluvial fans grow in size via the progradation of the fan toe across their accommodation space (Schumm et al., 1987). The accommodation space is the extent of the lowland area available to the fan, and acts as a limiting factor to fan growth (Davies and Korup, 2007).

During progradation, the fans are constantly adjusting the number of channels, channel geometry, and overall morphology, thereby creating a range of spatial and temporal patterns (Clarke et al., 2010). In an experimental fan these adjustments and patterns can be categorized into three stages (Figure 2.4). These stages can be used to explain fan evolution, as well as the response of the fan to changes in the supply of sediment and water, and other extrinsic controls such as tectonics and human interference such as river control works (Clarke et al., 2010).

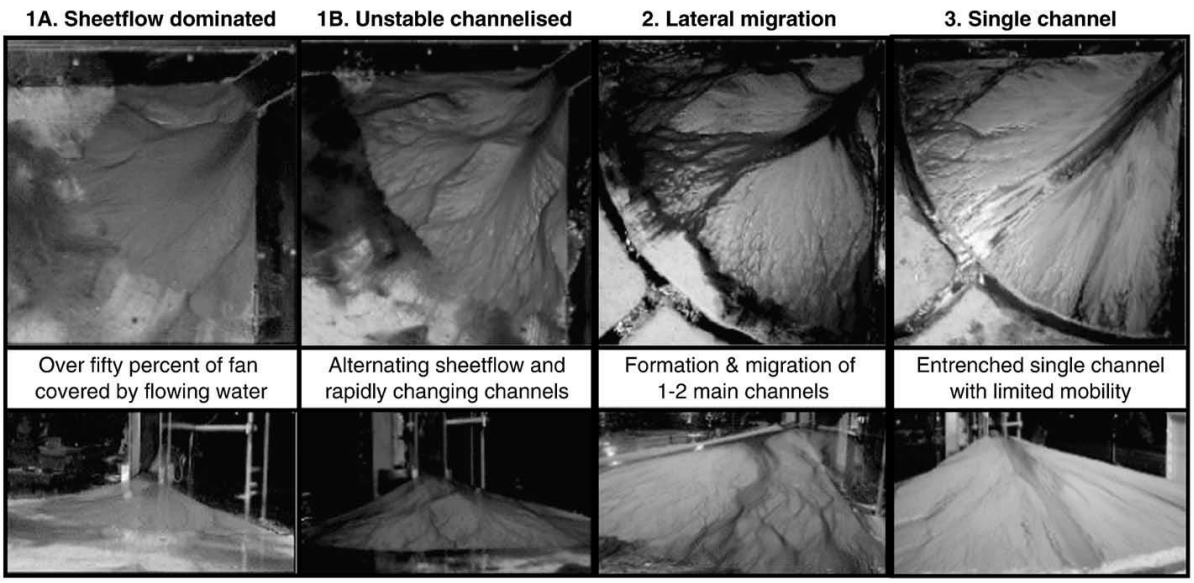

Figure 2.4: Diagram of the stages of experimental fan evolution; taken from Clarke et al (2010).

Stage one

This stage is deposition dominated; the fan grows rapidly, spreading out across the accommodation space (Clarke et al., 2010). Often there are no clear channels, thus avulsions do not occur; instead water moves as sheetflow, covering more than 50 % of the fan surface and spreading sediment across the fan surface (Bryant et al., 1995) (Figure 2.4 - 1a). However, the sheetflow does alternate with short lived and rapidly changing channelized flows (Clarke et al., 2010) (Figure 2.4 -1b).

Stage two

Fan growth continues; however, the rate of growth is slower. The fan toe in some places has reached the end of the accommodation space, meaning that not all the sediment is deposited onto the fan slopes but instead is transported out of the system (Clarke et al., 2010) (Figure 2.4 - 2).

In this stage the water has now become channelized into one or two distinct channels (Bryant et al., 1995). These channels are unstable and prone to bifurcation. There is a tendency for avulsion, which allows the channel network to migrate laterally across the fan, depositing and/or reworking sediment (Clarke et al., 2010). Short-lived crevasse splays that develop off the main channel also contribute to the deposition (Bryant et al., 1995).

An alluvial fan may alternate between stages one and two, switching between sheet flow and channelized flow, depending on where the bulk of the flow is and the occurrence of high flow or sediment supply events (Clarke et al., 2010; Davies and Korup, 2007).

In addition, fan lobes form in the mid to lower reaches of the fan during both stages 1 and 2. These reflect periods of deposition, when the main channels are focussed on that particular area (Clarke et al., 2010).

Stage three

In stage three a majority of the sediment load is transported out of the system (Clarke et al., 2010), and continued growth depends on whether the fan is confined or unconfined (Davies and Korup, 2007).

In confined fans, growth stabilizes once the fan toe has prograded to the capacity of the accommodation space. This stage is characterised by a single channel (Bryant et al., 1995) which is entrenched in the upper part of the fan at the apex, but continues to avulse and migrate laterally over the fan surface in the mid and lower reaches (Clarke et al., 2010) (Figure 2.4 - 3). In this stage the fan is considered to have reached a dynamic equilibrium in terms of its gradient and morphology. Therefore, the fans transport capacity meets the amount of material supplied, such that sediment accumulation on the fan surface is zero (Davies and Korup, 2007).

In comparison, an unconfined fan can continue to grow indefinitely (Davies and Korup, 2007). It will episodically aggrade and prograde under constant sediment and water supplies; and whilst the rate of growth may become very small, the fan can never reach the dynamic equilibrium that a confined fan can (Davies and Korup, 2007).

However, in both cases, the surface state of the fan experiences both short and long term changes, which can result in the fan exhibiting behaviour characteristic of the previous two stages (Clarke et al., 2010). In the short term, minor alterations to the water and sediment supply i.e. floods which introduce higher flow, or landslides which increase the sediment load, and induce continual alterations to the river profile and pattern (Harvey et al., 2005). In the long-term changes in the base level or climate, as well tectonic activity can alter the dynamic equilibrium to the point that the fan can become aggradational or degradational (Harvey et al., 2005).

2.2 The Waiho River and fan system

The Waiho River and fan system is situated in and west of the Southern Alps, on the South Island of New Zealand (Davies, 1997; Davies and McSaveney, 2001) (Figure 2.5). It lies just south of the Franz Josef Glacier (Waiau) township and is the location of the Franz Josef glacier, a major tourist attraction for the town and region (Davies, 1997).

Figure 2.5: Looking out over the upper Waiho Fan towards Canavan's Knob from the river right stopbank

The Waiho River drains a total of 170 km^2, a large portion of which is from the Callery River tributary, a complex system in its own right, whilst other smaller tributaries include the Tatare River and Dochertys Creek, as well as several small streams (Davies and McSaveney, 2001). A proglacial river, the Waiho flows west out of the Franz Josef glacier for 15 km, confined by steep mountainous terrain (Davies, 1997; Davies and McSaveney, 2001). The Callery tributary is in fact 20% larger in area than the rest of the Waiho catchment, and hosts 3 small glaciers; it joins the Waiho about 1 km upstream of Franz Josef Glacier township. The Waiho there departs the mountains to enter a wide valley which it flows through for another 15 km before meeting with the Tasman Sea (Davies and McSaveney, 2001). From where the Waiho River leaves the confines of the mountains, an elongated alluvial fan has formed, the Waiho Fan.

The Waiho Fan has formed in the 15 km long trough left behind by the once coalesced Callery - Tatare - Waiho glacier, which at the last glacial maximum extended some km beyond the present coastline (Davies and Scott, 1997; McSaveney and Davies, 1998). Its width is limited to 4 km at its widest

by lateral moraines 100 m high that extend down to the coast (Davies and Scott, 1997). At the coast the moraines form high cliffs which protect the fan from coastal erosion. Located where it is on the Western flanks of the Southern Alps, the fan experiences high sediment supply, extreme rainfall and flood events, glacial interference, and earthquake movements from the Alpine and other faults. The combination of these factors have created an incredibly powerful and dynamic system.

Water supply

The predominant source of water for the Waiho River is precipitation in the upper headwaters. This precipitation can fall as rain up to heights of 3500 m, however in colder weather, this may fall as snow down to 1000 m. Eighty one percent of the runoff generated by this rainfall interacts with glacial systems such as the Franz Josef Glacier, where it is transported under or through the glacier to the river network in the valley below; the remaining nineteen percent is delivered directly to the river (Davies and McSaveney, 2001).

The Waiho catchment is exposed to the 'roaring forties', a prevailing moist westerly airflow (Davies and Scott, 1997). This means that average annual precipitation is high. Whilst exact values are unknown, it has been estimated from scattered measurements, that annual precipitation is around 11,000 mm in the upper headwaters.

Contributing to this high annual rainfall are intense storm events which frequently occur in the region (McSaveney and Davies, 1998). At the township, rainfall from these storms can reach 200 mm over a 24 hour period at least once a year, whilst storms with rainfall up to 600 mm over a 3 day period can occur every few years. During these storms, maximum intensities are likely to be about 2 mm per minute. However, rainfall is unevenly distributed across the catchment, increasing inland, such that the upper headwaters are likely to receive greater rainfall than the township.

These storms typically produce large flood events. Catastrophic flooding, where the raging river has threatened and at times inundated both town and farmland, punctuates the history of the region (Figure 2.6). The braided nature of the river, especially in the 15 km of alluvial fan, means that its ability to hold floods varies depending on the braided formation at the time

(McSaveney and Davies, 1998). This makes predicting the response of the river and fan to flood events extremely difficult.

Figure 2.6: Waiho flood 2016. Photo RNZ/Conan Young.

Sediment supply

The Waiho River originates in very steep mountainous terrain, in some places 3000 m high. This terrain is a product of uplift resulting from the Pacific plate in sliding collision with the Australian plate (Davies and McSaveney, 2001). It is in an ongoing battle between the $\tilde{1}0$ mm of uplift per year, and rapid erosion caused by the high amounts of precipitation. As a result, large amounts of sediment (metamorphosed schist/gneisses, and greywacke) are constantly entering the Waiho catchment via subaerial erosion (i.e. rockfalls and landslides). Some of this debris falls onto the Franz Josef Glacier, a sediment source in its own right with high erosion rates at its base (Davies and McSaveney, 2001) (Figure 2.7).

Figure 2.7: The retreating Franz Josef glacier. Photo by Linden Brown

The glacier transports sediment at a much faster rate to the Waiho River as the stormwater drainage flows through pressurised conduits (Davies and McSaveney, 2001). Thus, the valley floor immediately downstream of the

glacier is constantly aggrading (Figure 2.8). Additionally, when a temporary blockage or change in the subglacial drainage system occurs, brief floods containing large pulses of sediment and quantities of broken ice can be expelled (Davies and McSaveney, 2001; Davies et al., 2003b). These generate temporary sediment oversupply events to the river and fan below. Sediment pulses from the Callery system also contribute to these and other oversupply events (Davies and McSaveney, 2001).

The upper Waiho valley has a large storage capacity, therefore changes in sediment delivery from the glacier will take a while to become evident at the confluence with the Callery, and the head of the Waiho fan (Davies and McSaveney, 2001). However the Waiho River is still able to deliver sediment to the fan head at its transport capacity (Davies and McSaveney, 2001). This process is only limited by the velocity, depth, and slope of the river. By contrast, the Callery tributary runs in a 10 km long gorge to its confluence with the Waiho, so any sediment input to this reach is immediately transported to the confluence.

Figure 2.8: the upper valley of the Waiho River, just below the glacier terminus. Photo by Linden Brown

2.2.1 Geomorphic history

Waiho fan formation

The following information has been summarised from McSaveney and Davies (1998).

Around 16,000 to 18,000 years ago, glacial activity dominated the south western Southern Alpine coastline, and stages of advance and retreat of the coalesced Callery — Tatare — Waiho glacier had carved out a broad deep valley across the coastal lowland, now known as the Waiho Flats. A few thousand years later (13,000 years ago) a huge rock avalanche onto the significantly retreated Callery — Waiho glacier covered the glacier to its terminus. The glacier transported the rock avalanche debris to the terminus and there built the Waiho Loop terminal moraine (Alexander et al., 2014).

It was only after the Callery — Waiho glacial lobe receded from the Waiho Loop, and the glacially-fed Tatare and Waiho Rivers began delivering sediment to this upper lowland region, that the Tatare and Waiho alluvial fans began to form. At this time, the Waiho Loop would have extended much further south than at present, and the isolated hillock known as Rata Knoll would have formed part of the continuous moraine deposit. River bed level would have been at least 100 m lower than the present, and sea level much lower, thus the Loop would have acted as an obstacle to the rivers and rapidly developing fans. In addition, 10,000 years ago the Loop was 400 m farther south-west relative to the Waiho Valley, due to tectonic movement on the Alpine fault.

The Tatare River with probable assistance from the Waiho River rapidly infilled the area upstream of the Waiho Loop, until approximately about a thousand years ago when its fan elevation became level with the lowest part of the Loop. The Tatare was then able to flow across the Loop, forming a substantial waterfall on the other side. Downcutting saw the Tatare become incised into its fan, and prevented further aggradation of the upper fan surface.

There is no evidence that the Waiho River ever flowed into the Tatare above the Loop. Instead the Waiho is believed to have aggraded its fan towards the outer sea coast. When sea level stabilized about 6,000 years ago,

so did the position and elevation of the fan toe. Therefore long term aggradation would have ceased shortly after that, evident by shallowly buried old soils close to the South end of the Waiho Loop, either side of the Waiho River bed.

Since its fan formation, it is believed that the Waiho River flowed south of Rata Knoll, its passage to the north being blocked by the higher Tatare fan. At the same time, farther upstream flow would have alternated either side of Canavan's Knob, slowly burying and eroding the former westward extent of the Waiho Loop moraine. However, in recent time, perhaps as a result of either large sediment input or fault movement (or both), the upper Waiho fan experienced considerable and unusual aggradation which induced a shift of the main Waiho channel to the east of Canavan's Knob on to the Tatare fan, and then through a low point between the loop and Rata Knoll. This is its current configuration, which has been unchanged for at least a century aside from an attempted break out to the south in 1982, which was pushed back by control measures.

Fan surface state

It is believed that by the time the Waiho river had shifted to occupy the land east of Canavan's Knob and the low point between the Loop and Rata Knoll, the fan surface had reached a state of long term dynamic equilibrium (Davies and McSaveney, 2001). Nevertheless, in the short term this equilibrium would be affected by brief sediment oversupplies or deficits. Oversupply, a result of storm or earthquake triggered landslides, induced aggradation and therefore the steepening of the fan surface profile (Davies and McSaveney, 2001). Alternatively, deficits (or water surpluses) caused episodes of degradation, resulting in lowering of the fan slope (Davies and McSaveney, 2001).

Overall, it is believed that the fan surface would have been operating about a well-defined mean profile, a result of steady long term sediment and water inputs, a confined accommodation space, and a toe kept constant by the stabilized sea level (Davies and McSaveney, 2001).

2.2.2 Human interference

The Waiho region was settled around the 1890s. The town location itself was chosen as it was considered safe from flood events, and provided close

access to the reasonably safe and stable river crossing. However, over time it became evident that the Franz Josef township and farmlands were in danger from flood events and the slowly aggrading river bed. As a result, stopbanks were gradually installed. These ad hoc works were designed to restrict the river to the far north western side of the valley, preventing it from utilizing a majority of its valley as well as protecting the township and highway. Aerial photography dating from 1948 to 2013, provides an excellent time lapse of the region since this time (Appendix A). It is interesting to note that since the initial stopbank installation in the 1930s the Waiho River has undergone dramatic and significant planform changes (Figure 2.9). The deeply incised gorge just below the confluence between the Waiho and Callery rivers is long gone, lost under an unprecedented level of aggradation. These dramatic changes have led to the belief that the stopbanks were the cause of the rapid rates of aggradation.

Brief history of control works

The first aerial photographs of the region were taken in 1948. Thus, the exact behaviour of the Waiho river and fan system prior to this time cannot be accurately reconstructed. However, photographs and written accounts do provide some insight into what was going on.

- In the late 19th century the river bed adjacent to the site of the township consisted of very large glacial lag boulders
- The earliest evidence of river control works comes from a photo in 1910 of the first car fording the Waiho River below a footbridge. A rock gabion had been put in place to control the location of the river crossing, and indicates that there was significant sediment movement and channel instability present.
- In 1927, relocation of infrastructure indicates that significant sediment movement was resulting in aggradation of the river bed. The original hotel had to be moved away from the lower terrace site because of flooding.
- By the 1930s the river borne sediment was causing further problems for the lower terrace site, such as flooding of the former airstrip. At

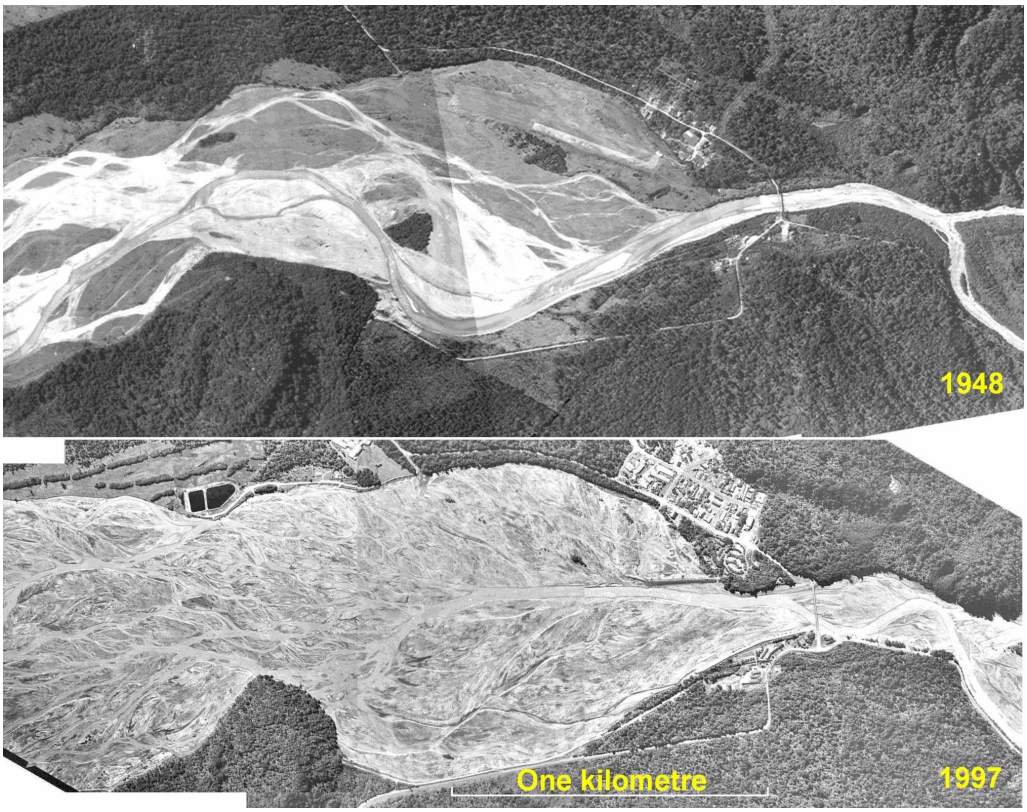

Figure 2.9: Aerial imagery of the upper Waiho fan from 1948 and 1997. Image from Davies and McSaveney (2001)

this time the first permanent stopbank was installed to keep the river away from this lower terrace site.

- The 1948 aerial photograph indicates several more stopbanks in place. Bank protection works are visible on the true right back opposite the Holiday Park, and there is a true left stopbank just upstream of the Canavan's Knob.

- From 1948 onwards, the aerial photographs provide an excellent record of the changes taking place on the upper fan, and of the increasing and on occasion decreasing number of stopbanks (Appendix A). One of the rare, but spectacular failures of the stopbank network, was of a long central bank installed in 1980 (figure 2.10). It was designed to restrict

the river to a narrow bed against the south western bank (true left), downstream of the motor home. It lasted only four years, and was breached in a flood event; no evidence of it remains.

Figure 2.10: Photo of the Waiho showing the 1980 stopbank. The (failed) stopbank runs down the centre of the fan.

Present day stopbank alignment

The present day stopbank system consists of nine main stopbanks (five on the left and four the right) which restrict the Waiho River to a third of its alluvial fan. These are described briefly below (Table 2.1). Other stopbanks do exist in the lower reaches of the Waiho River, Tatare River, and Dochertys Creek, but are not discussed here, as the focus is on the upper and middle sections of the Waiho fan.

Table 2.1: Description of the current stopbanks setup on the Waiho River (McSaveney and Davies, 1998)

	Type	Location	Reason
R1	Interlocked heavy rock spur groynes	Between the Callery Junction and the SH6 bridge	To deflect the river flow away from the base of the high terrace and therefore prevent further scour and loss of the terrace. Loss of this terrace edge would threaten the right bank (Northern) approach to the SH6 bridge and the Waiho River frontage of the Franz Josef Glacier township
R2	280m embankment of interlocked heavy rock	Upstream of the SH6 bridge to the downstream edge of the terrace where the Anglican church is sited. (Figure 2.11)	Scour protection. The embankment is 5 m deep to prevent future scouring, and provide ongoing protection to the terrace, and church.
R3	Stopbank	Lower terrace where the former airstrip was located. It is now a heliport.	This stopbank has been up to a kilometre long in an attempt to prevent the river overflowing onto the former airstrip.
R4	Upgraded R3 stopbank, as well as fill and rock rip rap and spur groynes	Lower terrace at the Franz Josef Glacier hotel and oxidation frontage. (This was breached in 2016; Figure 2.12)	To protect the Franz Josef Glacier hotel and the oxidation pond from the rapidly aggrading bed and flood events.
L1	Raised road, and rock rip rap	Between the Callery confluence and the SH6 bridge (Figures 2.13 and 2.14)	To protect the glacial access road from aggradation and bank scour
L2	Stopbank armoured in part by heavy rock, and as well as stub groynes	Downstream of the SH6 bridge along the frontage of the Holiday Park (Figure 2.15)	To protect the river frontage of the Holiday Park from continuing aggradation and scour.
L3	Stopbank with stub groynes	Overlapping with the L2 stopbank down to Canavan's Knob.	To protect the SH6 from aggradation and scour, and prevent the river from breaking out.
L4	Stopbank	Downstream of Canavan's Knob, acting as a continuation of a low terrace at its upstream end.	To protect the terrace from erosion by deflecting flow away from the left bank (towards the unprotected right bank).
L5	Stopbank faced with large rocks	Immediately downstream of Rata Knoll	Eatwells (formally Miltons) stopbank is designed to protect the farmland and Waiho Flats airstrip from flow break outs, which could potentially result in a shift across the flats into Dochertys Creek.

Figure 2.11: Looking downstream from the SH6 bridge at the true right stopbank that protects the church

Figure 2.12: The repaired lower terrace stopbank. The Heartland Hotel can be seen in the top right hand corner. The Waiho breached this stopbank and flooded the hotel in 2016. Photo by Rob Pieper

Figure 2.13: Looking upstream from the SH6 bridge at the true left stopbank and spur groynes

Figure 2.14: Looking downstream to the SH6 bridge at the spur groynes on the true left of the Waiho River

Figure 2.15: Looking downstream from the SH6 bridge at the true left stopbank. The river/fan bed is clearly much higher than the land on the other side of the stopbanks.

Chapter 3

Microscale modelling

Microscale models are extremely small scale physical hydraulic models (Peakall et al., 1996; Clarke, 2015; Gaines and Maynord, 2001; Malverti et al., 2008). Physical hydraulic models represent a selected fluvial geomorphic feature, allowing it to be studied under closely monitored or controlled experimental conditions (Mosley and Zimpfer, 1978). Microscale models have been successfully used to model alluvial fan behaviour and dynamics, and river engineering works (Davies et al., 2003a, 2013; Gaines and Maynord, 2001; Clarke, 2015).

The successful use of this type of modelling, and number of advantages as outlined below, has shown them to be an invaluable tool to both engineers and geomorphologists alike (Peakall et al., 1996; Mosley and Zimpfer, 1978).

- Due to their small size, usually tens of centimetres to a couple of meters (Malverti et al., 2008) these models are relatively easy and inexpensive to set up, and they take up very little space (Malverti et al., 2008; Mosley and Zimpfer, 1978) For example, the Davies et al. (2013) microscale model of the Waiho alluvial fan and river system was constructed on a 2m by 3m wooden table, using readily available polystyrene for the boundaries (Campbell, 2012). Aside from the initial assistance for the setup, the honours student was able to run the experiments alone (Campbell, 2012).

- The close control over the relevant variables that a small model allows, also means that they allow for precise measurement (Mosley and Zimpfer, 1978), as was found in a study on growth dynamics on gravel bed river deltas (Wild, 2012). The relatively small scaled models of 1:1500 and 1:2000, allowed the use of an instantaneous-profile laser scanner, providing bed elevation accuracy of +/- 0.5mm.

- In addition, microscale models evolve at much shorter timescales than other larger scaled models, which means that results can be achieved quickly (Malverti et al., 2008). This is particularly valuable when

considering that the timescale of river bed evolution through bedload transport is 10^{-1} to 10^{4} years. Microscale models dramatically reduce this timescale. This has allowed for the study of landscape evolution processes (Peakall et al., 1996). However, it must be borne in mind that, unlike a properly scaled model, the timescale of operation of microscale models is unknown.

- Finally and perhaps most importantly when considering the study of very dynamic systems, they allow the observation of fluvial phenomena that are otherwise difficult to observe in the field (Warburton, 1996; Davies and Lee, 1988). For example, braided gravel-bed rivers experience a majority of their planform change during flood conditions (Peakall et al., 1996). At this time, the highly turbulent and turbid nature of flow makes it virtually impossible to observe near-bed processes in the field (Peakall et al., 1996).

However, microscale modelling is a relatively new form of physical hydraulic modelling, and thus far has had only limited use, but received much criticism from the scientific community (Gaines and Maynord, 2001). Physical hydraulic models are required to meet three similarity criteria, which are geometric, kinematic and dynamic similarity (Schumm et al., 1987). Microscale models do not meet all of these criteria. They will maintain geometric similarity, and some kinematic similarity, but place little emphasis upon dynamic similarity (Davinroy, 1994; Hong and Davies, 1979; Malverti et al., 2008), instead appearing to adhere to a fourth criterion, Hooke's similarity of process (Mosley and Zimpfer, 1978). This has led to a number of concerns in regards to its size and similitude (Gaines and Maynord, 2001). However, several studies have been conducted to address these concerns, and subsequently justified the use of microscale modelling as a tool for scientific investigations.

The following sections will explore microscale modelling theory and practice, followed by an outline of the microscale model used in this study. The theory section will address underlying principles as well as the concerns over model size and similitude; whilst the practice section will discuss model construction, experimental procedures and measurement tools, providing a comparison between the two main users of microscale models. The outline of the microscale model used in this study will also include model construction, experimental design, and the data collection and analysis tools used.

3.1 Theory

3.1.1 Underlying principles

Physical hydraulic models are often classified into three types: one-to-one, scaled, and analogue (Peakall et al., 1996). Of these types, microscale models fall under the analogue category. This reflects the nature of the modelling. Analogue implies not the exact scaled representation of a prototype but that of the general population (Hooke, 1968; Peakall et al., 1996; Mosley and Zimpfer, 1978). The models reproduce a specific aspect of the form and function of the chosen feature, but the forces, materials and processes may be quite dissimilar to those in nature (Schumm et al., 1987). Thus, these models must be considered as small systems in their own right (Peakall et al., 1996; Mosley and Zimpfer, 1978). Analogue modelling is based upon Hooke's similarity of process criterion.

Hooke's similarity of process criterion

Roger Hooke's (1968) similarity of process technique was developed as an alternative to the formal scale-modelling procedures. He found the latter to be difficult to follow, restrictive and at times unsuitable to geomorphic studies where the aim was to develop general theory rather than represent a specific prototype (Schumm et al., 1987).

The similarity of process technique ignores true dynamic similarity (Barr, 1968), as Hooke (1968) viewed the quantitative extrapolation from a model to a prototype as dubious. Instead it is based on the concept that as the underlying principles are the same then the processes that occur in a laboratory system, and their morphologic effects, are similar to those in nature (i.e. in the field; Hooke, 1967).

The similarity of process criterion requires that:

1. *gross scaling relationship be met*
2. *the model reproduce some morphologic characteristic of the prototype*
3. *the processes which produced this characteristic in the laboratory can logically be assumed to have the same effect on the prototype.*

Under these criteria, the model is treated as a system in its own right (Hooke, 1968). This type of model is considered the true analogue model. However, the treatment of these models as systems in their own right can be seen as limited to a specific mode of investigation. As there is no similarity to a prototype, analogues are better suited to geomorphic problems that do not involve an individual (prototype) in the population (Hooke, 1968). Instead they can be used to investigate general relationships applicable to the entire population. For example, Hooke successfully conducted several similarity of process experiments to study the processes and steady-state relationships in arid region alluvial fans (1967; 1968). He did not focus on a particular fan, but on the behaviour of the group in general (Hooke, 1967, 1968). Similarly, Schumm (1977; 1987) successfully used analogue models to reproduce the fundamental features and processes that one would expect to see on natural alluvial fans (Clarke, 2015). These experiments were invaluable to the study of alluvial fans, and motivated a renewed interest into experimental modelling of these landforms (Clarke, 2015).

Whilst microscale models appear to adhere to the similarity of process criterion, they differ from the traditional analogue models that Hooke and Schumm used in that they retain some aspect of geometric and kinematic similarity between model and prototype (Hong and Davies, 1979; Malverti et al., 2008). This is because microscale models have and continue to be used to investigate specific systems (prototypes; Davies et al., 2003a; 2013, Gaines and Maynord, 2001). They are able to do this by meeting the geometric similarity criterion required of physical hydraulic models (Hong and Davies, 1979); and are calibrated to reproduce particular behaviours of the prototype (kinematic similarity).

Geometric similarity

Geometric similarity is one of the three similarity criteria required by a physical hydraulic model to precisely represent the prototype (Schumm et al., 1987). In microscale models, geometric similarity is achieved by the scaling down of the boundaries and landscape features of the prototype to the micro scale.

Microscale models have been used at a model to prototype ratio of as small as 1:20,000 (Gaines and Maynord, 2001). However, at such small scales it would be impossible to model the required flow rates and depths. Therefore,

in order to maintain adequate model flow depths, microscale models often take on a distortion effect (Gaines and Maynord, 2001; Peakall et al., 1996). This means that the vertical scale differs to the horizontal scale of the model, with vertical exaggeration (Gaines and Maynord, 2001; Peakall et al., 1996).

3.1.2 The justification for microscale modelling

Despite successful use (Gaines and Maynord, 2001; Davies et al., 2003a, 2013), microscale modelling has and continues to be treated with some trepidation and criticism by the scientific community (Gaines and Maynord, 2001). This is because these models do not meet all the basic similarity criteria required for other forms of physical hydraulic modelling (Gaines and Maynord, 2001).

Physical hydraulic models are required to meet three similarity criteria (Schumm et al., 1987):

1. *Geometric similarity (form): ratios of homologous dimensions are equal and equivalent angles are the same*
2. *Kinematic similarity (motion): paths and patterns of motion are geometrically similar to those of homologous occurrence in the prototype*
3. *Dynamic similarity (forces): the ratios of homologous masses and forces affecting matter are equal at all times.*

It is almost impossible to meet each of these similarity requirements exactly in a scaled model, and many types of scaled models will relax some of the dynamic similarity (Malverti et al., 2008; Mosley and Zimpfer, 1978). However, microscale models give little emphasis to these criteria. Whilst they conform to the (planform) geometric similarity criterion, and in part generate some kinematic similarity, there is no attempt made towards achieving dynamic similarity (Davinroy, 1994; Hong and Davies, 1979; Malverti et al., 2008).

Therefore, in the same way that Hooke (1968) had doubts about the quantitative extrapolation of results from model to prototype in scaled physical models, there are many concerns in regards to the accuracy and reliability of microscale modelling (Gaines and Maynord, 2001; Malverti et al., 2008; Mosley and Zimpfer, 1978; Peakall et al., 1996). The short time span that

microscale models have been in existence, and the relatively few studies that have used them, does not help their case, nor the present author's job. So, criticism and trepidation are justified. Thus, the concerns in regards to the accuracy and reliability of microscale modelling, as well as application to a specific prototype, must be discussed.

Size

Understandably concerns have focussed on the very small size of microscale models (Gaines and Maynord, 2001). This is because there is increasing evidence that some geomorphic processes are scale dependent (Schumm et al., 1987). However, considering that there is no direct quantitative extrapolation from model to prototype, then the errors that may occur during the interpretation of gross scaling relationships cannot occur. One must reiterate, that the microscale models are treated as systems in their own right (Hooke, 1968; Malverti et al., 2008).

Other points to consider with respect to the small size of these models are the effects of surface tension on channel development and the physics of channelized flow, as well as the severe vertical distortion required to maintain acceptable flow depths and rates (Malverti et al., 2008).

Surface tension is *"the tensile force which results from the difference between the internal molecular forces of a liquid and the forces between the liquid molecules and an adjacent* [material]" (Malverti et al., 2008) for example, the interface between water and air. Based on this definition, it seems logical that at such small flow depths, surface tension would have an effect on the model performance. However, studies by Peakall and Warburton (1996) and Mètivier and Meunier (2003) both found that the effect of surface tension was insignificant when the dimensionless Weber number was large i.e. between 10 and 100. Further, in a more recent study using laminar flow experiments, Malverti et al (2008) found that smaller Weber numbers ranging between 0.1 and 2 also had negligible effects on surface tension.

The very small size of microscale models also means that they employ very small horizontal scales (Gaines and Maynord, 2001). In order to maintain the flow depths and rates necessary to allow sediment transport, and accurate measurement with the available tools, a larger vertical scale must

be applied (Malverti et al., 2008). This creates a vertical distortion. Concerns exist about the accuracy of flow distribution under this distortionary effect (Gaines and Maynord, 2001) as experiments conducted by the US Army Corps of Engineers have shown that the vertical distortion means that riverbank effects extend over a greater portion of the model than the prototype (Gaines and Maynord, 2001).

However, microscale models are not the first type of physical hydraulic model to use distortions (Gaines and Maynord, 2001). Indeed distorted models themselves are considered a type of physical modelling (Peakall et al., 1996). Furthermore, scale distortion effects are irrelevant for analogue models, as discussed by Mosley and Zimpfer (1978).

Similitude

Microscale modelling appears to be almost flippant towards the similarity considerations that other physical hydraulic models are guided by (Gaines and Maynord, 2001). This is because there is no attempt made to meet the dynamic similarity criterion, meaning that dimensionless values such as the Froude, Reynolds and Shields numbers are ignored (Gaines and Maynord, 2001; Paola et al., 2009). For example, flow in microscale models is laminar, when in field rivers it is always turbulent (Davies et al., 2003a).

The use of laminar flow to model turbulent systems brings about several concerns about unrealistic friction coefficients, lack of suspended load transport, and as discussed earlier the effects of surface tension (Malverti et al., 2008). However, each of these can be defended.

- A study by Lajeunesse et al (2010) showed in their own experiments and in a discussion of other experimental studies (Armstrong, 2003) that the effect of unrealistic friction coefficients were negligible upon model performance (Lajeunesse et al., 2010; Malverti et al., 2008).
- Whilst the lack of suspended sediment transport is a valid concern, it is not applicable to studies where the focus is on bedload transport (Malverti et al., 2008), as is the case for braided gravel-bed rivers, and in the Waiho River and fan system.

In addition, Hong and Davies (1979) have shown that whilst processes of water flow and sediment motion may differ between turbulent and laminar flows, this does not suppress similarity between channel pattern variability or Froude numbers (Davies et al., 2003a).

- Hong and Davies (1979) were able to reproduce the braiding pattern of several east coast rivers of the South Island of New Zealand in a microscale model by adjusting flow rates, sediment supply, and slope, thus proving that microscale models can achieve kinematic similarity, at least in part.
- Hong and Davies (1979) and Grant (1997) also found that Froude numbers in microscale models are often similar to their prototype values regardless of the lack of attempt to achieve similarity.

Another concern related to the similitude between model and prototype is to do with the calibration of microscale models. The vertical scale represented by flow depth, as well as flows rates, sediment supply, and slope, are not included in the design of microscale models (Gaines and Maynord, 2001). In many cases, this is because field data are lacking, which is why the microscale model has been utilized in the first place (Davies et al., 2013). Therefore there are insufficient data to generate a hydrograph or sediment supply rates (Gaines and Maynord, 2001). Thus, during the calibration phase slope, flow depth and rate, and sediment supply are adjusted empirically to ensure general bed movement as well as reproduce some morphologic and behavioural aspect of the natural system they are representing (Gaines and Maynord, 2001). However, to reiterate a previous point, the microscale model is not an exact scaled replica of the prototype. It may be similar in process and geometry, but it is still a system in its own right, and does not require the scaled inputs that other physical models do.

Although there are concerns over the veracity of microscale modelling, these models have thus far been "unreasonably effective" (Paola et al., 2009), having been used very successfully to study a number of problems (Clarke, 2015). In both New Zealand and the United States of America, microscale models have been applied to investigate alluvial fan dynamics, and river engineering works. Davies et al (2003a; 2013) successfully reproduced the behaviour of the Waiho River on the upper part of its fan using 1:2000 and 1:5000 scale micromodels (Clarke, 2015). The US Army Corps of engineers have and continue to use microscale models for a number of channel

responses studies, including evaluation of how navigational channel widths and depths are affected by different channel designs on the Mississippi river (Gaines and Maynord, 2001). Given the success of the models in these studies, it would seem that microscale models present an opportunity for further use as well as exploration within the scientific community.

3.2 Practice

In the fluvial environment, microscale models have been successfully used to study a range of evolutionary processes (Peakall et al., 1996). These include sediment-flow interactions, bed morphology, channel morphology such as meandering and braiding, channel evolution, and knickpoint migration (Malverti et al., 2008; Davies et al., 2003a, 2013; Davies and Korup, 2007; Gaines and Maynord, 2001; Guerit et al., 2014). Of note, they have provided a valuable insight into landscape evolution processes, such as that of alluvial fan and channel dynamics (Clarke et al., 2010; Peakall et al., 1996).

In addition to developing general theory and understanding, they have been extensively applied to engineering and river management problems (Gaines and Maynord, 2001; Mosley and Zimpfer, 1978; Warburton, 1996). They have been used to investigate management upon specific reaches of river channel by studying the channels response to different control structures such as weirs, dikes, groynes, and stopbanks (Gaines and Maynord, 2001; Mosley and Zimpfer, 1978) as well as on the impact on fan behaviour when confined (Davies et al., 2003a, 2013); and to test engineering design equations (Warburton, 1996).

The following three sections will explore microscale model design and experimental procedure, as well as the tools used for measurements. This will draw on and explore the limited number of microscale modelling experiments associated with alluvial fans and braided gravel-bed rivers.

3.2.1 Model design

There appear to be two main centres of microscale modelling, one in the United States and the other in New Zealand.

- In the United States, the St Louis District of the United States Army Corps of Engineers (USACE) has been using microscale modelling for

some time now to investigate river training issues on the Mississippi and White rivers (Gaines and Maynord, 2001).

- In New Zealand a number of microscale modelling experiments have been used to study fan systems on the South Island west coast and the dynamics of braided gravel-bed rivers on the east coast (Davies et al., 2003a, 2013; Davies and Korup, 2007).

Comparison of the two microscale modelling styles reveals that whilst they do differ in some respects, there is general trend in model design. Other studies which have adopted the microscale or analogue approach (Clarke et al., 2010; Guerit et al., 2014; Mètivier and Meunier, 2003; Paola et al., 2009) also share similar practices.

The main components of microscale models include (Figure 3.1):

- Hydraulic flume (structure, sediment/water feeders, and flow controller)
- Geometric insert
- Bed sediment
- Materials to be used for control work structures (if required).

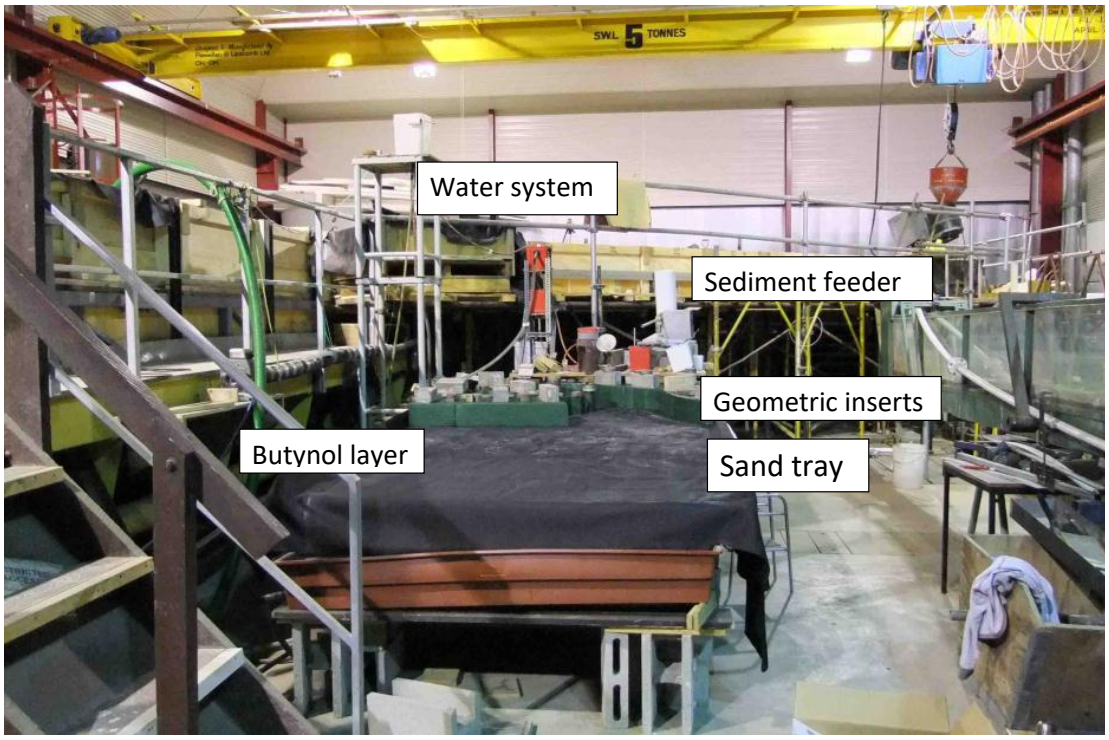

Figure 3.1: Campbell (2012) microscale model; components include the butynol layer, geometric inserts, sediment feeder, and water system (head and footer tanks, connecting tubes and siphon).

Hydraulic flume

Hydraulic flumes (Gaines and Maynord, 2001), also called sand trays (Davies et al., 2013), are the self-contained structures on which the microscale models are built.

- Whilst the USACE structures are more flume-like, the tray used by Davies et al (2013) is simply a flat, wooden table top, with raised edges, and a waterproof butynol layer to prevent water loss (Figure 3.1).
- In both cases, they can be sized to meet a range of requirements. However the size tends to be limited by the area physically reachable by the modeller (Gaines and Maynord, 2001). The USACE models

typically fall within 0.9 m wide by 1.90 m long dimensions, whilst the Davies et al. (2003a; 2013), Davies and Korup (2007) and Wild (2012) models shared a 2 m width, and a range of lengths between 2 and 5 m. These structures also have adjustable slopes in both the longitudinal and transverse direction, and planar tops (Gaines and Maynord, 2001; Wild, 2012).

Microscale models receive sediment and water from a singular point at the head of the model. In both centres of modelling, the water is recirculated via a pump, and header and footer tanks (Gaines and Maynord, 2001; Wild, 2012; Davies et al., 2013).

- The head tank is connected by a tube to the head of the outwash section of the river, where flow enters the model via the flow controller. This control is electronic in the USACE experiments (Gaines and Maynord, 2001), whilst in the NZ set of microscale models, flow is manually controlled by adjustable clamps (Campbell, 2012).
- Once the water has passed through the model, it enters a tray at the bottom. In the New Zealand models, a fine sieve mesh is secured at the end of this tray, to ensure only the water drains down into the footer tank below (Campbell, 2012). This tank is connected to the header tank, and water recirculation is maintained between the two by the pump and a pipe network.
- In the USACE and Davies et al (2003a; 2013) models, water was fed into the model at constant rates (Gaines and Maynord, 2001). However, in the Davies and Korup (2007) model, water was fed into the model via a series of repeated hydrographs between which flow would briefly stop. The hydrographs were regulated by an automatic siphon and reserve tank which were fed by a steady inflow. The tank in which the siphon sat, would fill up to the point that the surface of the water was higher than its bend, at which point the siphon would be triggered.

Sediment was also fed into the head of the models. In the USACE models the sediment was recirculated (Gaines and Maynord, 2001), whilst in the New Zealand set of models (Davies et al., 2003a, 2013; Davies and Korup, 2007), it was not.

- In the unrecirculating models, a Tinker sediment feeder was used to move the sediment at a controlled rate into a funnel where it would be

joined by the water. This allowed mixing of the two mediums before entering the actual model.

- Tinker sediment feeders consist of open topped sediment holding container, and a revolving metal pipe connected to the bottom of the container (Figure 3.2). Sediment is poured into the top of the feeder, and exits along the revolving pipe which is powered by the pump. The angle of the pipe and container, and speed of the pump, dictate the sediment supply rate to the model. The steeper the angle, the greater the feed rate. Crucial to successful operation, the sediment must be dry, or it won't move through the revolving pipe. (Campbell, 2012; Wild, 2012; Davies et al., 2013).

Figure 3.2: the Tinker sediment feeder used in the author's experiments. In this image, the double funnel and disc system used by Davies and Korup (2007) is present.

- In addition, Davies and Korup (2007) had the feeder pipe deliver the sediment onto a disc above the funnel (Figure 3.2). A conical angle of repose sand pile would then form on the disc, and the sediment would avalanche naturally from it into the funnel, where it would mix with

the water before entering the model. This generated irregular inputs of sediment in the short term.

- Once the sediment left the model, the water was strained out, and the sediment dumped to dry for later use. Sediment could not be recirculated as it is not possible to use wet sediment in a Tinker sediment feeder.

Geometric insert

The geometric inserts represent the fixed boundaries of the river reach (Gaines and Maynord, 2001) or fan system (Davies et al., 2013) being studied. These inserts have been cut out of high density expanded polystyrene that is typically between 50 and 250 mm thick (Clarkson, 1999; Gaines and Maynord, 2001; Campbell, 2012; Wild, 2012). It is then attached via strong, water proof glue (ADOS Styrobond), and sealed with a silicone sealant Silaflex ®RTV (Wild, 2012).

- The USACE designed the inserts from georeferenced aerial photographs of the prototype (Gaines and Maynord, 2001). The generated photomap was scaled to the chosen horizontal scale of the model. It was then placed over the singular rectangular sheet of planar polystyrene, and the channels cut out vertically (Gaines and Maynord, 2001).

- Wild (2012) designed her inserts from contours created in ArcGIS from a 25 m DEM of New Zealand which was produced by Land Information New Zealand using digital topography data. The inserts were chosen so that they represented the disparity of slope, where the mountains rose steeply from the gentle valley slopes.

- In the Davies et al. (2003a; 2013) experiments, inserts were cut from stencils that had been generated from a scaled 1:50,000 topographic map of the Waiho area (Clarkson, 1999; Campbell, 2012).

- The polystyrene inserts also received layer/s of paint to make them water tight (Wild, 2012; Clarkson, 1999; Campbell, 2012).

- In addition to these inserts, the Davies et al. (2003a; 2013) models also used a free overfall. This meant a base level could be set, effectively confining the fan systems they were working with. The overfall was a 1cm thick strip of wood that was glued and sealed to the butynol layer at a point where field studies had shown that very little aggradation

had occurred, suggesting that bed elevation downstream of that point had been fairly constant over the last few thousand years (Davies et al., 2003a).

Bed sediment

The bed sediment differed between the sets of microscale modelling.

- The USACE used a "Urea Type II plastic", which has a typical specific gravity of 1.48. The mix used in the microscale models consisted of four gradations: 0.25 - 0.42 mm, 0.42 - 0.58 mm, 0.48 - 0.84 mm, and 0.84 - 1.19 mm. The USACE had used a number of different types of sediment, but has settled on the Urea type II plastic because it is light enough to be transported, and retains the bed configuration after each model test so that the bathymetric data can be collected (Gaines and Maynord, 2001).
- The New Zealand set of models use a fine silica sand (Davies et al., 2003a, 2013; Davies and Korup, 2007; Wild, 2012), that has a median diameter of 0.19 - 0.22 mm.

Control work structures

Control work structures include but are not limited to dikes, bendway weirs, chevrons, closed structures, and stopbanks. In reality, these may be designed out of concrete, wood, a coarse mix of gravel, or large boulders. However, in the microscale models, they are not.

- The USACE microscale models use pervious, steel mesh structures (Gaines and Maynord, 2001). The St Louis District of USACE tested a number of different materials using flume experiments and model studies. The pervious, steel mesh structures were found to produce the most realistic effect of flow and sediment dynamics. This was confirmed by comparing localized scour and depositional trends between models and prototype.
- Alternatively, the Davies et al. (2003a; 2013) models had sand roughened galvanized steel strips to represent the stopbanks.

3.2.2 Experimental procedure

After initial construction, both sets of microscale modelling followed a general procedure to calibrate and prepare the models for experimentation. This procedure involved the running of the model with water and sediment inputs until the respective river (Gaines and Maynord, 2001) or fan system (Davies et al., 2003a, 2013) had achieved a state of equilibrium. Equilibrium or rather dynamic equilibrium as termed by Davies and Korup (2007) refers to the bed slope. It is assumed that under specified channel alignment or boundaries, sediment size and supply rate, flow, and enough time, the bed slope will reach an equilibrium state. In this state the average sediment input is equal to the average sediment output, and as a result there is no change in average sediment storage (Gaines and Maynord, 2001; Davies and Korup, 2007).

- For the USACE models initial water discharge was one half to two thirds of the channel bankfull depth. This higher discharge was designed so as to form the bed configuration with respect to the channel alignment and instream structures, as well as flume tilt, amount of sediment in the model and the tailgate elevation (Gaines and Maynord, 2001). A low water reference plane was also used in which the surface elevations of the micromodel corresponded to the water surface profile that is exceeded 97% of the time in the prototype (Gaines and Maynord, 2001).

- This procedure differed slightly for the Davies et al. (2003a; 2013), Davies and Korup (2007), and Wild (2012) models. In these models arbitrary values were initially used to develop a moderately sloped fan. After this, the values were gradually altered by trial and error to give a surface slope of about 7% (Davies et al., 2003a) and to provide kinematic similarity to the prototype, meaning that the channel patterns and behaviour occurring in the model were similar to that of the prototype (Wild, 2012).

  As the sediment was not recirculated in these models, supply rate was also adjusted with the flow rate.

Once the models were considered to be in "equilibrium", experiments could begin.

- For the USACE and Davies et al. (2003a; 2013) models this meant that different control work structures could be introduced and the results monitored.

- The Davies and Korup (2007) experiments involved testing the effect of large inputs of sediment on different alluvial fan systems which had formed via two types of steady input regimes.

3.2.3 Measurement tools

A large component of analysis for microscale modelling is done via qualitative measures.

- Analysis of channel response in the USACE models involved a qualitative comparison between model and prototype bathymetry, with a focus on localized scour and depositional trends (Gaines and Maynord, 2001).

- Qualitative measurements in the New Zealand set were made via direct observation of processes at play in the microscale models, as well as through time lapse photography (Campbell, 2012).

  Campbell (2012) used a Nikon D40 digital SLR camera (6 MP) for the long image sequences, capturing images every 30 seconds for analysis; whilst Wild (2012) used two 2-megapixel webcams with autofocus (Logitech QuickCam Pro 9000).

The New Zealand microscale modelling also placed substantial focus on quantitative measurements. In this case, values were arbitrary and not extrapolated to the prototypes.

- In the Davies et al. (2003a; 2013) models, bed surface elevation was recorded using a point gauge system. In the 2003 experiments, digital Vernier callipers collected the point measurements at 50 mm intervals, across 14 cross sections. The Bosch GLM150 laser range finder was used for the 2013 experiments.

  The laser range finder was attached to a sliding rail system on which it moved at 5 cm increments in both the longitudinal and transverse directions (Campbell, 2012), therefore generating a greater density of points compared to the 2003 mode.

  Each point measurement was imported into GIS, where subtraction between new and old measurements provided arbitrary values which represented the rate of change (Campbell, 2012).

- Both the laser range finder and the callipers were also used to measure knickpoint recession, fluvial incision, channel widening and other channel adjustments (Campbell, 2012).

- Davies and Korup (2007) generated longitudinal profiles using a hand-held laser scanner, which produced Digital Elevation Models of the fan surface at a vertical resolution of 1-2mm. This produced a spatial density far greater than the point system utilized by Davies et al. (2003a; 2013).
- Wild (2012) also used a laser scanner. Her instantaneous-profile scanner (Darboux and Huang, 2003) was mounted on a rail system. At various stages during the experiment it would take measurements at different cross sections of the model surface. These allowed for the surface profile of the delta and river system, and volume of accumulated sediment, to be quantified.

3.3 The Waiho microscale model

3.3.1 Model construction

The Waiho microscale model for this study was constructed in the Engineering Soil and Water Laboratory at Lincoln University, Canterbury, New Zealand, a purpose built facility containing a number of flumes as well as a sand tray (Figure 3.3). The sand tray had previously been used for similar modelling investigations on the Waiho River and fan system (Davies et al., 2003a, 2013), and was therefore considered suitable for this study.

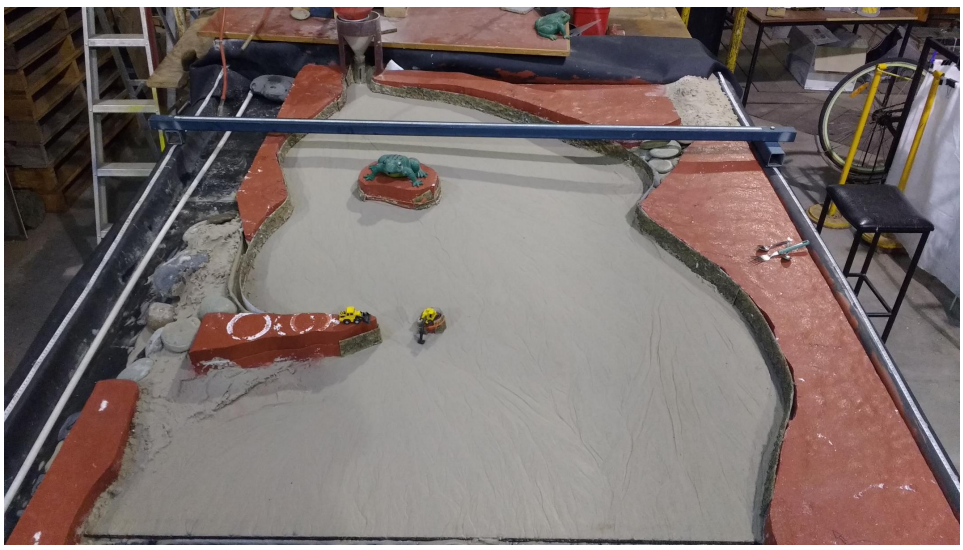

Figure 3.3: labelled microscale model used for this study; components include the butynol layer, bed sediment, geometric insert, sediment feeder, water feeder, header and footer tanks

Construction of the Waiho microscale model was based on the New Zealand set of microscale models discussed earlier in this chapter, and therefore consists of four main components: the hydraulic flume, geometric inserts, supply of sediment and water, and stopbanks (Figure 3.4).

- The **hydraulic flume** is the 2 by 3 m sand tray; a flat wooden structure with an adjustable slope, covered by a waterproof butynol layer.

- **Geometric inserts** were built out of 100 mm thick painted polystyrene. Google Earth imagery and a scaled 1:50,000 Land Information New Zealand topographical map were used for the boundary dimensions and shapes. For ease of scaling and to ensure all key boundaries and landforms were included, a 6 km by 6 km area was chosen, creating a 1:3000 scale model.

  Corresponding to the previous studies by Davies et al. (2003a; 2013), the free overfall was positioned at the scaled location where Davies et al. (2003a) reasoned there to have been fairly constant elevation over the last few decades as there is significant evidence of very little aggradation. By shifting the base level inland, the length of the fan was reduced. This meant that the length of experimental time would also be reduced, as there would be less change of sediment volume for given change in circumstances.

- The **supply of sediment and water** was delivered to the top (upstream) end of the model via a funnel connected to two adjustable feeders.

  An elevated constant head tank fed water through a rubber tube to the funnel, where it mixed with the sediment entering from the Tinker sediment feeder. The header tank was connected to a tray at the bottom of the model which collected the exiting water. This was then pumped back up to the header tank creating a looped system.

  The **sediment (silica sand)** was collected and removed from a separate catcher to the one in the water circuit at the bottom of the sand tray, and was not reused. Instead new sediment, sifted through a 500 micron sieve, was supplied when needed into the feeder up top.

- Unlike the Davies et al. (2003a; 2013) experiments, strips of moulded fibre glass were used for the **stopbanks**. Coarse sediment was glued to the strips to create a rough surface. Two stopbank alignments were used in the experiments: the current confinement (Figure 3.5) and the intermediate option (Figure 3.5). The extreme stopbank option was simply the fan in its natural unconfined state.

To allow the alluvial fan to evolve naturally, sediment and water only entered the model area via the funnel system. This meant that the fan was formed by aggradation as it would have done in the prototype. Initial sediment supply and flow rates were taken from previous experiments

by Davies et al. (2003a; 2013). Experimentation only began once the entire accommodation space had been filled with waterborne (and deposited) sediment.

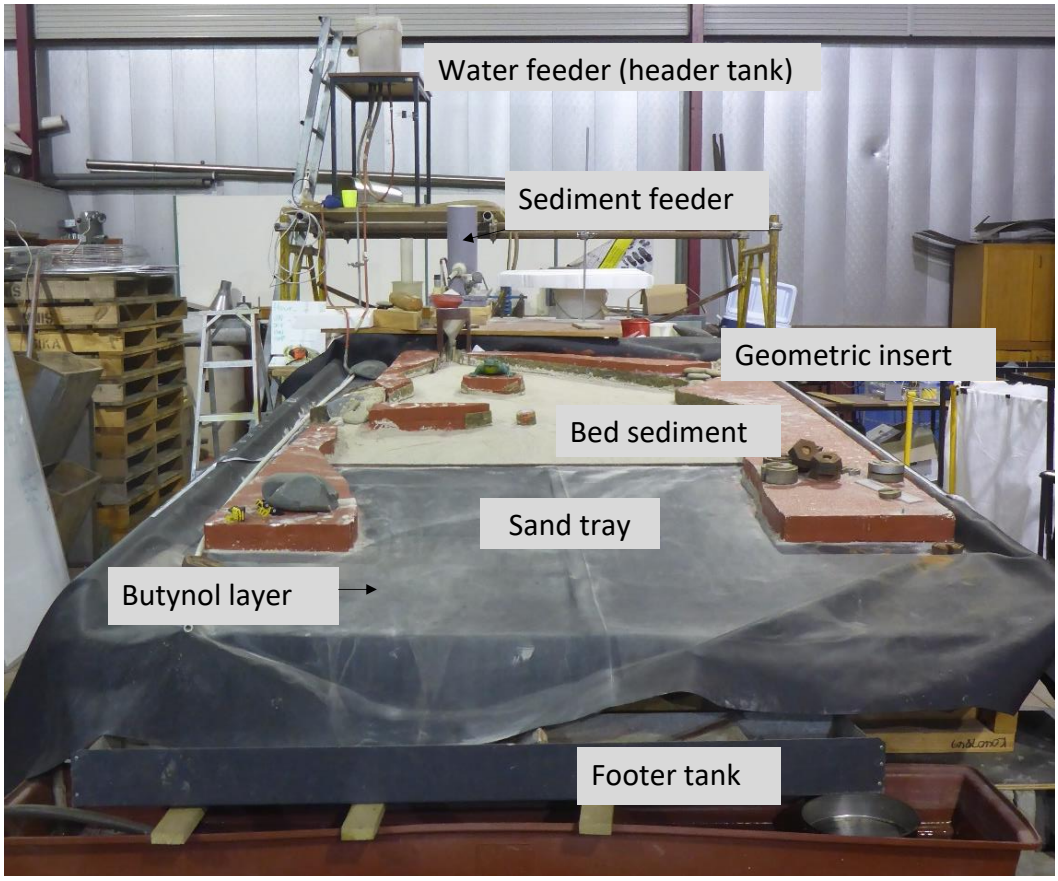

Figure 3.4: Labelled microscale model used for this study; components include the butynol layer, bed sediment, geometric insert, sediment feeder, water feeder, header and footer tanks

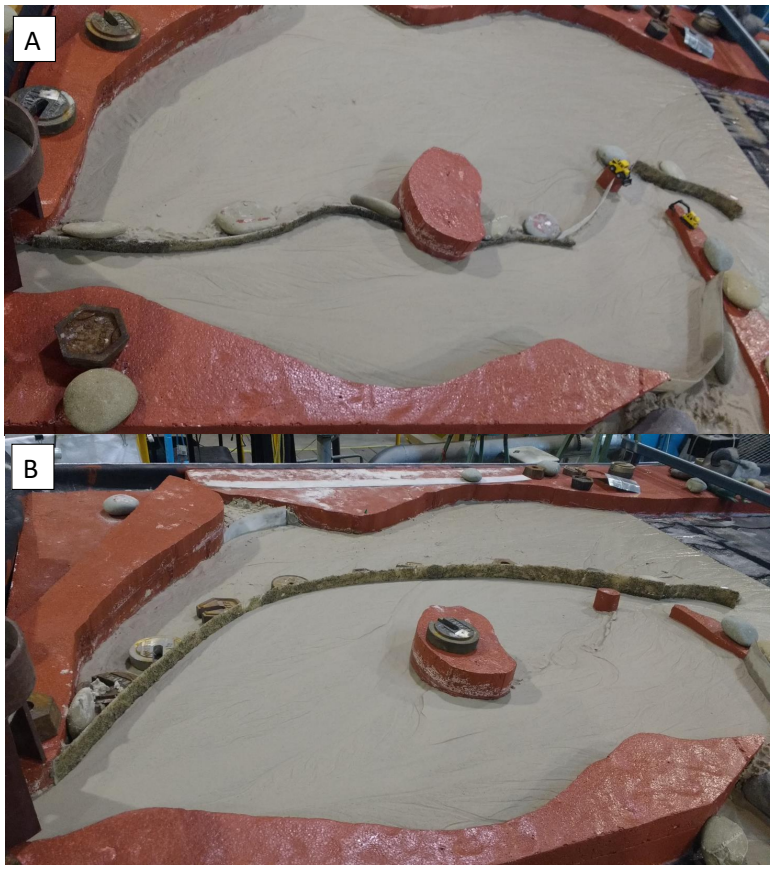

Figure 3.5: The two stopbank alignments used in the experiments. A) is the current stopbank alignment, whislt B) is the intermediate option. No stopbanks were used for the extreme option as it is simply the fan in its natural state

3.3.2 Experimental procedure

In total, eight experiments were conducted using the Waiho microscale model. These were based around four different types of conditions that varied about the type of input, and the surface state of the fan when the stopbanks were installed (Table 3.1). Steady input refers to a constant feed of sediment and water for the entirety of the experiment, whilst the variable input involved having alternating 15 minute intervals of base and flood water flows. A state of aggradation was identified when it was visually (and

quantitatively) obvious that the fan was growing in steepness and height. By comparison, in a state of dynamic equilibrium, change was little to none. Using the DEMs generated from the laser scanned point cloud, dynamic equilibrium was considered to have been achieved when:

- the bed surface elevation had a net change with an absolute value less than 1 mm
- the minimum and maximum (degradation and aggradation) values of change were equal
- the histogram of net change showed a bell shaped curve centred at 0
- the maximum elevation of the area scanned was no longer increasing

In addition, sediment output was measured during one experiment to ascertain the surface state of the fan. Dynamic equilibrium was identified when the sediment output was within +/- 1 g min^{-1} of the input. This corresponded well to the data collected using the laser scanner, and so further use of sediment output data was considered unnecessary.

Table 3.1: Brief summary of the 8 sets of experiments conducted

Number	**Input**	**Surface state**
S1	Steady	Dynamic equilibrium
S2	Steady	Dynamic equilibrium
S3	Steady	Dynamic equilibrium
S4	Steady	Aggrading
V1a	Small variability	Dynamic equilibrium
V1b	Small variability	Aggrading
V2a	Large variability	Dynamic equilibrium
V2b	Large variability	Aggrading

The experiments were designed to replicate the prototype timeline of events. Therefore no stopbanks were in place for the initial hours of all experiments. This was to replicate the natural state. The stopbanks were then installed when the fan surface reached a certain state, either dynamic equilibrium or aggrading, replicating the anthropic interference with the system. Each experiment therefore consisted of a number of stages. However, not all stages were tested in each experiment.

- Natural
- Current stopbank alignment
- Intermediate option
- Natural/extreme option

The experiments also differed based on water flow and sediment supply rates. Initial experiments were found to have input rates too large for the model. Subsequently these were gradually dropped down to be similar to those of Davies et al. (2003a; 2013).

Run durations varied between the experiments, and depended on the models response to the rate and type of input as well as to the stopbanks. The aggrading fan scenarios all fell under the 15 hour mark, whilst the equilibrium fan scenarios extended up to 139 hours.

3.3.3 Data collection and analysis

Bed surface elevation

Bed elevation data were extracted from the sand tray via two different methods.

- Digital Vernier Callipers (DVC) were used for the first set of experiments (Figure 3.6)
- The Aranz Medical Laser (AML) scanner was used for the remaining seven experiments

The DVC measured cross sectional lines of points over the entire fan surface. The cross sections were chosen so that each of the upper, middle and lower sections of the fan were represented (Figure 3.7), whilst the points

measured were evenly spaced out across each cross section. Earlier point values were subtracted from the latest measurement to provide arbitrary rates of change (Table 3.2).

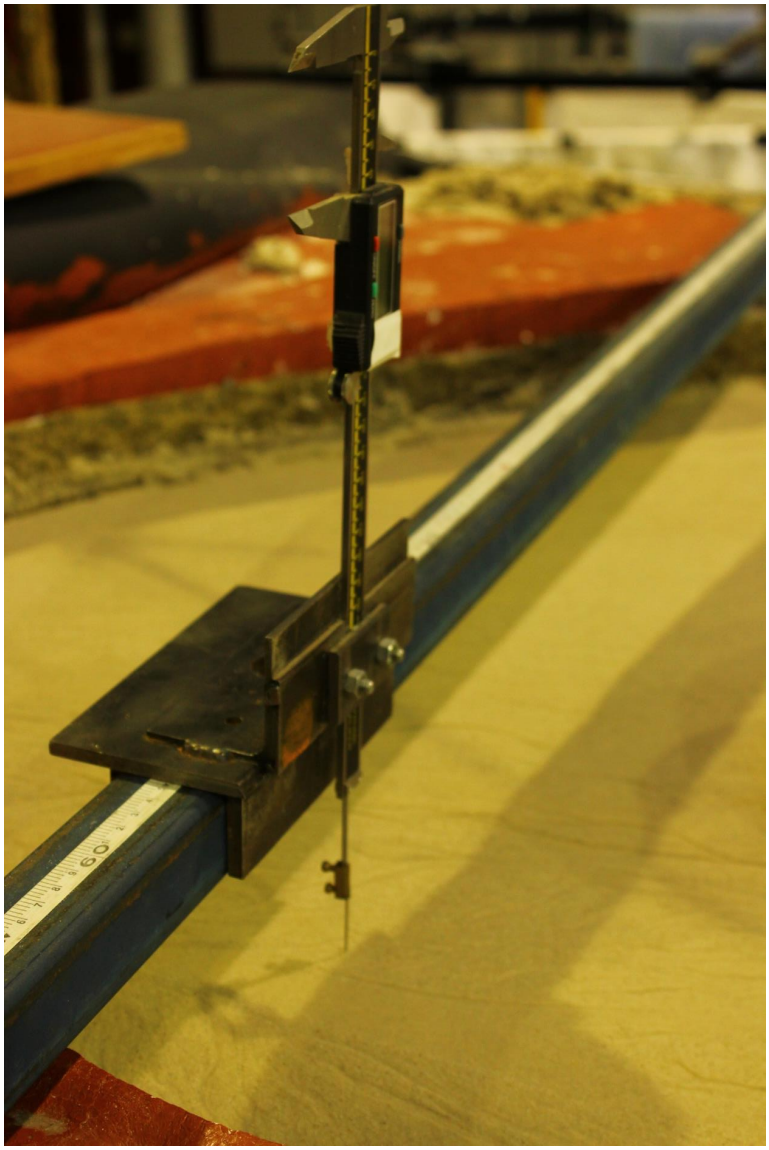

Figure 3.6: Digital Vernier Callipers in action

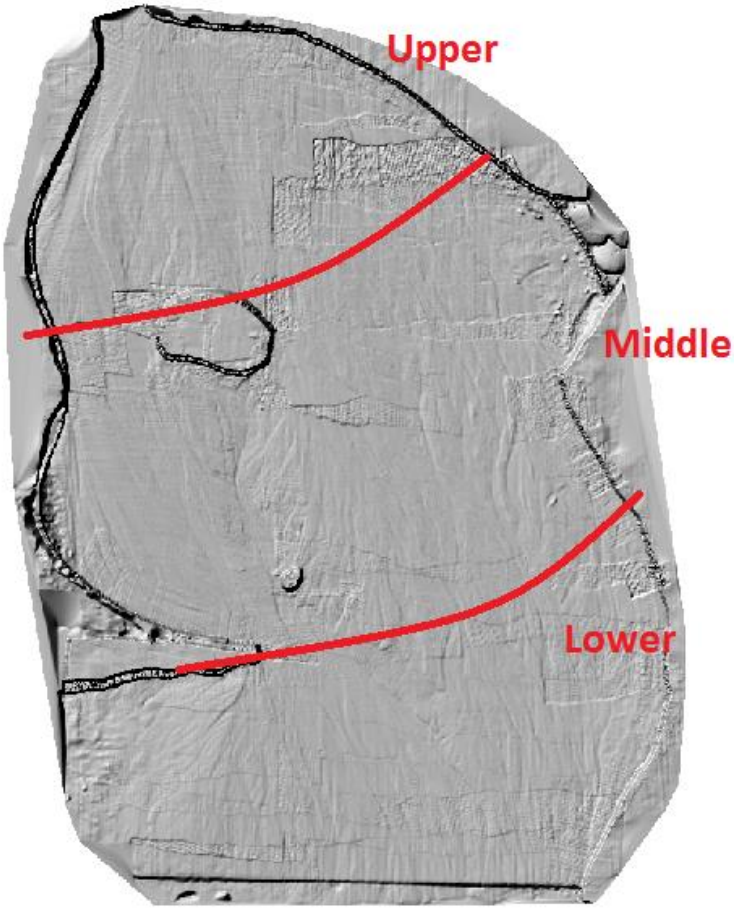

Figure 3.7: The upper, middle and lower sections of the model fan

Table 3.2: Table of bed surface elevation points and calculated rates of change for the S1 experiment. Pink = aggrading, green = degrading, blue = no change. EC = elevation change

Nrth	East	945 - 1015am	1215 - 1230pm	EC (2hrs)	130pm - 350pm	EC (1hr)	450 - 5pm	EC (1hr)
30	20	35.49	35.46	0.03	31.78	3.68	30.16	1.62
30	40	26.33	23	3.33	20.64	2.36	21.4	-0.76
30	60	17.45	12.62	4.83	13.85	-1.23	12.06	1.79
45	20	35.31	33.35	1.96	31.4	1.95	32.07	-0.67
45	40	29.32	25.05	4.27	23.97	1.08	24.1	-0.13
45	60	22.01	17.47	4.54	17.5	-0.03	16.11	1.39
60	20	38.56	35.58	2.98	34.44	1.14	39.33	-4.89
60	40	31.04	28.49	2.55	24.86	3.63	25.72	-0.86
60	60	25	21.22	3.78	20.55	0.67	20.54	0.01
105	90	51.32	49.57	1.75	49.37	0.2	48.94	0.43
105	120	43.59	40.34	3.25	39.99	0.35	40.01	-0.02
105	150	34.1	32.36	1.74	31.61	0.75	29.93	1.68
165	65	51.79	51.86	-0.07	51.66	0.2	51.38	0.28
165	90	54.12	52.98	1.14	52.97	0.01	53.9	-0.93
165	115	47.02	46.41	0.61	45.32	1.09	46.33	-1.01

The AML scanner was used to create point clouds for Digital Elevation Models (DEMs) before, during and after each experiment. DEMs of Difference (DoDs) could then be generated to show how the model was changing over time.

The Aranz Medical Laser scanner consists of a receiver, transmitter and handheld laser scanner. The receiver was placed below the sand tray and levelled. It communicated with the moveable transmitter on top of the model to increase the range of the laser scanner, and allow the full extent of the model to be measured. The handheld laser scanner was then waved methodically and slowly over the surface of the model to collect the elevation data into a point cloud, assigning x, y, and z values to each point of elevation (Figure 3.8). The elevation data were then exported from the Fastscan software to ArcGIS programs.

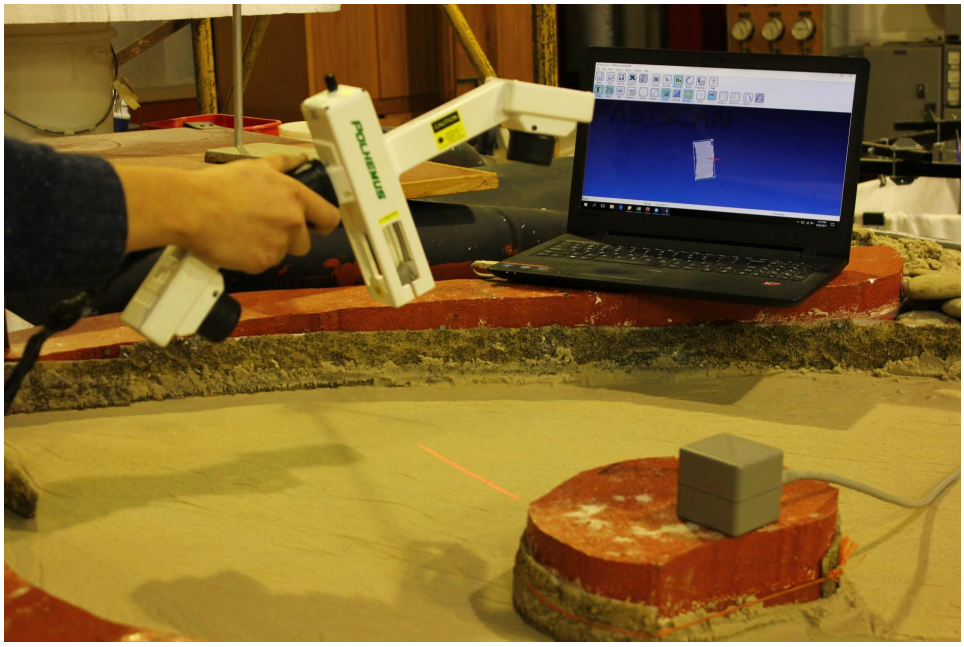

Figure 3.8: Aranz Medical Laser scanner in action

In ArcMap, to create the DEM, each set of elevation data was interpolated using natural neighbour to an output cell size of 2.5 cm (2.5 by 2.5). Other interpolation tools were tested, with no major differences. The hillshade tool was then applied to the DEM (Figure 3.9) as it simulates the

fall of shadows on terrain, and therefore allows the surface topography to be seen more clearly. The DEM was then imported into ArcScene and converted into a 3D map to allow for a thorough examination of the surface for any glitches.

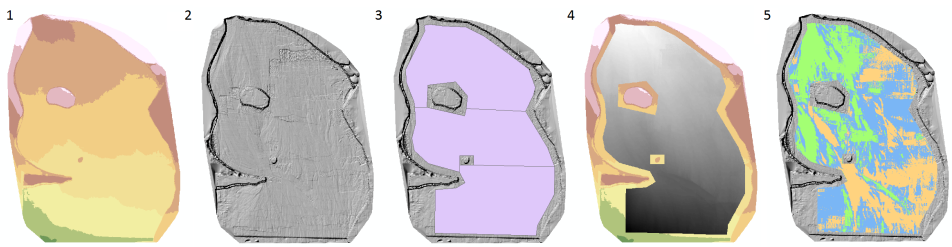

Figure 3.9: The five stages involved in generating the DEM and DEM of Difference in ArcGis. 1) Interpolated DEM using natural neighbour. 2) DEM with hillshade applied 3) the purple cookie cutter shapefile, used to extract the area of information required 4) the cut out area 5) the DEM of difference created by subtracting two cut out areas (4)

DEMs of Difference (DoDs) were created by subtracting the newer DEM from the older, this involved several steps (Figure 3.9). First, a 'cookie cutter' was made. This consisted of a shapefile that covered the area of interest and excluded the boundaries. For each experiment natural, current stopbank alignment, and the intermediate and extreme options, a different 'cookie cutter' were created. The 'clip (data management)' tool used the shapefiles to cut out the same area and elevation data from each DEM. The DEM cutouts could then be subtracted from each other using the 'raster calculator' tool to show where the model had changed. The range of values and their symbology were manually classified into three groups, aggrading (>1), degrading (<-1) and unchanged (-1< X < 1) to provide a clear picture of the change. The range for the unchanged category was chosen corresponding to the error of the scanner (±1mm).

Sediment output

Sediment output rate from the base of the free overfall was compared to input rate delivered via the sediment feeder to provide insight into the equilibrium state of the model. The output was measured at the start of each hour of run time for a period of five minutes before being dried and weighed.

At the end of an hour, the sediment and water feeders were turned off and the lower section of the sand tray (below the overfall) cleared of sediment. A 1 m-long tray with a 75 micron sieve sheet across the back to allow water through was then placed squarely against the base of the overfall and held down with weights. The sediment and water feeders were turned on again, and the five-minute period began when the flow of water entered the tray.

After five minutes the tray was removed and the sediment washed through a coarse gridded sieve, into a 75 micron one. It was then dried before being weighed. The bulk weight measurement was converted to grams per minute, and compared to the rate at which sediment is entered via the feeder at the top of the model.

Qualitative time sequencing

Photography was used to provide a qualitative measurement of change in the model. For each experiment, different angles were chosen to provide the optimal viewpoint for key areas of change. In the initial hour, photos were taken every ten minutes. After this, change was considered to occur less rapidly, and photos were taken on the hour. When the photos of the same angle were arranged and viewed in order, it provided an accurate visual record of change over time (Figure 3.10).

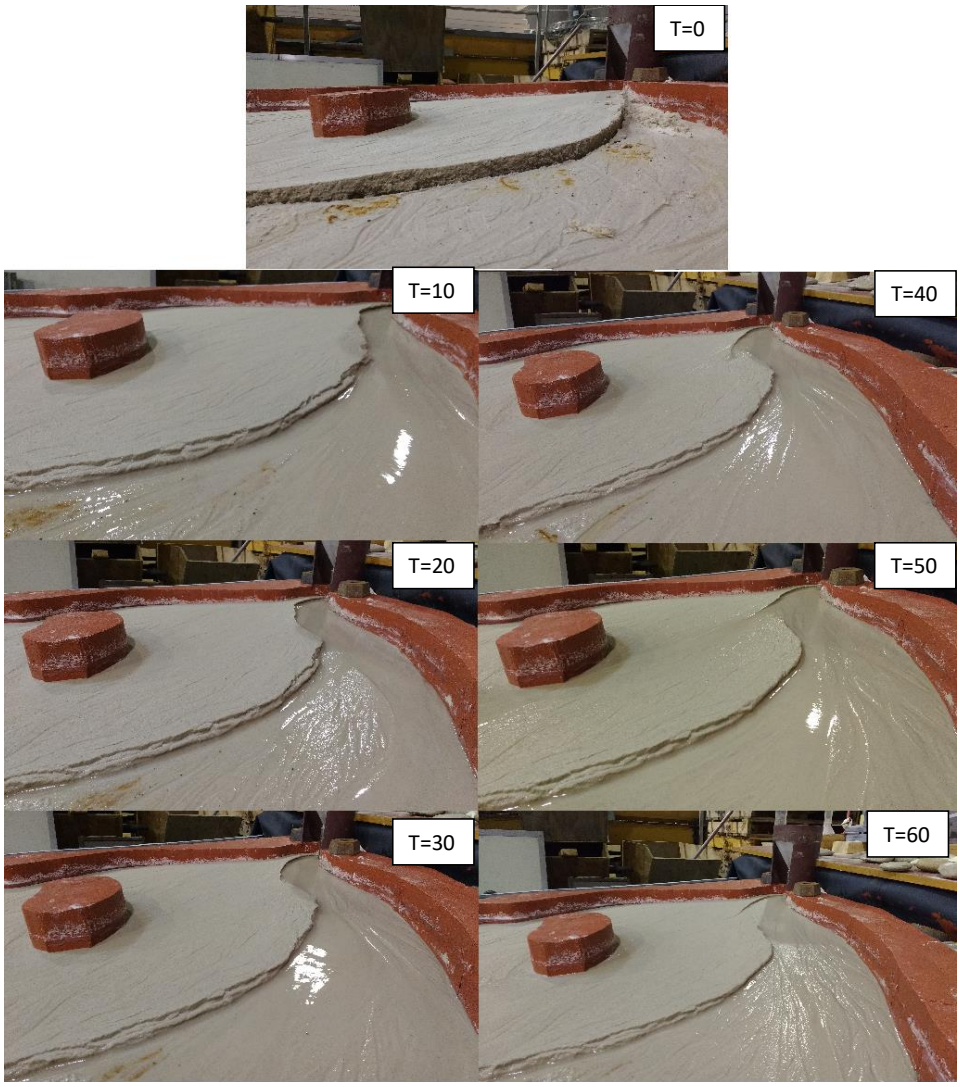

Figure 3.10: Time lapse of change after the intermediate stopbank has been removed. Images are spaced 10 minutes apart

Chapter 4

Data analysis: steady input experiments

4.1 Introduction

This chapter reviews the results from the four steady input experiments conducted on the Waiho River and fan microscale model. These experiments were based on the methodology of the previous Waiho River and fan microscale model experiments (Davies et al., 2003a, 2013). In the Davies et al. (2003a; 2013) experiments, steady inputs of water and sediment were used to build microscale model fans to states of dynamic equilibrium. Installation of the current stopbank alignment then resulted in similar aggradational behaviour to that of the prototype (Davies et al., 2003a). Ongoing confinement and therefore aggradation, induced an avulsion of the experimental Waiho River into the Tatare River (Davies et al., 2013).

In the present study, the steady input experiments were initially designed to take the previous work a step further, so as to investigate how the microscale model river and fan would respond to the removal of the current stopbank alignment, and installation of two alternative alignments. However, as the experiment sequence progressed, focus gradually switched to an investigation of the microscale modelling techniques. This was to address inconsistencies that were occurring with data collection and the effect of boundary surface roughness on fan behaviour; but above all to understand the difference between the present experimental results and those of Davies et al. (2003a).

4.2 Results

The following steady input experiments differ based on the surface state of the fan when the stopbanks were installed, water and sediment input rates, scenarios tested and measurement tools used (Table 4.1).

Table 4.1: Summary of the four steady input experiments, including; surface state when stopbanks were installed, input conditions (sediment and water); scenarios tested (Nat = natural, CC = current confinement, Int = intermediate stopbank option, Nat2 = released from confinement (also the extreme stopbank option); measurement tools and outcomes.

Number	Surface state	Input conditions		Scenarios	Measurement tool/s	Outcome
		Sediment (g/min)	Water (ml/s)			
S1	Equilibrium	36	18	Nat, CC, Int, Nat2	Callipers Time lapse photography	Fan aggraded when confined, and then continued to aggrade when released.
S2	Equilibrium	25	20	Nat, CC, Nat2	Laser scanner Sediment output Time lapse photography	No aggradation when confined.
S3	Equilibrium	16	8	Nat, CC	Laser scanner	No aggradation when confined.
S4	Aggrading	20	8	Nat, CC, Nat2	Laser scanner	Fan continued to aggrade when confined, and then when released.

4.2.1 S1: equilibrium fan

Experiment S1 was the first experiment to be run following the development to equilibrium of the fan on the sand tray. It was designed to address the primary aim of this thesis, which was investigating the response of the fan to removal of the current stopbank alignment and installation of less restrictive alternatives. Based on the previous studies (Davies et al., 2003a, 2013) it was believed that after achieving a state of dynamic equilibrium, the installation of the current stopbank alignment would result in aggradation, followed by degradation upon removal.

In this experiment, the fan bed surface elevation was measured at a number of points using the digital Vernier Callipers. Observed equilibrium was based on the amount of change that occurred in these points over time. When a majority of the points showed no change (absolute values less than 1 mm) the fan was considered to be in a state of dynamic equilibrium (Appendix B). Once this had been established, the current stopbank alignment was installed and monitored, followed by the intermediate alignment option, and finally released back to its natural state, the extreme option (Appendix B).

The experimental fan did not behave in the way it was expected to. When confined by the current stopbank alignment, the fan did aggrade, as it has done in the prototype situation, and in the previous studies (Davies et al., 2003a, 2013). However, it did not degrade to the ‘dynamic equilibrium‘ bed surface elevation when released from this confinement. Instead it infilled the newly available areas of the fan, and once these were level with the bed surface elevation of what had been the confined fan, the whole surface continued to aggrade (Figure 4.1).

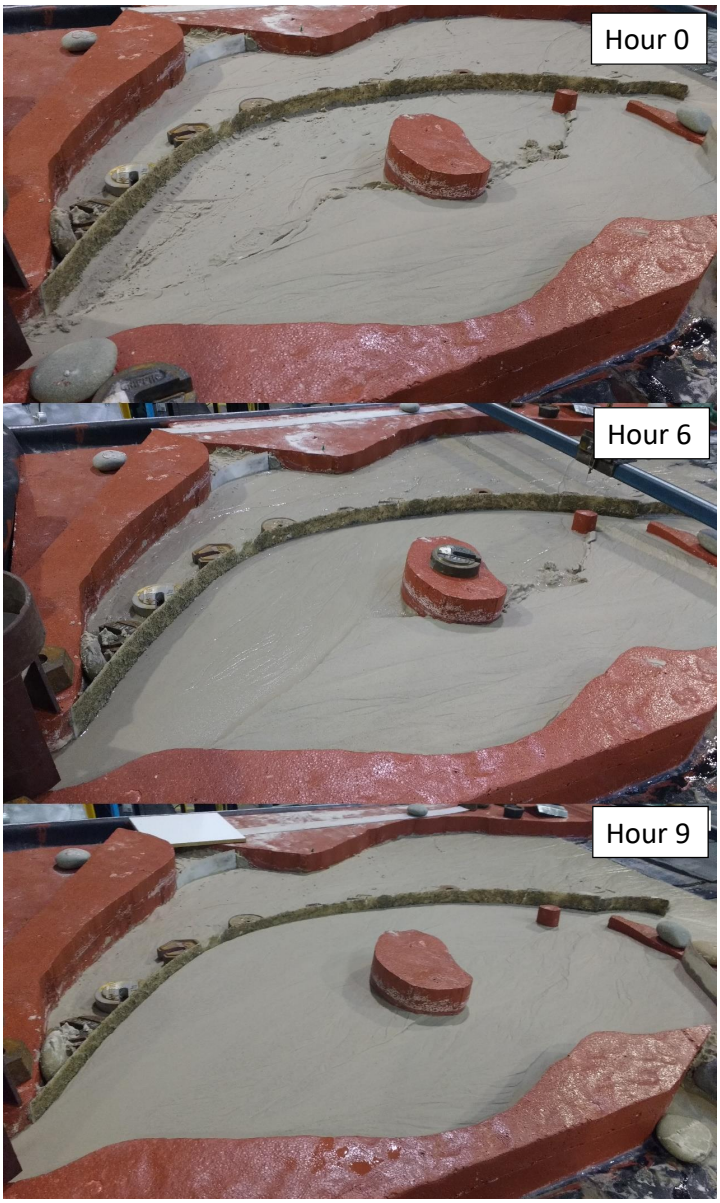

Figure 4.1: Photo time lapse of the fan behaviour when the current stop-bank alignment was removed and the intermediate alternative installed. The three photos show the initial, 6 hour and 9 hour stages. The fan is aggrading.

The aggradation also occurred at different rates depending on the degree of confinement (Figure 4.2). The rate of aggradation was highest during the current confinement at 1.77 cm per hour, and lowest with no confinement (extreme option) at 0.48 cm per hour. The intermediate option had an average aggradation rate of 1.12 cm per hour.

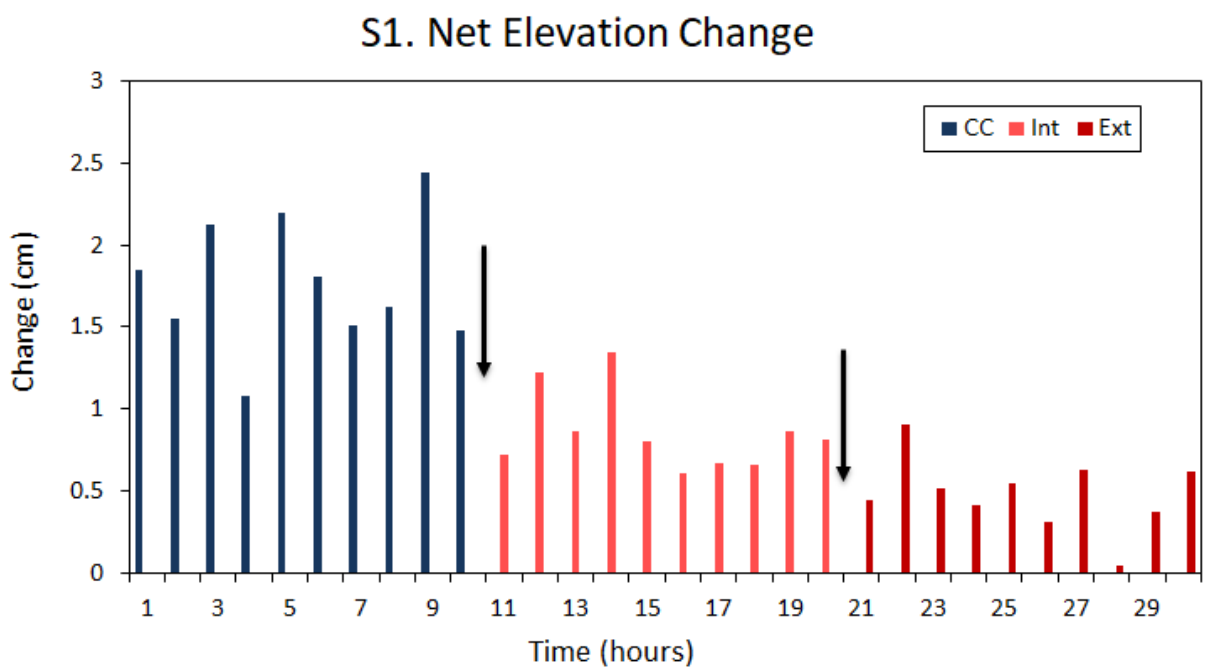

Figure 4.2: plotted net elevation change during the current confinement (CC), intermediate option (int) and natural (extreme option - Ext) scenarios. Change in confinement is indicated by the black arrows. The rate of aggradation decreased as confinement decreased.

The outcome of this experiment did not correspond with what was expected to happen according to geomorphic theory. That is, that there exists one and only one fan surface configuration that uniquely corresponds to planform geometry under specified input rates of water and sediment. Therefore, following surface geometry disturbance the geometry will return to the equilibrium state. The fan did not return to its defined state of dy-

namic equilibrium after the current stopbank alignment was removed. This prompted further experimentation involving the use of the Aranz Medical Laser scanner. The Aranz Medical Laser scanner can be used to generate high density spatial data. Therefore, in these experiments it was able to establish bed surface states with greater accuracy to ensure more reliable results than the widely-spaced data from the vernier Callipers.

In addition, the experimental focus widened to include investigation of how the fan responded to the installation and removal of the current stopbank alignment when it was in an aggrading state. This was to provide a comparison to the steady state dynamic equilibrium experiments.

4.2.2 S2: equilibrium fan

This experiment was designed to repeat the steps of the previous experiment (S1), with some modifications to supply rates, run time, boundary surface roughness and measurement tools. As the river had been unable to braid when confined, both the water flow and sediment supply rates were arbitrarily lowered. In addition, the time allowed for the fan to achieve ‘equilibrium‘ was significantly greater (130 hours, compared to the 40 hours of the S1 experiment).

In addition, during the experiment it was identified that the smooth surface of the lateral boundaries resulted in the flow getting stuck against them and not migrating elsewhere on the fan. This was solved by the installation of coarse-sediment coated strips along the boundaries, after which the flow returned to migrating across the fan surface (Figure 4.3).

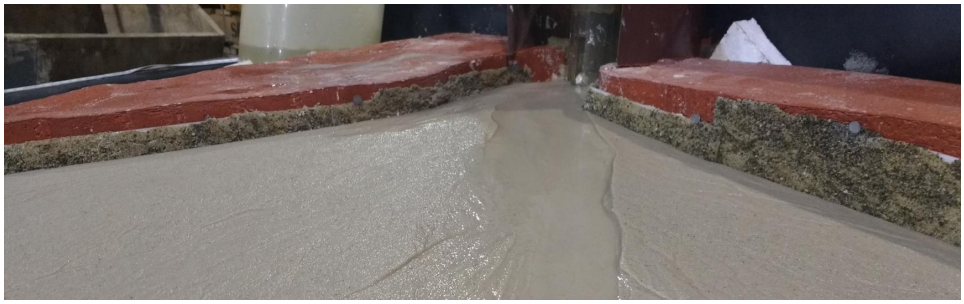

Figure 4.3: Coarse strips of sediment nailed to the boundaries to increase surface roughness

In order to obtain more detail on the behaviour of the model, the Aranz Medical Laser scanner was used to measure bed surface elevation at hourly intervals, and a sediment output collector tray was used to capture the sediment leaving the fan for five minutes every hour. Dynamic equilibrium was considered to have been reached when both sets of data matched up; that is, the scanner showed minimal total surface change and sediment output rate equalled sediment input rate. For the laser scanner, this meant that the Digital Elevation Models (DEMs) of Difference (DoD) showed minimal net change (i.e., absolute values less than 1 mm averaged over the entire surface)(Figure 4.4), whilst for the sediment output tray, the dried and weighed output sediment fell within ± 1 g/min of the input amount (Figure 4.4). Once both measurement tools were indicating equilibrium, the stopbanks were installed, monitored, and then removed.

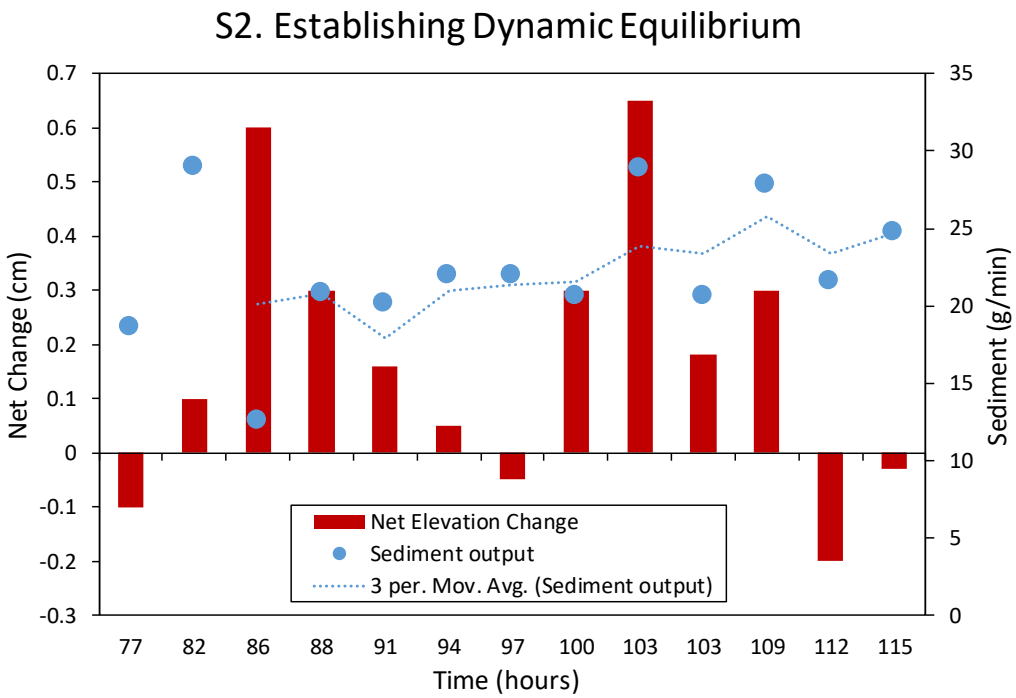

Figure 4.4: The graph shows the final hours before dynamic equilibrium was established in the S2 experiment. The columns show the net change (overall change in elevation) whilst the line shows the sediment output values (input was 25g/min)

In contrast to the previous experiment, in its equilibrium state, the fan did not aggrade when confined. Instead in the first six hours of confinement, net change was negative (degradation), and in the following six hours whilst net change was positive, it was minimal (<1 mm) (Figure 4.5). In addition, during the confined state it was noted that no braiding in the upper reach of the fan occurred, only sheet flow.

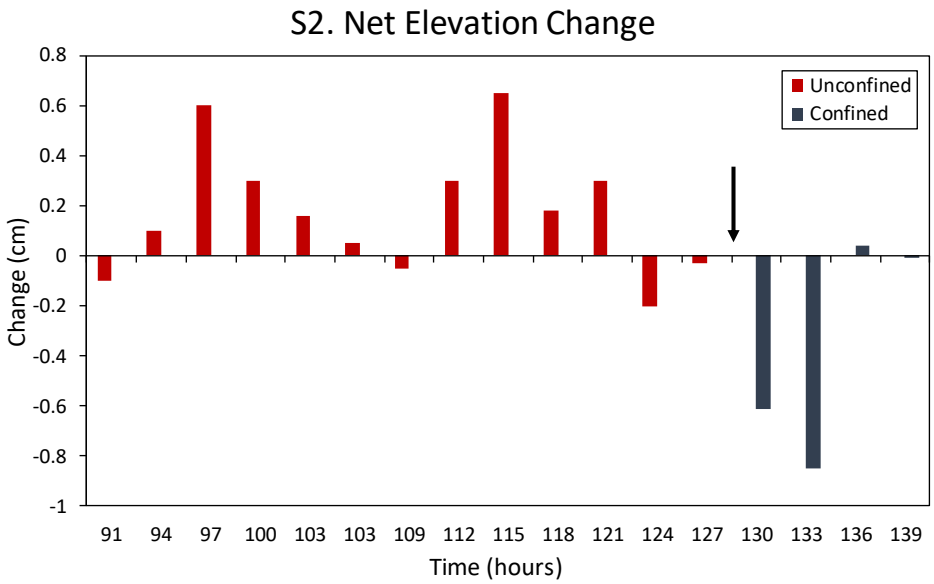

Figure 4.5: Plot of the net change between hours 91 and 139. Hours 91 to 127 were the lead up to the fan being considered to be in a state of dynamic equilibrium, with hours 109 to 118 to be ignored as a batch of finer sediment unfortunately entered the model causing significant incision into the fan apex extending down to the middle of the fan and subsequently extra additions of sediment were added to infill the trench effecting the net change. The installation of the current stopbanks configuration is marked by the black arrow between hours 127 and 130, and then from hours 127 to 139 the net elevation change in the fan corresponding to the installation of the current stopbank alignment is shown.

As the experimental river was unable to braid when it was confined, and the Waiho braids in its confined state, it was thought that the flow to sediment ratio was incorrect. This prompted the need to repeat the S2 experiment with reduced supply rates and a smaller flow to sediment ratio.

4.2.3 S3: equilibrium fan

In the S3 experiment sediment and water supply rates were adjusted to be similar with those of the Davies et al. 2003 and 2013 models (Table 4.2).

Table 4.2: Comparison of water flow and sediment supply rates vs model scale between different studies

	Model scale	Water flow rate	Sediment supply rate
Clarkson, 1999	1:2000	10 ml/s	20 g/min
Campbell, 2012	1:5000	6 ml/s	18 g/min
This study, 2017	1:3000	8 ml/s	16 g/min

The fan was allowed to reach equilibrium and then the stopbanks were installed. The model was then run for eight hours (Figure 4.6) before the stopbanks were removed, and the fan continued as before, in its natural state.

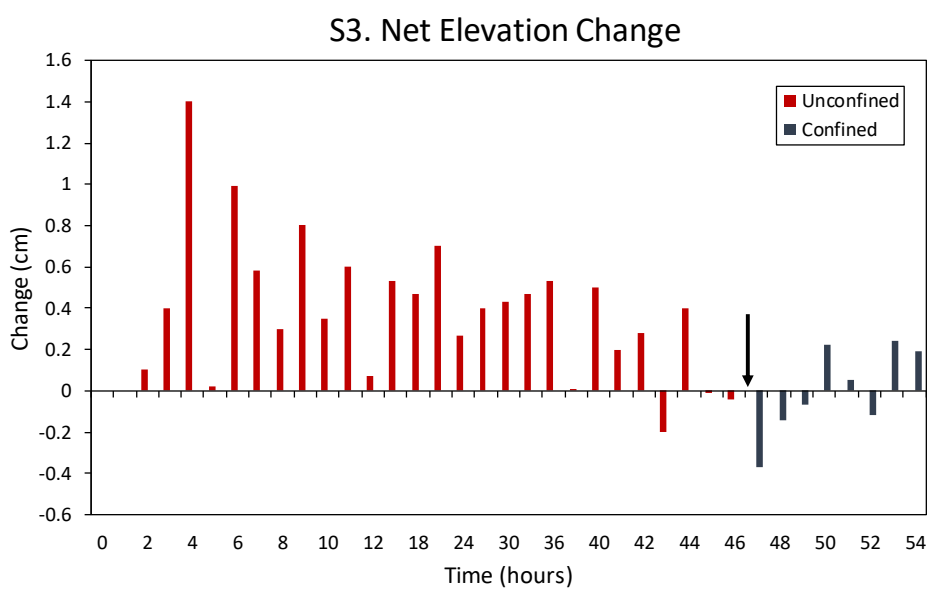

Figure 4.6: Plotted net elevation change values over time. The natural state was monitored for its final 46 hours, at which point it was considered to be in dynamic equilibrium, and the stopbanks were installed confining it (the black arrow indicates this change). The confinement was monitored for eight hours.

In this experiment aggradation did occur when the stopbank was confined. However, this aggradation occurred in the middle reach of the fan,

not in the upper reach (Figure 4.7). The DEM generated from the point cloud data collected by the laser scanner included both the upper and middle reaches of the fan; and because the aggradation was significantly high in the middle reach, the net change over both upper and middle was positive (Figure 4.8). However, when a second DEM was generated, focussing only on the upper reach, it was found that net change was negative, the fan surface was actually degrading in response to the installation of the stopbanks (Figure 4.8).

The behaviour of the confined S3 experimental fan did not correspond to the prototype behaviour or that of previous studies because no aggradation occurred in the upper reach when the fan was confined. This prompted two further sets of experiments. The first one was to test the response of an aggrading fan to confinement. The second involved the use of variable sediment and water inputs, as it was thought that perhaps some degree of variability was required to induce similar behaviour in the model to that of the prototype.

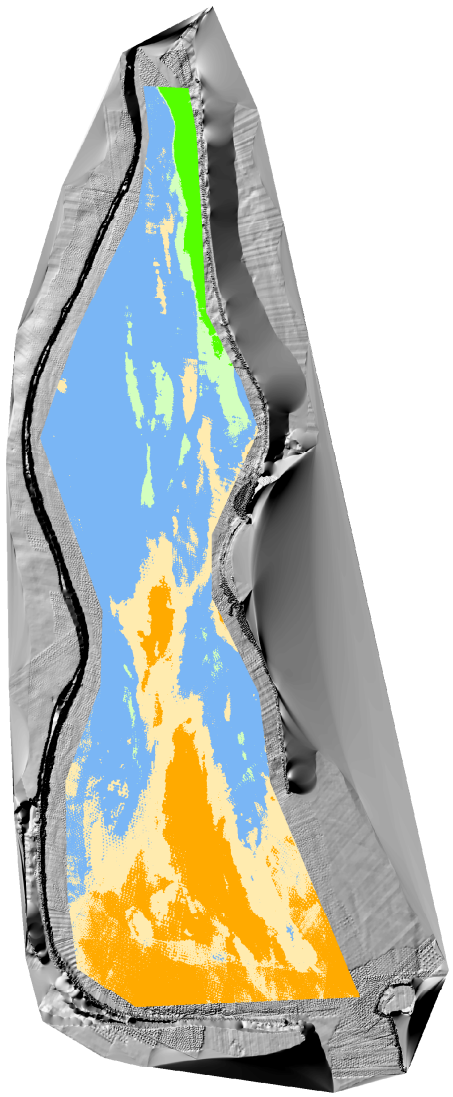

Figure 4.7: DoD image showing aggradation (orange) in the middle reach and degradation (green) in the upper reach (Change between hours 0 and 1)

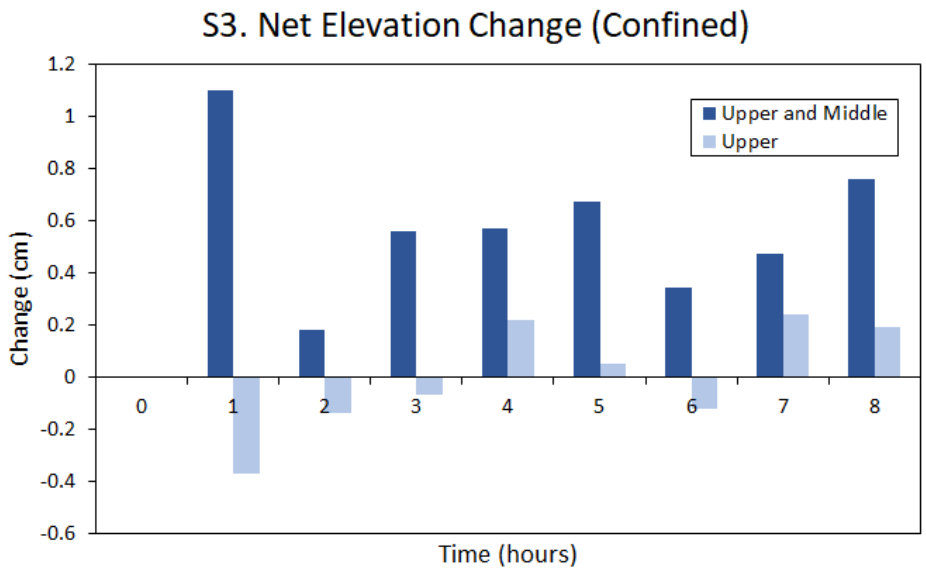

Figure 4.8: Plotted mean net change values over time, upper and middle vs. upper only

4.2.4 S4: aggrading fan

This experiment was designed to investigate the response of an aggrading fan to the current stopbank alignment. The response was then compared to the S1 experiment results, to show that the 'dynamic equilibrium' defined in the initial work of Davies et al. (2013) was unlikely to have been true.

The sediment input was increased to 20 g/min inducing an aggrading fan, the stopbanks were installed and the model was run for 4 hours until substantial (1 cm) aggradation occurred (Figure 4.9). The stopbanks were then removed, and the model run for 6 hours in its natural state.

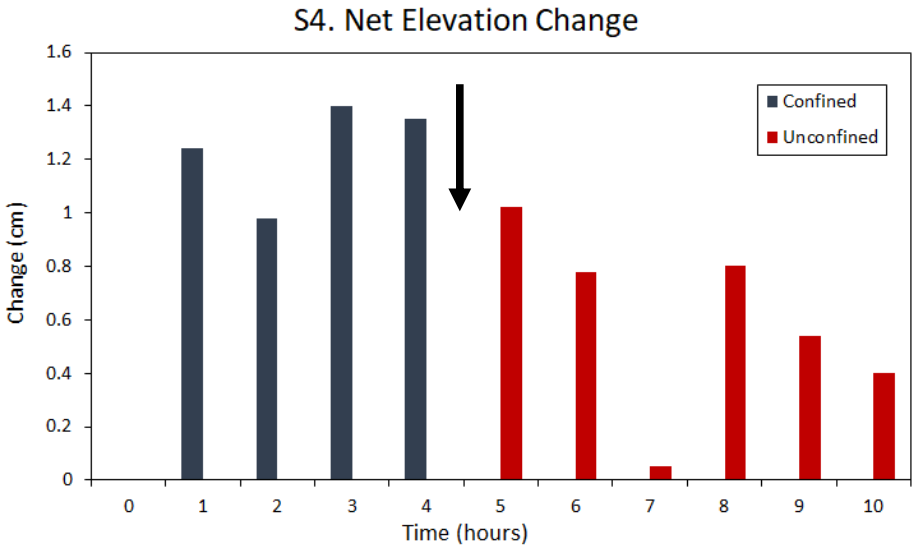

Figure 4.9: Plot of net elevation change for the four hours of confinement, and following (indicated by black arrow) 6 hours of unconfinement.

In both the confined, and the following unconfined states the fan aggraded (Figure 4.10a and 4.10b). This aggradation occurred in the upper reaches, similar to that of the prototype.

The continued aggradation in both the confined and released states of the fan, whilst at greater rates, is similar to the behaviour of the fan to confinement and release in the initial experiment (S1), in which the fan experienced aggradation after the removal of the stopbanks (Figure 4.2).

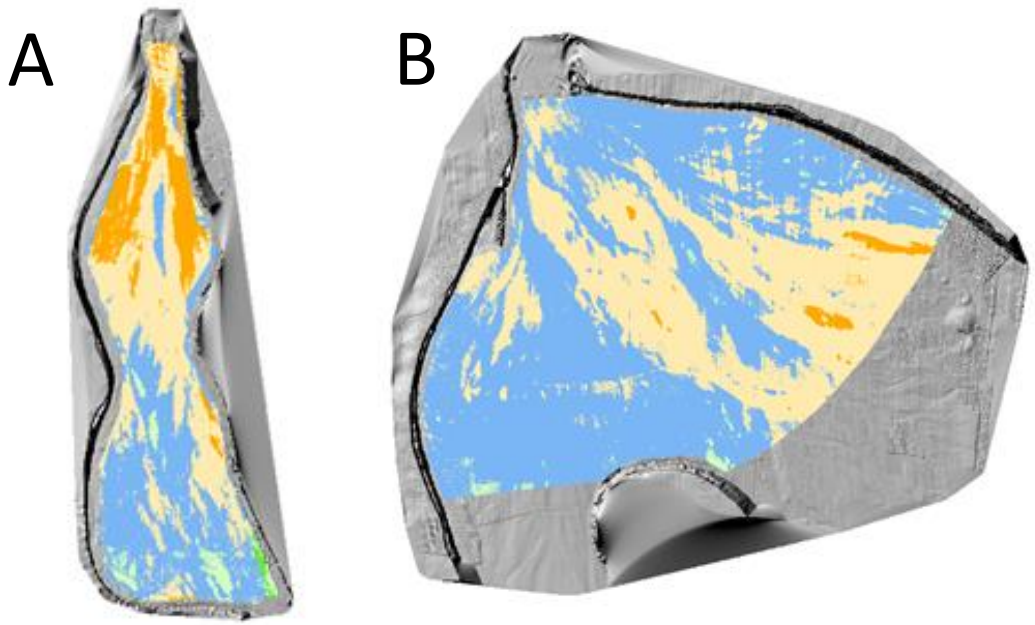

Figure 4.10: Aggradation in both the (a) confined, and then (b) unconfined (after the stopbanks had been removed) fan. Orange = aggradation, blue = no change, green = degradation

4.3 Discussion

4.3.1 Importance of spatially dense data

A comparison between the results of the four steady input experiments in this study indicated that a greater depth of detail is required to accurately measure change and establish surface states in microscale fan systems. In the initial studies of the Waiho River and fan system, Digital Vernier Callipers, time lapse photography and Structure from Motion (SfM) techniques were used to measure change in the bed surface elevation, and subsequently establish dynamic equilibrium in the experimental fans (Campbell, 2012; Clarkson, 1999). In those dynamic equilibrium experiments, the fan aggraded when confined. However in the present study, in experiments where dynamic equilibrium was established using the Aranz Medical Laser scanner which provides high density spatial data, aggradation did not occur when the fan was confined. It was only in the test where the occurrence of dynamic equilibrium fan was established using Digital Vernier Callipers that aggradation occurred. This suggests that the dynamic equilibrium surface states achieved in this and earlier studies may have been false.

In this study, Digital Vernier Callipers were only used to measure change and establish dynamic equilibrium for the first experimental fan (S1). Upon reaching the defined dynamic equilibrium, the S1 fan aggraded when confined and then continued to aggrade when released from its confinement. According to geomorphic theory in regards to the concept of dynamic equilibrium and the effects of perturbations, the fan should have degraded when released from confinement. The fan should have degraded to its surface state prior to the confinement, if it really had been in state of dynamic equilibrium.

Dynamic equilibrium refers to the oscillation about a system state or stable equilibria (Knighton, 1998). This oscillation occurs because of self-regulation, and relies on the mean values of the governing variables remaining relatively constant (Knighton, 1998). Self-regulation is characteristic of negative feedback mechanisms. These mechanisms moderate the effect of perturbations, allowing the approximate return of the previous state provided the perturbation is damped down (Knighton, 1998). They can also tend to overcompensate which causes an ongoing adjustment process, characterised by oscillations. In the case of the S1 experiment, the perturbation was the stopbank which confines the river and fan, and the governing vari-

ables were the geometric inserts and sediment and water inputs, all of which were kept constant. If the S1 experimental fan was operating about a dynamic equilibrium prior to confinement, once the perturbation (stopbank) was removed, according to geomorphic theory, it should have been able to degrade back down to the dynamic equilibrium it had achieved earlier under the given sediment and water inputs, constant fan toe location, and confined space. However, it did not.

The next two experiments, which were repeats of the S1 experiment but with slight changes, behaved differently. They did not aggrade when confined, behaviour continued as it had been prior to confinement in its dynamic equilibrium state. In these experiments, dynamic equilibrium was established using a high spatial density point cloud system achieved by the Aranz Medical Laser Scanner and GIS.

As a comparison to the dynamic equilibrium fan scenarios, a fourth experiment was conducted on an aggrading fan. It also used the laser scanner and GIS. In this experiment the fan behaved in the same way as the initial S1 experimental fan. Aggradation increased once confined, and continued once the confinement was released (albeit at a reduced rate).

The similarity in fan response to stopbank installation and removal between the S1 and S4 experiments, and the difference when compared to the S2 and S3 experiments, suggests that *the first experimental fan had not achieved dynamic equilibrium when the stopbanks were installed.* The digital Vernier Callipers did not provide a spatial density of points high enough to accurately capture change in the fan compared to that of the laser scanner in the other three experiments. This also then suggests that the microscale fans in the studies by Davies et al. (2003a; 2013) had also not reached a state of dynamic equilibrium. In his thesis Campbell (2012) does mention that he is unsure if his micro fan had reached equilibrium when the stopbanks were installed. However, in neither study was the response of the fans to the removal of the stopbanks investigated, and as all three microscale models differ in scale and inputs, this makes comparisons unreliable. Nevertheless, it emphasises an important point for microscale modelling; the importance of collecting spatially dense data to ensure the veracity of the experiment and results.

Microscale models are very small replicas of nature, so change itself is also quite small. Therefore, measuring and monitoring such systems does require a close attention to detail. Based upon the results from this study, and a comparison with the previous two studies on the Waiho system, the digital Vernier Callipers and qualitative methods such as time lapse photography and Structure from Motion techniques cannot collect data at the spatial density required for accurate results. However, tools such as laser scanners which produce high density point cloud systems, can do this, as shown in this study. This is not the first study to have utilized laser scanner technology to generate high density point cloud systems. Both Wild (2012) and Davies and Korup (2007) have utilized laser scanners successfully for studies on the Dart and Rees rivers, and Westland fan systems respectively.

However, further work could be done to investigate how accurate different measuring techniques are for microscale modelling. Of interest would be to run an experiment using a range of measurement techniques including the Callipers, SfM, time lapse photography, and laser scanners to directly compare the behaviour of the fan and the dynamic equilibrium established.

4.3.2 Effect of boundary surface roughness

Observations from the steady input experiments, particularly the S2 experiment, indicate that the surface roughness of the boundary inserts has an effect on model performance. Previously, it was believed that the effects of surface tension and friction coefficients were negligible at the micro scale (Lajeunesse et al., 2010; Peakall and Warburton, 1996; Mètivier and Meunier, 2003; Malverti et al., 2008). However, in this study, the polystyrene geometric boundary inserts adversely affected model river and fan behaviour.

In the S2 experiment it became obvious that the flow was getting ‘stuck‘ against the true right boundary insert. At first it was thought that the persistent flow down that side of the fan was indicating the fan surface had achieved a state of dynamic equilibrium. But by observing the rest of the fan it was obvious that this dynamic equilibrium was false, as the rest of the fan surface was lower than the true right, with low spots untouched by the flow. What was actually happening was that the smooth wall of polystyrene was creating a path of least resistance for the water, resulting in the flow remaining ‘stuck‘ to that side for up to ten hours. Tal and Paola (2010) also noticed this tendency in their flume studies. However by lining the walls of their flume with coarse mesh, constructing a buffer zone of wet sand

and installing wooden groins, they were able to create a rougher surface which prevented the flow from sticking to the walls (Tal and Paola, 2010). Introducing surface roughness also worked for this study. Coarse strips of sediment were added to all of the geometric boundary inserts, after which flow returned to migrating back and forth across the fan.

This seems like quite an obvious incident to observe in a microscale model, particularly as in both the New Zealand and the United States of America studies polystyrene is the material of choice for a majority of microscale models. However, perhaps due to the length run of times it may not have been noticeable in these experiments.

In this study, the S2 experiment was run for 130 hours before it was considered to be in dynamic equilibrium, with the coarse sediment strips being introduced around the 70 hour mark. This was in addition to the 73 hours of run time for the S1 experiment. By comparison, in the study conducted by Clarkson (1999), experiments were monitored on average for 6 hours; whilst in studies conducted by the USACE, hydrograph cycles ranged from 1.8 to 6 minutes (Gaines and Maynord, 2001; Maynord, 2006). In the UK, the maximum run time for a series of experiments conducted on alluvial fans by Clarke et al. (2010) was 12 hours. None of these times appear to be long enough to observe flow tendencies in the model. Furthermore, in his study of the Waiho River and fan system, Campbell (2012) noted that at the time of the stopbank installation it was unlikely that the fan had reached a state of equilibrium, despite having been run for 81 hours. Perhaps this was due to unobserved interference from the smooth polystyrene boundary walls.

Microscale models have been used successfully to predict prototype fan behaviour (Davies et al., 2003a, 2013), further understanding of alluvial fan processes (Davies and Korup, 2007), and facilitate the design of control work structure in rivers (Gaines and Maynord, 2001). However, they have not been exposed to a thorough exploration of the underlying principles or practice. The results of this study suggest an exploration is necessary, particularly in regards to the effects of surface roughness. Such a study could investigate and compare how models fans respond to polystyrene and other materials.

Chapter 5

Data analysis: variable input experiments

5.1 Introduction

In this chapter the results from the variable input experiments are described and reviewed. This set of experiments follow on from the previous set of steady input experiments (Chapter 4). The steady input experiments did not produce the fan behaviour that was expected, and it was hypothesized that by introducing input variability, this might be rectified. Rather than testing the fan response to the two alternative stopbank alignments, these experiments address the more fundamental topic of the response of the fan to variability, in terms of its behaviour and its ability to reach a state of dynamic equilibrium.

The variability introduced was based on experiments conducted by Davies and Korup (2007). In their study of fan surface dynamics, a siphon was used to simulate a fluctuating hydrograph of floods, base flows and no flow. In addition the Tinker sediment feeder, instead of delivering a constant rate of sediment into the flow, deposited sediment onto a circular disc. The sediment built up on this disc creating a conical angle of repose which generated intermittent, variably-sized avalanches off the sides; these were collected by a funnel and delivered to the water inflow. This created irregular sediment input in the short term, with a long term measurable average.

The siphon was initially used in this study, however it became unfeasible due to the very low flows required. Instead, an electronic timer was used to generate the fluctuating hydrograph. The hydrograph consists of two periods, a high flow (flood) and low flow (base).

5.2 Results

The variable input experiments differed based on the surface state of the fan when the stopbanks were installed, and the hydrograph used (Table 5.1). Two different hydrographs were used, however they shared the same mean flow of 9.25 ml/s.

5.2.1 V1: small variability

The V1 experiments were designed to be comparable to the S3 and S4 steady input experiments in order to investigate the effect of variability on microscale model fan behaviour and its ability to reach dynamic equilibrium. The V1a and V1b experiments operated with a hydrograph of fifteen minutes at 8 ml/s followed by fifteen minutes at 10.5 ml/s, with a mean flow of 9.25 ml/s. The response to confinement was tested for both an equilibrium fan (V1a) and an aggrading fan (V1b).

In the V1a equilibrium experiment, the model was turned on and left to run for 54 hours. Hourly scans began at hour 20, and by the 54th hour, the fan was considered to be in dynamic equilibrium (Figure 5.1). The time taken for the model fan seemed to be longer than that under the steady input conditions. However as it is uncertain whether the experiments all started from the same bed surface elevation, this cannot be categorically confirmed. Once dynamic equilibrium was established, the current stopbank alignment was installed and the model monitored for four hours (Figure 5.1).

Table 5.1: Summary of the four variable input experiments, including surface state when stopbanks were installed, input conditions (sediment and water), scenarios tested (Nat = natural, CC = current confinement, and Nat2 = released from confinement), measurement tools and outcomes. (15min = 15 minutes)

Number	Surface state	Input conditions		Scenarios	Measurement tool/s	Outcome
		Sediment (g/min)	Water (ml/s)			
V1a	Equilibrium	18	Mean 9.25 15min (8) 15min (10.5)	Nat CC	Laser scanner	No aggradaation when confined.
V1b	Aggrading	18	Mean 9.25 15min (8) 15min(10.5)	Nat CC Nat2	Laser scanner	Fan continued to aggrade when confined, and also when released
V2a	Attempted equilibrium	18	Mean 9.25 15min (6.5) 15min (12)	Nat CC	Laser scanner	Model DID NOT reach equilibrium
V2b	Aggrading	18	Mean 9.25 15min (6.5) 15min (12)	Nat CC Nat2	Laser scanner	Fan continued to aggrade when confined, and also when released.

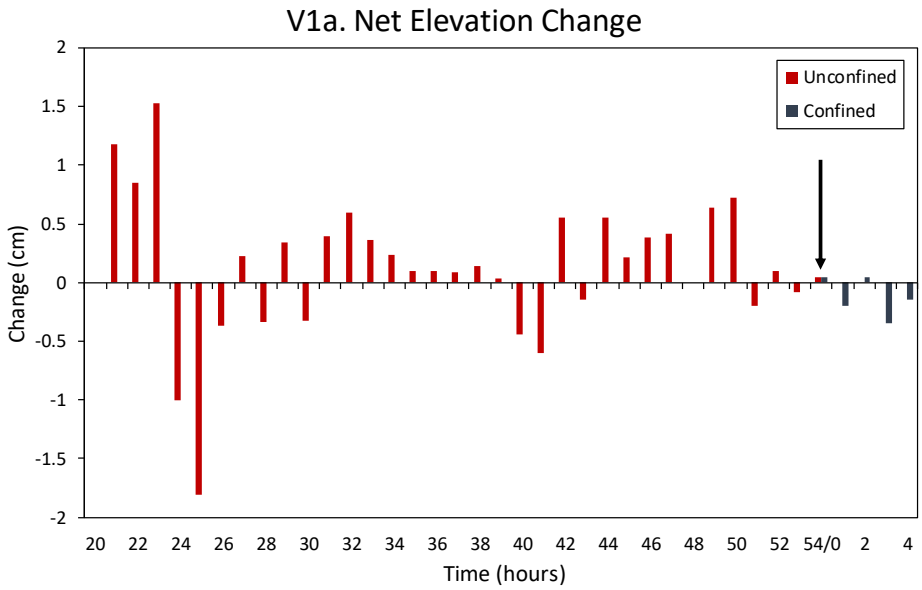

Figure 5.1: Plotted net elevation change of the V1a experiment between hours 20 and 58. Hours 20 to 54 are of the fan in its natural state, whilst hours 54 to 58 are of the confined fan (beginning marked by the black arrow).

In the lead up to achieving dynamic equilibrium the fan behaved quite differently to that of the steady input experimental fans. In particular, fan head trenching became much more obvious. Towards the end of the 10.5ml/s fifteen minute interval, a relatively deep trench would form in the fan apex (Figure 5.2a and b), shifting sediment deposition to the middle and lower reaches of the fan where it would then be transferred out of the model. Sediment accumulation below the free over fall was observably higher than in the steady input experiments.

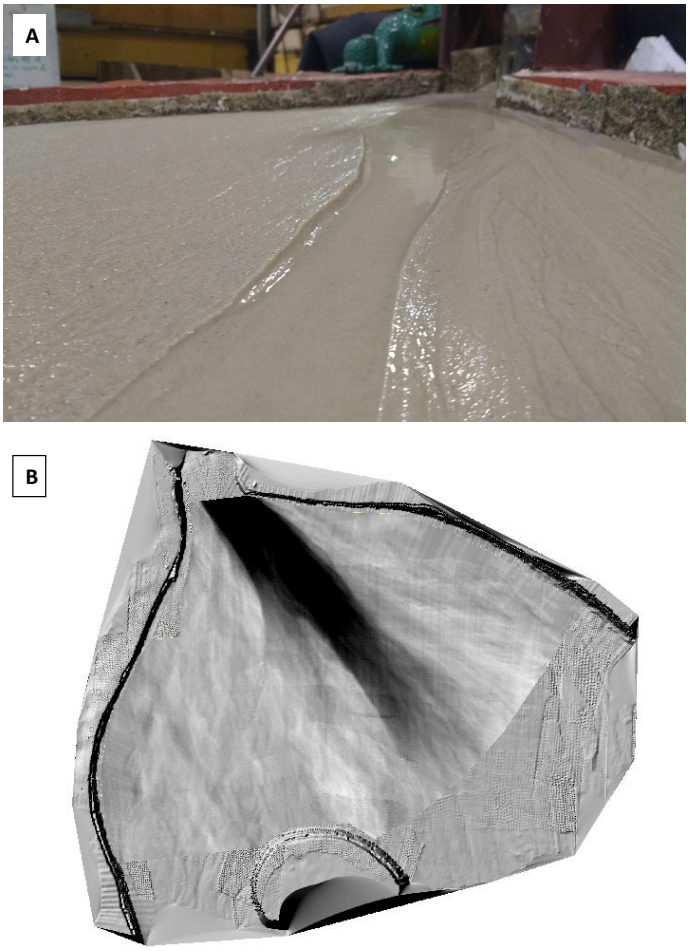

Figure 5.2: Photo (A) and DEM of Difference (B) of the unconfined fan showing a definite trench in the apex at hour 24

In addition, the fan exhibited catch up behaviour in response to the fan head trenching. During the first half of the smaller flow interval, the fan head trench would remain obvious (Figure 3a). However, as the flow to sediment ratio was smaller, sediment could accumulate in the trench until in the second half of the interval the trench would be infilled and braiding would reoccur (Figure 3b and c).

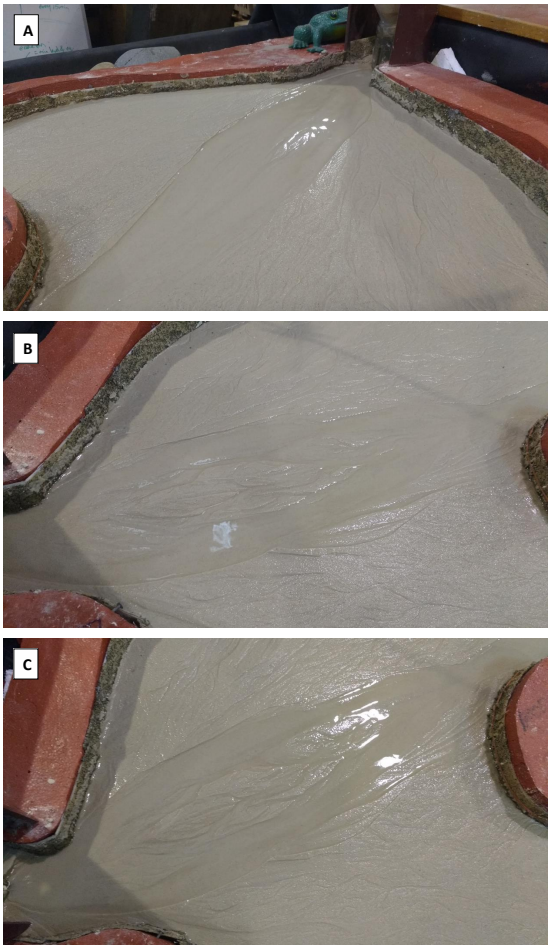

Figure 5.3: Fan exhibiting catch up behaviour. A)first half of low flow interval and the trench is still obvious B) second half of the low flow interval and sediment has begun to accumulate C) end of the low flow interval and braiding is obvious.

As with the S2 and S3 equilibrium fan experiments, the fan did not aggrade when the current stopbank alignment was installed. Consequently, the V1b aggrading experiment was conducted in order to confirm the fan would respond in the same way the S4 aggrading fan had to confinement.

In the V1b experiments, the fan was monitored for four hours as it built up in its natural state, and then whilst it was still aggrading the stopbanks were installed and it was monitored for a further four hours (Figure 5.4). The stopbanks were then removed and the fan monitored for a final five hours (Figure 5.4).

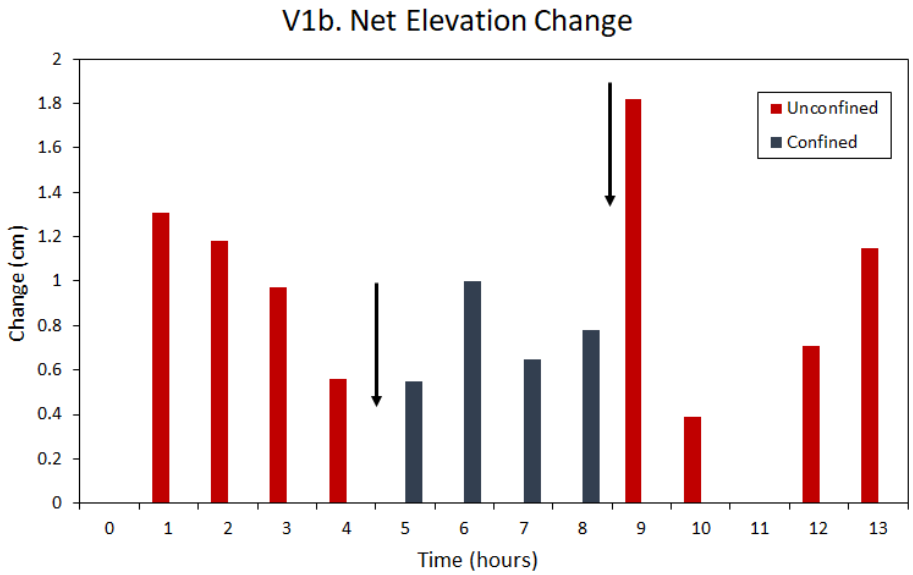

Figure 5.4: Plotted net elevation change of the V1b experiment. The graph shows three different states of the experiment, the initial natural state, the confined state and then the return to natural state. These changes are marked by the black arrows.

As in the steady input aggrading fan experiment (S4), the fan aggraded when confined, and then when the stopbanks were removed it continued to aggrade, infilling the newly available space (Figure 5.5).

Figure 5.5: Time lapse of change after the current stopbank alignment is removed. A) 0 mins B) 20 minutes c) 40 minutes. Fan is continuing to aggrade regardless of stopbank removal.

5.2.2 V2: large variability

The V2 experiments were designed as a comparison to the V1 experiments. They were run under a hydrograph with a much larger difference between the two fifteen minute flows whilst still maintaining the mean of 9.25 ml/s. The two fifteen minute intervals comprised a 6.5 ml/s flow and a 12 ml/s flow. As with the V1 experiments, both an equilibrium fan (V2a) and an aggrading fan (V2b) were tested. In addition, the maximum elevation from each DEM was recorded, to show the change in fan head height over time.

In the V2a experiment the model was turned on and left to run for 62 hours, with scans from hour 20 at hourly intervals. In addition to the mean net change data extracted from the DoD, maximum elevation data was also recorded (Figure 5.6).

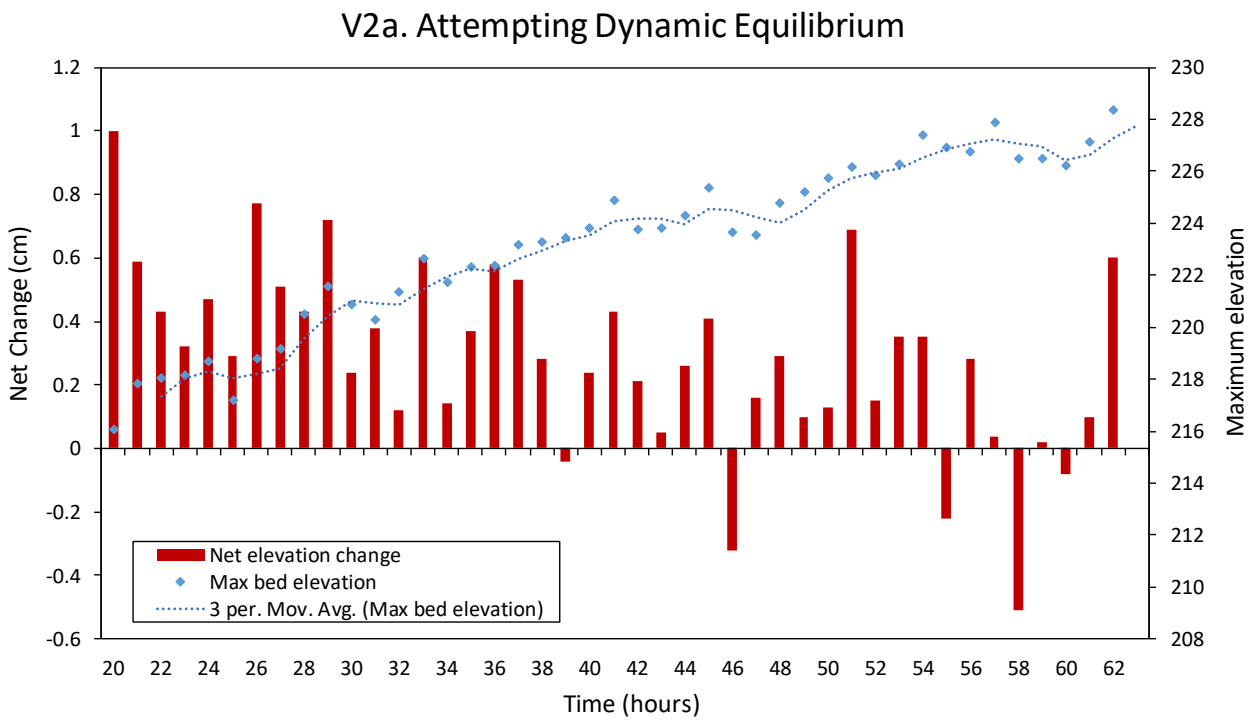

Figure 5.6: Plotted net elevation change and maximum elevation values for the V2a experiment. No stopbanks were installed, as this experiment was ended before dynamic equilibrium was reached.

During the experiment for a period of 2 hours (hours 55 and 56) scans were taken every 15 minutes to see if much was being missed by only scanning at the end of the flood flow (Figure 5.7). The 2 hour period of 15 minute interval scans showed much the same fluctuating pattern about 0, just at a smaller scale because of the reduced time between scans.

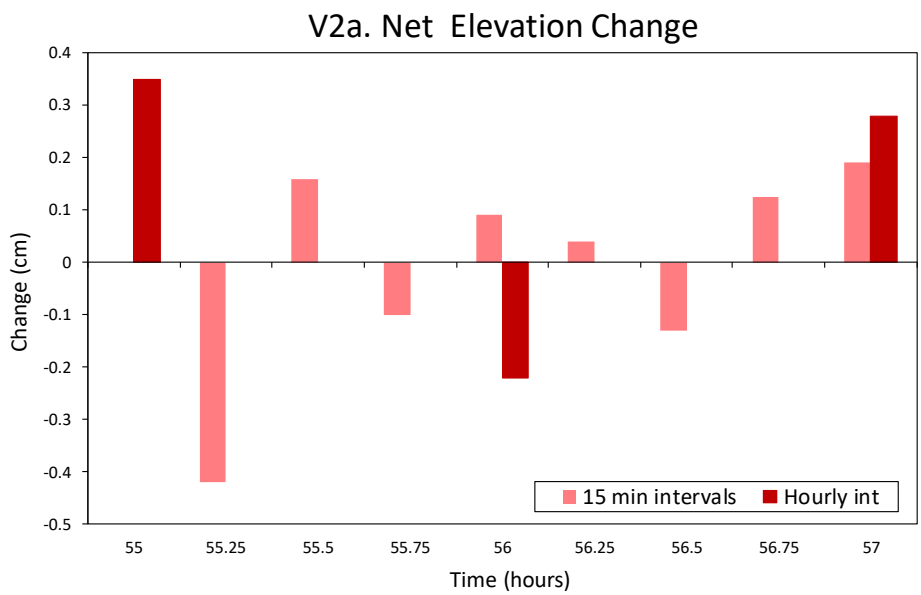

Figure 5.7: 2 hour period with scans completed every fifteen minutes in order to capture the change between each stage in the hydrograph.

The upper fan region did not reach dynamic equilibrium in this experiment (based on the definition of equilibrium for this study). Instead, the model fan continued to aggrade slowly. At 62 hours its maximum elevation at the head was only 227. At 54 hours the previous variability experiment (V1a) with the same water flow mean, had reached equilibrium with a head elevation of 240. The experiment was ended at 62 hours.

In hindsight this experiment would have benefited from a longer run time. This would have allowed observation of the pattern that seems to begin at hour 51. From this point onwards net change undergoes large fluctuations about zero. This could be evidence of a very dynamic equilibrium. The net change data suggests that during this time the microscale fan experienced episodes of high aggradation followed by periods of slower aggradation, as well as episodes of degradation. Overall, in the long term the fan was aggrading.

A second experiment (V2b) using the same hydrograph as V2a was then run to check the response of an aggrading fan. The V2b experiment proceeded in a similar fashion to the V1b aggrading fan experiment. The model was run for 3 hours in its natural state, and then while it was still aggrading the current stopbank alignment was installed and monitored for a further 3 hours. The stopbanks were then removed and the fan monitored for another 3 hours (Figure 5.8).

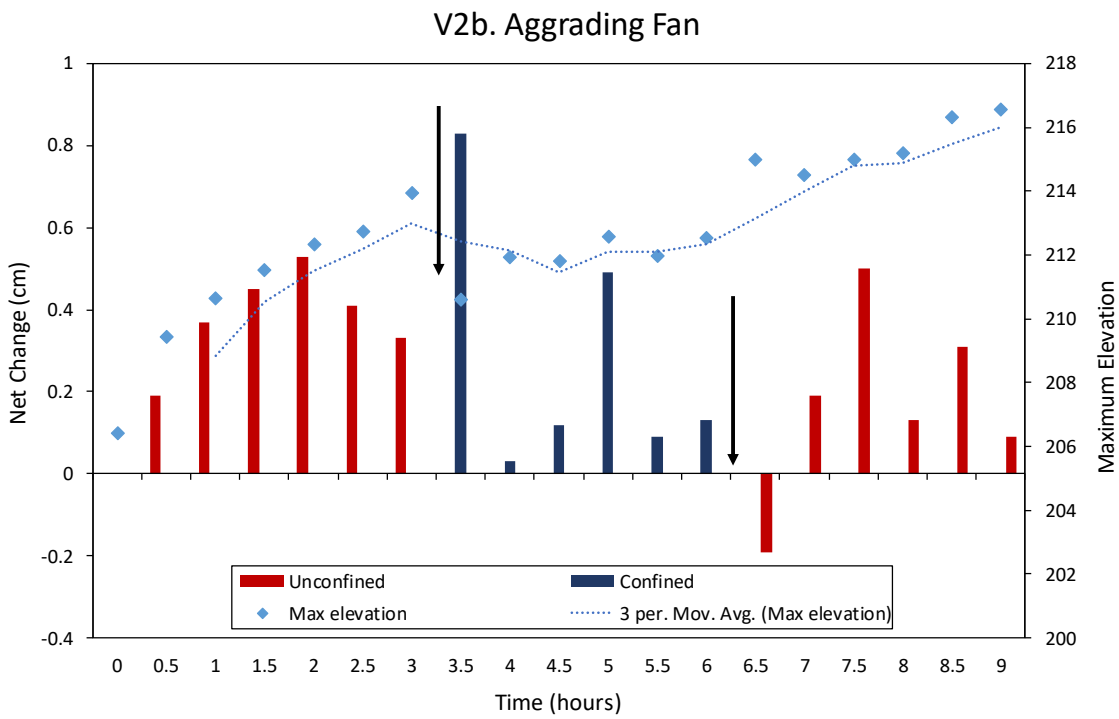

Figure 5.8: Plotted net elevation change and maximum elevation values for the V2b aggrading fan scenario. The experiment consisted of three stages, natural, confined and natural again, these are marked by the black arrows.

There was an initial spike of high positive net change when the stopbanks were installed, however this did not last. A small fluctuating aggrading pattern developed after that first half hour (Figure 5.8). When the stopbanks were removed there was another initial spike, this time of negative net change. Again, this did not last, the fluctuating aggrading behaviour resumed after that initial spike (Figure 5.8).

5.3 Discussion

5.3.1 Fan behaviour

The variable input experimental fans behaved differently to the steady input experimental fans. Many alluvial fan studies use constant input conditions (Davies et al., 2003a, 2013; Clarke et al., 2010; Whipple et al., 1998; Reitz and Jerolmack, 2012; Reitz et al., 2010). Under these steady input conditions, the experimental fans follow a predicted set of developmental steps (Bryant et al., 1995), that involve a range of behaviours (Clarke et al., 2010). Of these behaviours, fan head trenching tends to occur in the later stages of fan formation, when it has neared or reached maximum growth (Clarke et al., 2010; Whipple et al., 1998). This was not the case for the variable input experimental fans in this study.

In both the V1 and V2 sets of experimental fans, fan head trenching occurred every time the water discharge was increased. In the V1 experiments, this was a 31% increase whilst for the V2 experiments this was a 85% increase. In both cases, after the water input was increased flow would become unchannelized forming sheet flow for several minutes before a deep wide trench in the apex of the fan formed (Figure 5.2). The trench always formed in the apex, but it would switch to different alignments out into the middle and lower reaches of the fan between each cycle of the hydrograph. During the higher flow intervals sediment accumulation below the free overfall was also high. These behaviours appear to be a result of the increased water discharge increasing the ability of the fan to move sediment across its surface. As there was no increase to sediment supply or lowering of the gradient when the water discharge was raised, the stream power was increased and therefore the ability of the fan to transport sediment.

By contrast, in the steady input experiments, fan head trenching occurred only when the fan began to approach a state of dynamic equilibrium.

The response of the experimental fans to variability in this study is similar to another study. In their study of the Westland fan network, Davies and Korup (2007) constructed a microscale model of the Poerua river and fan system. This model was fed by variable sediment and water inputs, and the results showed that the irregular inputs of sediment had a direct effect upon fan head trenching behaviour that were not apparent in the steady input experiments.

When steady input conditions are used, the assumption must then be that the fluctuations in sediment and water supply in nature can be averaged out over the scale of interest in a model i.e. long term evolution (Jerolmack, 2011). However, alluvial fans are incredibly dynamic systems, whose behaviour is often dictated by variability as has been shown by this study and that of Davies and Korup (2007). The variability experiments have produced behaviours that are not present in steady input experiments. This has implications for prototype-related investigations which use steady inputs. A prototype fan will frequently experience and respond to some random higher than normal flood event or large sediment input. However, this response will not be expected by engineers or hydrologists, if a steady input experiment has been used where there is no variability to produce such a response. For the sake of accurate and reliable investigations, it would appear that modellers must find a way to incorporate variability into their models if they wish to reproduce those behaviours that occur in nature.

5.3.2 Fan surface state

The variable input conditions also affected the ability of the experimental fan to reach a state of dynamic equilibrium. This effect differed depending on the degree of variability. Small variability in the hydrograph between the base and flood flow appeared to have less of an impact than larger variability. Similarly Davies and Korup (2007) showed that larger, irregular inputs of sediment also had a greater impact on experimental fan behaviour.

The V1a and V2a experiments were designed to allow the fans to reach dynamic equilibrium under variable conditions before the stopbanks were installed. In the V1a experiment, variability was small. The base flow was 8 ml/s, whilst the flood flow increased by 31% to 10.5 ml/s. Therefore there was a 2.5 ml/s increase in flow between the two 15 minute intervals that formed the hydrograph cycle. In this scenario, whilst the fan did reach a dynamic equilibrium, it appeared to behave differently to the steady input experiments, with fluctuations between net change more gradual. However, when dynamic equilibrium was reached and the stopbanks installed, it responded in the same way as the steady input experiments. No net aggradation occurred.

By contrast the V2a experiment was ended before dynamic equilibrium was reached, because of the extremely slow growth of the fan. In both the V1a and V2a experiments maximum elevation was measured at the head of

the fans. In the V1a experiment, by the time the fan had reached a state of dynamic equilibrium (fifty four hours), the head of the fan had aggraded to a relative elevation of 240. By 62 hours in the V2a experiment, the head of the fan was only at 228. Despite the same mean input values as the V1a experiment, the greater variability in the V2a experiment with a base flow of 6.5 ml/s, and flood flow of 12 ml/s, clearly affected the progress of the fan towards dynamic equilibrium. In addition whilst the V1a fan was able to develop a fluctuating net elevation change pattern early on (hour 21), the V2a did not. However the V2a fan does appear to achieve the beginnings of a fluctuating pattern at hour 51. Perhaps if the V2a experiment had been left to run for much longer, it would have reached a higher maximum elevation, established its fluctuating pattern further and even achieved a state of dynamic equilibrium. Unfortunately, due to slow fan development and time constraints, it did not.

These results raise the question of what effect irregular and large landslides or flood events have upon a natural fan system and its evolution. For example, the Waiho river and fan system is in a location where sediment input from landslides and glacial activity is high and irregular, and intense high rainfall storms frequently occur in the area causing high flow variability. In addition the fan is located on the Alpine fault, which ruptures several times per millennium, resulting in earthquakes which generate extreme shaking that causes very high sediment inputs due to coseismic land sliding (Robinson and Davies, 2013). The combination of these factors make for an extremely dynamic system. Can such active systems with so much variability reach a state of dynamic equilibrium? And if they can, how long would this take or last? And how dynamic would this equilibrium be? These types of questions need to be addressed and investigated, as they have implications for how we understand and manage such systems.

Further studies on the impact of flow and sediment input variability on alluvial fan processes and evolution would be beneficial to our understanding of the dynamic nature of alluvial fans, and could perhaps improve our management of these systems. An avenue for research lies in further investigation of the effects of irregular sediment and water inputs in laboratory conditions and comparisons to both steady input experiments as well as observations made in the field.

Chapter 6

Application to the Waiho River

The purpose of this study was to investigate alternate stopbank alignments for the Waiho River and fan system that would facilitate the return of the bed to more manageable levels. This would reduce the severe flood risk posed by the system to the neighbouring town, State Highway 6, and surrounding farmland, and alleviate the need for ongoing and potentially dangerous height additions to the current stopbank network. However, the results of this study, discussed in depth in chapters four (steady input experiments) and five (variable input experiments) have produced some unexpected conclusions and questions which indicate that a solution the Waiho-Franz Josef problem may not be able to be usefully based on micro-scale modelling until better field information can be acquired.

6.1 Outcome of the alternate stopbank alignments

The two stopbank alignments tested released the Waiho River from its present confined state to different degrees of confinement on the southern side of the fan. The intermediate option doubled the area that the river could utilize, whilst still protecting a large portion of the farmland for continued human use. Alternatively, the extreme option freed the river completely, allowing it full access to the farmland and the entirety of its natural accommodation space.

The rationale and theory behind these options was based on the concepts of dynamic equilibrium and the effects of channel confinement discussed earlier in chapter four. These assumptions have led to the belief that the current stopbank alignment confined the river to an area of the fan that was too small for it to behave naturally. Traditionally, confinement of a river has been designed to increase the depth of the flow, thereby increasing

transport capacity and subsequently promoting degradation. However, the Waiho River is still able braid at a range of flows within the confined reaches. This ability to braid suggests that confinement has not increased the depth, only limited the ability for it to laterally migrate. For this reason, the Waiho River has departed from its state of dynamic equilibrium, into one of rapid aggradation (Figure 6.1). Therefore, realigning the stopbanks to reduce the degree of channel confinement should result in degradation, and the return of the fan surface to its previous state of dynamic equilibrium. However, neither the extreme nor the intermediate realignment schemes induced degradation in the micro-scale model.

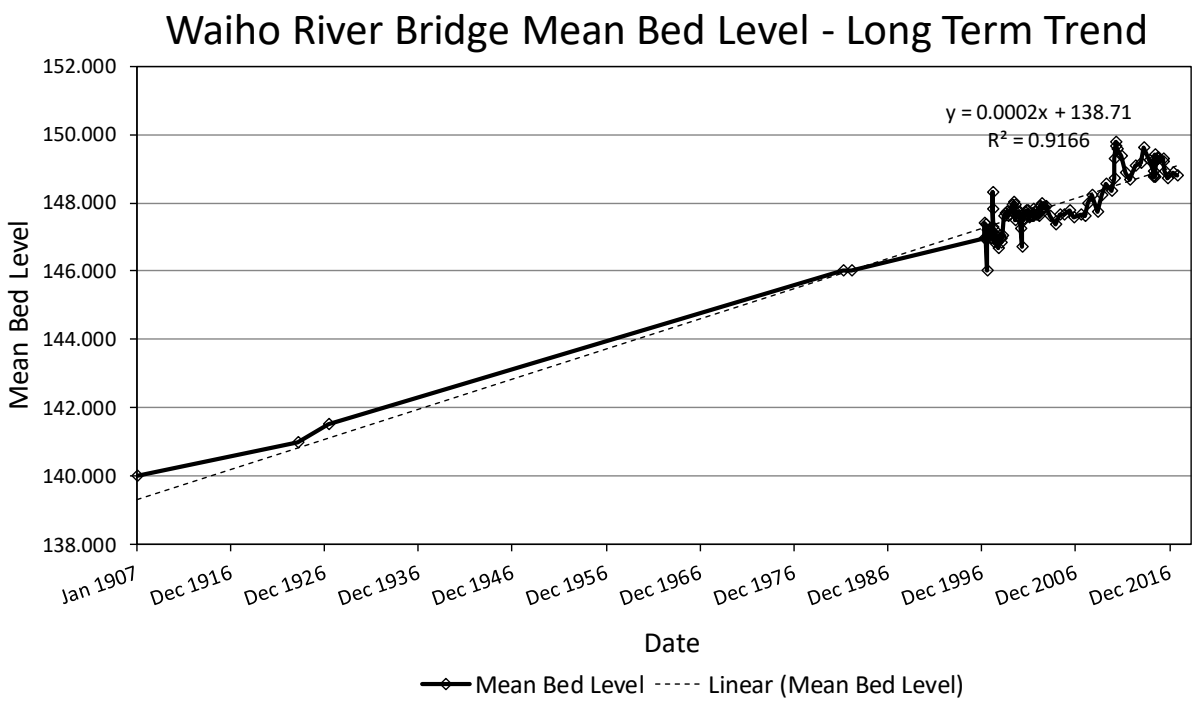

Figure 6.1: Mean bed level data at the Waiho River bridge site plotted from 01/01/1907 to 11/09/2017 provides evidence for the aggrading river bed over the last 111 years. Data was collected by NIWA and NZTA, and compiled by Mark Healey at Opus Consulting Inc.

In all of the dynamic equilibrium fan scenarios for the present modelling exercise, the fan did not aggrade when confined by the current stopbank

alignment, and additionally did not degrade or aggrade when the degree of confinement was reduced (Figured 4.5, 4.6 and 5.1). During the aggrading fan scenarios, channel confinement increased the local rate of aggradation by reducing the accommodation space available to the fan, which matches observations of the Waiho River in the field. However, when the degree of confinement was reduced or removed altogether, the fan continued to aggrade albeit at a slower pace (Figures 4.9, 5.4 and 5.8). This suggest that there must be some aggradation present for the confinement to exacerbate.

These results cast doubt on the assumptions that have been made with respect to the behaviour and surface state of the Waiho fan prior to human interference.

6.2 Surface state of the Waiho fan

When people first arrived and settled across the Waiho fan surface, it is believed that the fan had reached a long term state of dynamic equilibrium for a number of reasons based on:

- Fan theory for dynamic equilibrium: constant fan toe position, limited accommodation space, river entrenched into the fan head
- Assumed long-term steady inputs of water and sediment (based on assumed constant climate and tectonics)
- Other fans in the Westland region appear to have (or are assumed to have) reached a state of dynamic equilibrium
- Young surface soil stratigraphy

Following human settlement, stopbanks were gradually installed to protect the growing town, highway and farmland from flood hazards. A recent concept is that it was the confinement of the Waiho River by these stopbanks which prompted the rivers shift from a state of dynamic equilibrium to one of aggradation (e.g. Davies et al, 2003a).

As outlined above, none of the dynamic equilibrium fan scenarios in this study exhibited aggradation when confined by the current stopbank alignment. It was only the aggrading fan scenarios in this study which exhibited aggradation when confined. Similarly, Campbell (2012) suggested that his

Waiho experimental fan was also not in a state of dynamic equilibrium when the stopbanks were installed, but rather one of aggradation. In his model the fan aggraded when confined. Furthermore, in the various aggrading fan scenarios, confinement resulted in an increased rate of aggradation, which is similar to what has been observed in the field over the past few decades. These discrepancies call the assumptions about the equilibrium nature of the Waiho fan into question.

6.2.1 Was the Waiho in dynamic equilibrium?

Alluvial fan theory and quantitative relationships

Alluvial fan theory suggests that the Waiho fan surface had reached a state of dynamic equilibrium when people first arrived because the river had become entrenched into its fan head (Davies and McSaveney, 2001), sea level had been constant for 6,000 years, and therefore so had the Waiho fan toe (Davies and McSaveney, 2001), and the fan has a limited accommodation space, confined as it is by steep moraine walls on both sides. Therefore, it should have had enough time to fill its accommodation space to an equilibrium state. However, a review of the quantitative relationships established between drainage basin and fan size and steepness suggest otherwise.

During the mid-20th century, Bull (1964) found that the larger the basin, the larger the fan. In addition, drainage basins composed of mudstone or shale produced larger fans compared to those composed of sandstone due to the higher erodibility of the former materials. Ryder (1971) also linked drainage basin relief to fan steepness. Steeper average basin relief resulted in steeper fans. More recently, experimental fan slopes have been shown to vary as a result of the sediment-discharge ratio, with steeper slopes associated with a higher ratio (Clarke et al., 2008; Zarn and Davies, 1994).

When applying these relationships to the Waiho fan system, it would seem that whilst the Waiho fan cannot increase its surface area it could still be larger in volume, and hence steeper in slope. Many of the mountains in the Waiho drainage basin exceed 3000m and as a result of their location in an area of high tectonic uplift rate, the relief is on average very steep (McSaveney and Davies, 1998). The geology of the region is that of greywacke and schist, and when combined with the high rainfall of the region, the result is a high erosion rate and therefore high sediment supply (McSaveney and Davies, 1998). Finally, the 170 km^2 area could be considered quite large

compared to the 64 km^2 fan. Thus, it would seem reasonable that the Waiho fan could still have been growing when people first arrived. Despite its fixed toe it could still have been aggrading, increasing in elevation and therefore in steepness.

Furthermore, a constant fan toe does not necessarily imply equilibrium, as shown by the experiments in this study. Prior to any experimentation, the fan was allowed to build up without interference to where its toe had reached the free overfall. This overfall acted as a constant fan toe. In all of the experiments aggradation continued despite the fan toe being reached, and sediment being expelled from the system.

Long term steady inputs and a severe lack of data

Davies and McSaveney (2001) suggest that the Waiho and the other Westland fans would have been experiencing long term steady water and sediment inputs, and as this has been for a substantial amount of time, the fans should therefore be in a state of dynamic equilibrium. However, this is based upon the average uplift of the mountains, and average rainfall data from an assumed climate. These are not recorded data. There are no such data for the Waiho's past, only an inferred history.

The assumed history for the Waiho, whilst plausible, is not consistent to what is understood about the impact of glacial behaviour or tectonic activity upon sediment production rates. Nor is this history definite enough to determine what the surface state of the fan or its behaviour was prior to human interference. Notes and sketches made by the early explorers and inhabitants do not extend further back than 150 years, and these accounts are not accurate or reliable enough to make such a decision. Aerial photography does not go back to when the fan was unconfined by stopbanks.

In addition, it is known that climate has changed dramatically over the last 200 years (recovery from the Little Ice Age) and that the Franz Josef Glacier has undergone several advance and retreat phases during this time. The last Alpine fault earthquake was 1717, and would have had a major sediment input; Davies et al. (2005) found evidence for several metres of aggradation on the Waiho fanhead since before that event, again casting suspicion on the steady-state assumption. These incidences could cause short term deviation away from a long term equilibrium. By inferring long

term inputs, the perturbations and resulting aggradational or degradational episodes are ignored.

Long term sediment and water inputs can be inferred, but it is only an inference. Variability which exists everywhere in nature, and which may be a critical component of behaviour, is lost when something becomes considered as steady in the long term. By doing this, the effect of large and small flow events, sediment deficits and surpluses, climate change, glacial recession and advance, and Alpine fault movements on fan behaviour and development are not taken into account and therefore not understood. People were not around to measure and monitor such events, so inferences are made which act to simplify fundamentally dynamic and complex systems. Ultimately this leaves us without the knowledge of how these events may have impacted and continue to impact fan behaviour and development.

Even now, regular and ongoing collection of data sets of this system are non-existent. Flow rates are not measured, bedload transport not monitored. There is little knowledge of sediment and water inputs and transport rates within the Franz Josef glacier, or how the glacier has and continues to affect the river and fan below. If our knowledge of this system is limited now, how can we accurately infer its past behaviour and surface state, or predict future changes for the Waiho Fan?

Soil stratigraphy

Soil stratigraphy shows that the soils on the inactive fan surface are all recent, with few more than about 500 years old due to constant reworking of the face surface by the shifting river (Davies and McSaveney, 2001; Davies et al., 2003a). This indicates rapid process rates which suggests that there should have been enough time for the longitudinal profile of the fan to have been in long term dynamic equilibrium (Davies and McSaveney, 2001). However, rapid process rates do not necessarily mean that there has been enough time for the Waiho fan to have reached a state of dynamic equilibrium 150 years ago. A review of how fans develop suggests that these young soil layers are also indicative of a fan still in development.

Fans develop via a migrating channel network which shifts back and forth across the entire fan surface, reworking, transporting and depositing sediment (Blair and McPherson, 1994b). This migrating behaviour has been

described as the "windescreen-wiper effect" (Zarn and Davies, 1994). It occurs as a result of local sediment deposition. The accumulating sediment raises the channel bed until it is higher than that of the surrounding land, resulting in the river breaching its banks and forming a new channel (Reitz and Jerolmack, 2012). This process has been observed to gradually shift laterally across the fan from one side to the other and back (Zarn and Davies, 1994).

How many times would the Waiho channel network need to migrate back and forth across the fan surface to reach dynamic equilibrium? What was the past avulsion rate? Was it slow? If so, inactive areas would remain inactive for some time before the channel network returned. More importantly how did having a large feature like the Waiho Loop, which would originally have extended across the entire fan width, have affected fan development? The exact behaviour of the Waiho River beyond 150 years ago is unknown because humans were not a round to record it. Therefore behaviour is only inferred. The age of the soils in the inactive part of the fan could indicate dynamic equilibrium, but they could also indicate growth.

In this study, of the two dynamic equilibrium fan scenarios under variable conditions (Chapter 5), only one reached dynamic equilibrium after 54 hours. At the 62 hour mark the second experiment was ended, and that fan never reached a state of dynamic equilibrium. Both experiments shared the same sediment input and mean water input. In the steady input experiments (Chapter 4), all dynamic equilibrium fan scenarios took similarly long time periods to reach a state of dynamic equilibrium. Given also, that the records indicate that the stopbanks were originally installed to protect the surrounding land from a slowly aggrading river bed, then it would seem reasonable to infer that the young age of the soils on the inactive part of the fan are from a phase of development for the migrating channel system. Therefore, the soil stratigraphy could suggest that the Waiho fan was still increasing its elevation, and had not reached a state of dynamic equilibrium when people first arrived.

Westland region fans and the complexity of the Waiho

Davies and Korup (2007) argue that many of the fans along the West Coast have reached dynamic equilibrium, therefore inferring that the Waiho

has also had enough time to establish dynamic equilibrium. However, despite being subject to identical environmental forces during their evolution, landforms in the same region can be in different stages of geomorphic development (Schumm et al., 1987). For instance, alluvial fans along the same region may be experiencing active growth (Beaty, 1970), dissection (Hunt and Mabey, 1966) or steady-state equilibrium (Denny, 1967). This seems a likely diagnosis for the Waiho, given the difference between its catchment and that of its neighbours.

Of the West Coast river and fan networks, only two have glaciers that persist down to near sea level, the Waiho and the Fox. Yet, the two networks differ significantly in terms of the shapes of the valleys, tributaries, and glacial deposits. For these reasons, it seems that the two may not necessarily be in the same stage of development (Carrivick and Rushmer, 2009).

There has been little study of the Fox glacier, river, and valley, therefore, the following information has been gleaned from topographical maps of the region (NZTopo50-BX15). The proglacial Fox river emerges from the Fox Glacier, flowing through several kilometres of confined valley before exiting into more open terrain (Figure 6.2). This point of exit is symmetrically placed, and feeds down into an elongated valley, where the Fox river eventually joins the Cook River. The Cook, a larger river, emerges on the Southern point of the valley and has formed a gently sloped fan. Glacial activity in the open section of valley has been dominated by the steady retreat of the Fox glacier, from which no distinct deposits remain. However, there has been a very large volume of ice buried beneath the upper part of the Fox River since the 1960s. This has been slowly melting since then, providing accommodation space for Fox sediment and reducing sediment input to the Fox system (Bull, 2004). There has been no such buried ice in the Waiho during this time (Bull, 2004).

Figure 6.2: Looking upstream through the transport reach of the Fox River towards the Fox Glacier terminus. The channel is dominated by large boulders, very different to the Waiho where such boulders have been buried beneath the aggrading bed. Photo by Greg Hewgill

Similarly in the Waiho catchment, the proglacial Waiho River emerges from the Franz Josef Glacier and also flows through several kilometres of confined valley before exiting into open terrain. However this is where some differences occur.

- Prior to leaving the confined valley, the Waiho is joined by the Callery River. The Callery contributes a greater percentage of catchment to the Waiho system (Davies and McSaveney, 2001). However, apart from inferences made about its sediment and water contributions to the Waiho River very little is known about the Callery. There are no sediment or water supply data sets (Davies and Scott, 1997). There have been no studies of how sediment slugs are moved through the system, or the effects of the glaciers upon sediment and water inputs. The narrow, steep gorge, surrounded by rugged terrain and dense vegetation make study difficult (Davies and Scott, 1997).

- To the true right side of the Waiho River after it has emerged from mountains the substantial Tatare fan has formed and prevented the

Waiho from accessing this Northern area of the valley. The Tatare River is a much smaller river than the Cook River; where the Fox is a tributary to the Cook, the Tatare is a tributary to the Waiho.

- Carrivick and Rushmer (2009) found that despite sharing the same climatic conditions, and neighbouring catchments, the Fox and Franz Josef glaciers and their proglacial systems differ considerably. These differences relate to glacier area and length, lower glacier debris coverage, valley orientation, and glacial behaviour, with subsequent effect on the sandur (outwash plane) below (Carrivick and Rushmer, 2009). The result is that the Franz Josef glacier sandur features massive, poorly sorted sediments with outsized clasts, whereas the Fox glacier sandur is of much finer-grained material (Carrivick and Rushmer, 2009).

- Finally, the glacial history of the Waiho valley may differ to that of the Fox. Two very obvious features are observed on the Waiho fan and flats, Canavan's Knob, and the Waiho Loop. These are ancient relics of past glacial behaviour. The Waiho Loop is in fact only a portion of a terminal moraine deposit that reached around to the southern side of the valley (Davies and McSaveney, 2001). The missing portion was eroded by the Waiho river where it was not protected by the higher Tatare fan (Alexander et al., 2014). How would this moraine wall, and the substantial infilling which eventually buried it, have affected the behaviour of the Waiho as it has developed? There is no evidence of a feature like the Waiho Loop in the Fox valley, however having no equivalent to the Tatare fan to keep the Fox and Cook Rivers away from such a feature, it may have been eroded. Aside from Rachocki's (1981) studies of the Polish fans in post glacial environments, there have been no experiments to look at how fan behaviour and development is affected by glacial remains.

Considering these differences, it seems likely that the Fox and Waiho Rivers could behave differently, and that their fans could also behave and have developed differently.

6.2.2 An aggrading Waiho scenario

If, in fact, the Waiho fan was still developing when humans first settled there, then removal of the current stopbank alignment and installation of

one of the alternatives might not solve the problem of the aggrading river bed in the long-term.

The results from the aggrading fan scenarios (S4, V1b, V2b) in this study indicate that removal of the current stopbank alignment will result in some initial degradation, but the fan will eventually fill up the newly available space, continuing its aggradation trend. This does buy some time, but as time cannot be quantitatively scaled up from the microscale model to its prototype, it is unknown how much time could be bought.

However, continuing to increase the current stopbank crest height and add more stopbanks to the current setup is certainly not going to solve the problem of the aggrading river bed, even in the short-term. It serves only to exacerbate an already dangerous situation. Steps need to be taken now to alleviate the pressures on the township of Franz Josef Glacier, SH6 and flats farmland.

In this study, the aggrading fan scenarios showed that the two alternative stopbank alignments resulted in a reduced rate of aggradation. Therefore, a controlled shift of the Waiho River to the South of the valley could be put in place using the two alternatives from this study or similar. This would allow time for the gradual relocation of farmland owners and the township, and shifting of the SH6 to the 160 m contour along the bush line where it is out of harms way. Whilst this solution does not solve the aggrading river bed, it should reduce the rate of aggradation, pressures on the northern stopbanks, and buy some time for relocations.

Ultimately, if the river was aggrading when people first arrived, and if its basic tendency is to aggrade, then aggradation will go on regardless of how many stopbanks are installed and however high they are built, with inevitable impact upon the surrounding land use.

6.3 Implications for the Waiho

The results of the microscale modelling experiments from this study have important implications for the management of the Waiho River and Fan.

Previously it has been believed that it was the combination of the fan being in a state of dynamic equilibrium and then severe confinement by the stopbanks which resulted in the rapid aggradational trend in the Waiho system. However, in none of the dynamic equilibrium fan scenarios in this study did the current stopbank alignment induce aggradation. It was only in the aggrading fan scenarios that an aggradational response occurred. This outcome suggests that the Waiho fan was not in a state of dynamic equilibrium when humans first settled there. If so, then the alternative stopbank alignments tested in this study will not solve the problem of a rapidly aggrading river bed, but will reduce the rate of the aggradation and relieve the current pressures on the northern stopbanks. This will provide the Franz Josef Glacier township with time to develop a long-term flood risk management strategy. How much time is unknown, as time in microscale models cannot be quantitatively scaled up to the prototype.

6.3.1 Recommendations

The rate at which the Waiho river bed is currently aggrading, and the hazards posed by this aggradation, are an immediate concern to the neighbouring Franz Josef Glacier township, State Highway 6, and landholders of the Waiho flats farmland. However, as the results of this study have indicated that a solution is not straightforward, the following recommendation is only a suggestion for the future which could provide some time, in the hope of finding a more favourable outcome for the town, highway and farmland.

At present, ongoing height additions to the current set of stopbanks keeps the rapidly aggrading river at bay, but for how much longer? Increasing the stopbank height is not going to solve the problem. Whilst maintenance and height additions do protect the town, road and farmland, they are only a temporary solution. Ultimately the additions add to the already dangerous situation. Each time the stopbanks are made higher, the river bed is also able to aggrade higher within its confines so that it sits considerably higher than the surrounding land and town (Figure 1.2). This is an extremely hazardous situation.

Alternatively, one of the stopbank alignments tested in this study could be installed to replace the existing one, or even both which would allow a gradual shift of the river to the south (Figure 1.2; Langridge et al., 2016). This would involve considerable effort, time and money, to move both highway and stopbank, and as shown by the results of this study, is unlikely to

stop the river bed aggrading. However, it would allow the river more space, reduce the current pressures on the northern stopbank alignment and Franz Josef township (Langridge et al., 2016), potentially slow down the rapid rate of aggradation and provide time before other action such as town relocation can be taken.

Chapter 7

Conclusions

This study was designed to investigate the response of an experimental fan to confinement and release, in order to provide information relevant to the management of the Waiho River on the South Island of New Zealand. Through a series of experiments it was demonstrated that fan behaviour in response to confinement by stopbanks, and its ability to reach equilibrium, were affected by the surface state of the fan prior to its confinement and by introduced variability in the water and sediment inputs.

The surface state of the experimental fan prior to confinement affected how the fan responded to the installation of the stopbanks. When the fan had reached a state of dynamic equilibrium before the stopbanks were installed, in both the steady and the variable input experiments, no aggradation took place as a consequence of confinement. Alternatively, when the fan was in a state of aggradation and the stopbanks were installed, in both the steady and the variable input experiments, aggradation continued. However, while the aggradation rate was increased by confinement under the steady input conditions, this was not the case for the variable input experiments.

Introduced variability in the sediment and water inputs of the microscale model had a noticeable effect on the behaviour of the experimental fan. The achievement of equilibrium on the fan with strongly varying water and sediment inputs took much longer than when the degree of variation was less or zero. In addition, when the degree of variation was greater than zero, particular fan behaviours such as fan head trenching occurred more frequently and under different circumstances than when variation was zero.

These findings have implications for both microscale modelling and for the relevance of this technique to management of the Waiho River.

7.1 Implications for microscale modelling

Microscale modelling has proven to be a valuable alternative to other forms of modelling as it does not require a large amount of input data. However, as it is a relatively new form of modelling it has not received the attention that more traditional forms have. Therefore, the underlying theory and the practices used are still open to modification and improvement.

The microscale modelling experiments of the Waiho River and Fan in this study have demonstrated that:

- It is extremely important to assess accurately whether or not the fan has achieved equilibrium prior to modification, in order to draw correct conclusions about its behaviour in response to modification.
- There are grounds to question whether a microscale model under steady water and sediment input conditions, thus lacking any variability in the form of turbulence, flow and sediment input variation, and sediment grain-size, can be expected to realistically represent the behaviour of a river that has all these variations.

There are thus opportunities for future investigation into the underlying theory and practice of microscale modelling. Opportunities exist in:

- The effect of surface roughness at such a small scale. In the present study, moulded fibre glass was used to represent stopbanks, similar to the non-porous stainless steel used by Clarkson (1999) and Campbell (2012). How do these materials affect the model behaviour compared to the pervious, steel mesh structures utilized in the USACE models (Gaines and Maynord, 2001)?

  In addition, the smooth surface of the polystyrene used for the model boundaries in this study and a majority of other microscale models had a definite effect on the model fan behaviour, and this could do with further investigation.
- The methods used to measure change in the model. The present study demonstrated that point-gauging could not provide the detail required to accurately establish fan surface states, whilst laser technology could. Further work could be done in exploring how accurate and reliable different measurement tools are to ensure reliable results.

- The study of the effects of variations in water and sediment inputs on alluvial fans.

In addition to these opportunities, there are no guidelines on microscale modelling practice. Therefore, an exploration and reporting of the techniques would be beneficial for anyone wishing to employ this type of modelling.

7.2 Implications for the management of the Waiho River

The findings of this study have important implications for relevance of the previous microscale modelling work completed by Davies et al (2003a; 2013, as well as for the current and future management of the Waiho River.

Davies et al. (2003a; 2013) were able to demonstrate a good match between model and Waiho River relative aggradation rates. However, the present study has shown that this match was probably achieved by confining a model fan that was a aggrading, and not in dynamic equilibrium as previously thought. The present study also indicated that the assumption by Davies et al. (2003a; 2013) that the Waiho was in dynamic equilibrium in the late 20th century when the stopbanks were first installed, is questionable. Therefore, the modelling of Davies et al (2003a; 2013) may still be appropriate, and so the implication from their work that reducing the degree of confinement of the Waiho will lead to degradation at the fanhead seems likely to be correct. However, as shown by this study, this degradation may not be permanent and in the longer term aggradation is likely to resume, albeit at a slower rate than with the present degree of confinement.

Ultimately, in order to be able to predict and understand the future behaviour of the Waiho River, a better understanding of the system itself is required. As this study has shown, understanding is presently limited. In addition, there is a severe lack of data for the behaviour of the Waiho River and its fan, which makes it difficult to model and manage effectively. Ongoing and regular monitoring of a number of components in this system would provide valuable information for how and where it is changing.

At present Lidar data are being collected, and are proving to be invaluable to understanding where the fan is aggrading and future aggradation

patterns. In addition, advances in Structure from Motion software may allow for event-scale aggradation patterns, volumes and rates to be calculated from aerial imagery.

However, other data sets would be valuable. These include:

- Bedload and suspended sediment load. At present bedload data acquisition is extremely difficult, and in reality unfeasible, due to the braided nature of the Waiho River and its large-calibre bedload during floods. However, should a method of acquisition become available, then it its use on the Waiho would be invaluable.
- River flow. Flow data are also difficult to collect due to the reasons described above. However, to accurately model a river system, this information is vital.
- Impact of glacial behaviour and fault rupture upon sediment supply
- Rainfall
- Braid formations

With these types of data sets, other forms of physical models as well as numerical models could be used to study the behaviour of the Waiho River and fan, assist with further microscale modelling studies, and in general improve our understanding of such a complicated, powerful and dynamic system so that we may better manage its impact on the human environment.

Bibliography

Acheson, A. R. (1968). *River control and drainage in New Zealand: and some comparisons with overseas practices*. Ministry of Works.

Alexander, D., Davies, T. R. H., and Shulmeister, J. (2014). Formation of the Waiho Loop terminal moraine, New Zealand. *Journal of Quaternary Science*.

Armstrong, L. (2003). *Bank erosion and sediment transport in a microscale straight river*. Doctoral thesis, Universite Paris, 7, Denis Diderot, France.

Ashmore, P. (1991). Channel morphology and bed load pulses in braided, gravel-bed streams. *Geografiska Annaler. Series A. Physical Geography*, pages 37–52.

Aulakh, B. and Mills, L. (2016). Franz Josef flooding: right in the firing line. NZ Herald.

Barr, D. I. H. (1968). Discussion of scale model of urban runoff from storm rainfall. *Journal of Hydraulics Division (American Society of Civil Engineers)*, 94(2):586–588.

Beaty, C. B. (1970). Age and estimated rate of accumulation of an alluvial fan, White Mountains, California, U.S.A. *American Journal of Science*, 268:50–70.

Bertoldi, W., Zanoni, L., and Tubino, M. (2009). Planform dynamics of braided streams. *Earth Surface Processes and Landforms*, 34:547–557.

Blair, T. C. and McPherson, J. G. (1994a). Alluvial fans and their natural distinction from rivers based on morphology, hydraulic processes, sedimentary processes and facies assemblages. *Journal of Sediment and Research*, A64:450489.

Blair, T. C. and McPherson, J. G. (1994b). *Geomorphology of Desert Environments*, Alluvial fan processes and forms, pages 354–402. Chapman and Hall, London.

Bristow, C. and Best, J. (1993). Braided rivers: perspectives and problems. *Geological Society, London, Special Publications*, 75(1):1–11.

Bryant, M., Falk, P., and Paola, C. (1995). Experimental study of avulsion frequency and rate of deposition. *Geology*, 23:365–368.

Bull, M. P. (2004). *New Zealand Tales and Tours: South Island Adventures*, Tour four - Westland, page 268. Trafford Publishing.

Bull, W. B. (1964). Geomorphology of segmented alluvial fans in western Fresno County, California. *U.S. Geological Survey Professional Paper*, 352-E:89 – 128.

Campbell, B. (2012). A microscale modelling experiment to investigate the effects of an avulsion of the Waiho River into the Tatare River, south Westland, New Zealand. Honours dissertation, University of Canterbury, New Zealand.

Carrivick, J. L. and Rushmer, E. L. (2009). Inter-and intra-catchment variations in proglacial geomorphology: an example from Franz Josef glacier and Fox glacier, New Zealand. *Arctic, Antarctic, and Alpine Research*, 41(1):18–36.

Chorley, R. J. (1967). Models in geomorphology. *Models in Geography*, pages 59–96.

Clarke, L. E. (2015). Experimental alluvial fans: advances in understanding of fan dynamics and processes. *Geomorphology*, 244:135–145.

Clarke, L. E., Quine, T. A., and Nicholas, A. P. (2008). *Sediment Dynamics in Changing Environments*, An evaluation of the role of physical models in exploring form-procss feedbacks in alluvial fans, pages 175–183. International Association of Hydrological Sciences.

Clarke, L. E., Quine, T. A., and Nicholas, A. P. (2010). An experimental investigation of autogenic behaviour during alluvial fan evolution. *Geomorphology*, 115:278–285.

Clarkson, P. J. (1999). Small-scale hydraulic modelling of alluvial fans. Master of engineering, Lincoln University, New Zealand.

Darboux, F. and Huang, C. (2003). An instantaneous profile laser scanner to measure soil surface microtopography. *Soil Science Society of American Journal*, 67(1):92–99.

Davies, T., Campbell, B., Hall, B., and Gomez, C. (2013). Recent behaviour and sustainable future management of the Waiho River, Westland, New Zealand. *Journal of Hydrology (New Zealand)*, 52(1):27–42.

Davies, T. and Lee, A. (1988). Physical hydraulic modelling of width reduction and bed level change in braided rivers. *Journal of Hydrology (New Zealand)*, pages 113–127.

Davies, T. R. and McSaveney, M. (2006). Geomorphic constraints on the management of bedload-dominated rivers. *Journal of Hydrology (New Zealand)*, 45(2):111.

Davies, T. R. H. (1987). *Sediment Transport in Gravel-Bed Rivers*, Problems of bedload transport in gravel-bed braided rivers, pages 793–828. J. Wiley and Sons.

Davies, T. R. H. (1997). Long-term management of facilities on an active alluvial fan Waiho River fan, Westland, New Zealand. *Journal of Hydrology (New Zealand)*, 36(2):127–145.

Davies, T. R. H. and Korup, O. (2007). Persistent alluvial fanhead trenching resulting fromlarge, infrequent sediment inputs. *Earth Surface Processes and Landforms*, 32:725742.

Davies, T. R. H. and McSaveney, M. J. (2001). Anthropogenic fanhead aggradation, Waiho River, Westland, New Zealand. In Mosley, M. P., editor, *Gravel-Bed Rivers V*, pages 531–553, Wellington. New Zealand Hydrological Society.

Davies, T. R. H. and McSaveney, M. J. (2008). Principles of sustainable development on fans. *Journal of Hydrology (New Zealand)*, 47(1):43 – 65.

Davies, T. R. H., McSaveney, M. J., and Clarkson, P. J. (2003a). Anthropic aggradation of the Waiho River, Westland, New Zealand microscale modelling. *Earth Surface Processes and Landforms*, 28:209–218.

Davies, T. R. H., McSaveney, M. J., and Doscher, C. (2005). Final report on research project no. 03/499 monitoring and effects of landslide-induced aggradation in the Poerua valley, Westland. Technical report, Earthquake Commission, Wellington, New Zealand.

Davies, T. R. H. and Scott, B. K. (1997). Dambreak flood hazard from the Callery River, Westland, New Zealand. *Journal of Hydrology (New Zealand)*, 36(1):1 –13.

Davies, T. R. H., Smart, C. C., and Turnbull, J. M. (2003b). Water and sediment outbursts from advanced Franz Josef glacier, New Zealand. *Earth Surface Processes and Landforms*, 28:1081–1096.

Davinroy, R. D. (1994). Physical sediment modelling of the Mississippi River on a micro scale. Master of science, University of Missouri-Rolla, Rolla, Mo.

Denny, C. S. (1965). Alluvial fans in the Death Valley region of California and Nevada. *U.S. Geological Survey Professional Paper*, 466:62pp.

Denny, C. S. (1967). Fans and pediments. *American Journal of Science*, 265:81–105.

Eckis, R. (1928). Alluvial fans of the Cucamonga district, southern California. *Journal of Geology*, 36:225–247.

Fleming, G. (2002). *Flood risk management: learning to live with rivers.* Thomas Telford.

Gaines, R. and Smith, R. (2002). Micro-scale loose-bed physical models. In *Hydraulic Measurements and Experimental Methods*, pages 1–12.

Gaines, R. A. and Maynord, S. T. (2001). Microscale loose-bed hydraulic models. *Journal of Hydraulic Engineering*, 27:335 – 339.

Grant, A. P. (1948). Channel improvements in alluvial streams. *Proceedings, New Zealand Institute of Engineers*, 34:231–279.

Grant, G. E. (1997). Critical flow constrains flow hydraulics in mobile-bed streams: a new hypothesis. *Water Resources Research*, 33:349–358.

Guerit, L., Mètivier, L. G., Devauchelle, O., Lajeunesse, E., and Barrier, L. (2014). Laboratory alluvial fans in one dimension. *Physics Review*, 90.

Harvey, A. M., Mather, A. E., and Stokes, M., editors (2005). *Alluvial Fans: Geomorphology, Sedimentology, Dynamics*, volume 251. Geological Society Special Publications, London. PP 1- 7.

Henderson, F. M. (1966). *Open-Channel Flow.* Macmillan.

Henderson, R. and Thompson, S. M. (1999). Extreme rainfalls in the Southern Alps of New Zealand. *Journal of Hydrology (New Zealand)*, 38:309–330.

Hoink, T., Lenardic, A., and Jellinek, A. M. (2013). Earths thermal evolution with multiple convection modes: A monte-carlo approach. *Physics of the Earth and Planetary Interiors*, 221:22–26.

Hong, L. B. and Davies, T. R. H. (1979). A study of stream braiding. *Geological Society of American Bulletin*, 90:10941095.

Hooke, R. (1967). Processes on arid-region alluvial fans. *Journal of Geology*, 75:438–460.

Hooke, R. (1968). Model geology; prototype and laboratory streams; discussion. *Geological Society of American Bulletin*, 79:391394.

Hunt, C. B. and Mabey, D. R. (1966). Stratigraphy and structure, Death Valley, California. *U.S. Geological Survey Professional Paper*, 494-A:162pp.

Jerolmack, D. J. (2011). Causes and effects of noise in landscape dynamics. *EOS, transactions, American geophysical Union*, 92(44):385–386.

Jerolmack, D. J. and Mohrig, D. (2007). Conditions for branching of depositional rivers. *Geology*, 35(5):463466.

Kleinhans, M. G., Ferguson, R. I., Lane, S. N., and Hardy, R. J. (2013). Splitting rivers at their seams: bifurcations and avulsion. *Earth Surface Processes and Landforms*, 38:47–61.

Knighton, A. D. (1998). *Fluvial Forms and Processes: A New Perspective*, Chapter five. Edward Arnold, London.

Kochel, R. C. (1990). *Alluvial fans: a field approach*, Humid alluvial fans of the Appalachian Mountains, pages 109 – 129. Wiley, Chichester.

Lajeunesse, E., Malverti, L., Lancien, P., Armstrong, L., Mètivier, F., Coleman, S., Smith, C. E., Davies, T., Cantelli, A., and Parker, G. (2010). Fluvial and subaqueous morphodynamics of laminar and near-laminar flows: A synthesis. *Sedimentology*, 57(1):1–26.

Langridge, R. M., Howard, J. D., Buxton, R., and Ries, W. F. (2016). A natural hazard assessment for the township of Franz Josef, Westland district. Consultancy Report 2016/33, GNS Science.

Lenardi, A., Moresi, L.-N., and Mulhaus, H. (2003). Longevity and stability of cratonic lithosphere: insights from numerical simulations of coupled

mantle convection and continental tectonics. *Journal of Geophysical Research*, 108(B6):2303.

Malverti, L., Lajeunesse, E., and Mètivier, F. (2008). Small is beautiful: upscaling from microscale laminar to natural turbulent rivers. *Journal of Geophysical Resarch of Earth Surfaces*, 113.

Maynord, S. T. (2006). Evaluation of the micromodel: an extremely small-scale movable bed model. *Journal of Hydraulic Engineering*, 132(4):343–353.

McKendry, I. G. (1992). Numerical simulation of sea breeze interactions over the Auckland region, New Zealand. *New Zealand Journal of Geology and Geophysics*, 35(1):9–20.

McSaveney, M. J. and Davies, T. R. H. (1998). Natural hazard assessment for the township of Franz Josef Glacier and its environs. Technical Report Client Report 43714B.10, Institue of Geological and Nuclear Sciences Limited.

Mètivier, F. and Barrier, L. (2012). *Gravel-bed rivers: processes, tools, environments*, Alluvial landscape evolution: what do we know about metamorphosis of gravel-bed meandering and braided streams?, pages 474–501. John Wiley and Sons, Ltd., Chichester.

Mètivier, F. and Meunier, P. (2003). Input and output mass flux correlations in an experimental braided stream. implications on the dynamics of bed load transport. *Journal of Hydrology*, 271:2238.

Mosley, M. P. and Zimpfer, G. L. (1978). Hardware models in geomorphology. *Progress in Physical Geography*, 2:438–461.

Nevins, T. H. F. (1969). River training the single thread channel. *New Zealand Engineering*, 15:367–73.

Paola, C., Straub, K., Mohrig, D., and Reinhardt, L. (2009). The "unreasonable effectivenes" of stratigraphic and geomorphic experiments. *Earth Science Review*, 97:143.

Peakall, J., Ashworth, P., and Best, J. (1996). *The Scientific Nature of Geomorphology*, Physical modelling in fluvial geomorphology: principles, applications, and unresolved issues, pages 221–253. John Wiley, Chichester, U. K.

Peakall, J. and Warburton, J. (1996). Surface tension in small hydraulic river models the significance of the weber number. *Journal of Hydrology (New Zealand)*, 35:199212.

Piegay, H., Grant, G., Nakamura, F., and Trustrum, N. (2006). *Braided rivers: process, deposits, ecology and management*, Braided river management: from assessment of river behaviour to improved sustainable development. International Association of Sedimentologists.

Popescu, I. (2014). *Computational Hydraulics*, Chapter 1: modelling theory, pages 1 – 10. IWA Publishing, London.

Rachocki, A. (1981). *Alluvial Fans*. John Wiley and Sons Ltd., Chichester, London.

Reitz, M. D. and Jerolmack, D. J. (2012). Experimental alluvial fan evolution: channel dynamics, slope controls, and shoreline growth. *Journal of Geophysical Research*, 117.

Reitz, M. D., Jerolmack, D. J., and Swenson, J. B. (2010). Flooding and flow path selection on alluvial fans and deltas. *Geophysical Research Letters*, 37.

Robinson, T. R. and Davies, T. R. H. (2013). Review article: potential geomorphic consequences of a future great (mw = 8.0+) alpine fault earthquake, South Island, New Zealand. *Natural Hazards and Earth System Science*, 13:22792299.

Ryder, J. M. (1971). Some aspects of the morphometry of paraglacial alluvial fans in south-central British Columbia. *Canadian Journal of Earth Science*, 8:1252–1264.

Schumm, S., Mosley, M., and Weaver, W. (1987). *Experimental Fluvial Geomorphology*. John Wiley, New York.

Schumm, S. A. (1977). *The Fluvial System*. Wiley, New York.

Schumm, S. A. (1985). Patterns of alluvial rivers. *Annual Review of Earth Planetary Science*, 13:5–27.

Tal, M. and Paola, C. (2010). Effects of vegetation on channel morphodynamics: results and insights from laboratory experiments. *Earth Surface Processes and Landforms*, 35:1014–1028.

Thornbury, W. B. (1954). *Principles of Geomorphology.* John Wiley, New York.

Trenberth, K. E., Branstator, G. W., Karoly, D., Kumar, A., Lau, N. G., and Ropelewski, C. (1998). Progress during toga in understanding and modelling global teleconnections associated with tropical sea surface temperatures. *Journal of Geophysical Research*, 103(C7):14291–14324.

Warburton, J. (1996). A brief review of hydraulic modelling of braided gravel-bed rivers in New Zealand. *Journal of Hydrology (New Zealand)*, 35(2):157–173.

Wasson, R. J. (1977). Last-glacial alluvial fan sedimentation in the lower Derwent valley, Tasmania. *Sedimentology*, 24:781–799.

Whipple, K. X., Parker, G., Paola, C., and Mohrig, D. (1998). Channel dynamics, sediment transport, and the slope of alluvial fans: experimental study. *Journal of Geology*, 106:677 –693.

Whitehouse, I. E. and McSaveney, M. J. (1990). *Alluvial fans: a field approach*, Geomorphic appraisals for development on two steep, active alluvial fans, Mt Cook, New Zealand, pages 369–384. Wiley, Chichester.

Wild, M. A. (2012). *Growth dynamics of braided gravel-bed river deltas in New Zealand.* phdthesis, University of Canterbury, New Zealand. 215p.

Zarn, B. and Davies, T. R. H. (1994). The significance of processes on alluvial fans to hazard assessment. *Zeitschrift fr Geomorphologie*, 38(4):487–500.

Appendices

Appendix A: aerial imagery of the Waiho fan

Aerial imagery of the Upper Waiho Fan taken from 1948 to 2013.

Figure 1: 1948 aerial imagery

Figure 2: 1964 aerial imagery

Figure 3: 1973 aerial imagery

Figure 4: 1979 aerial imagery

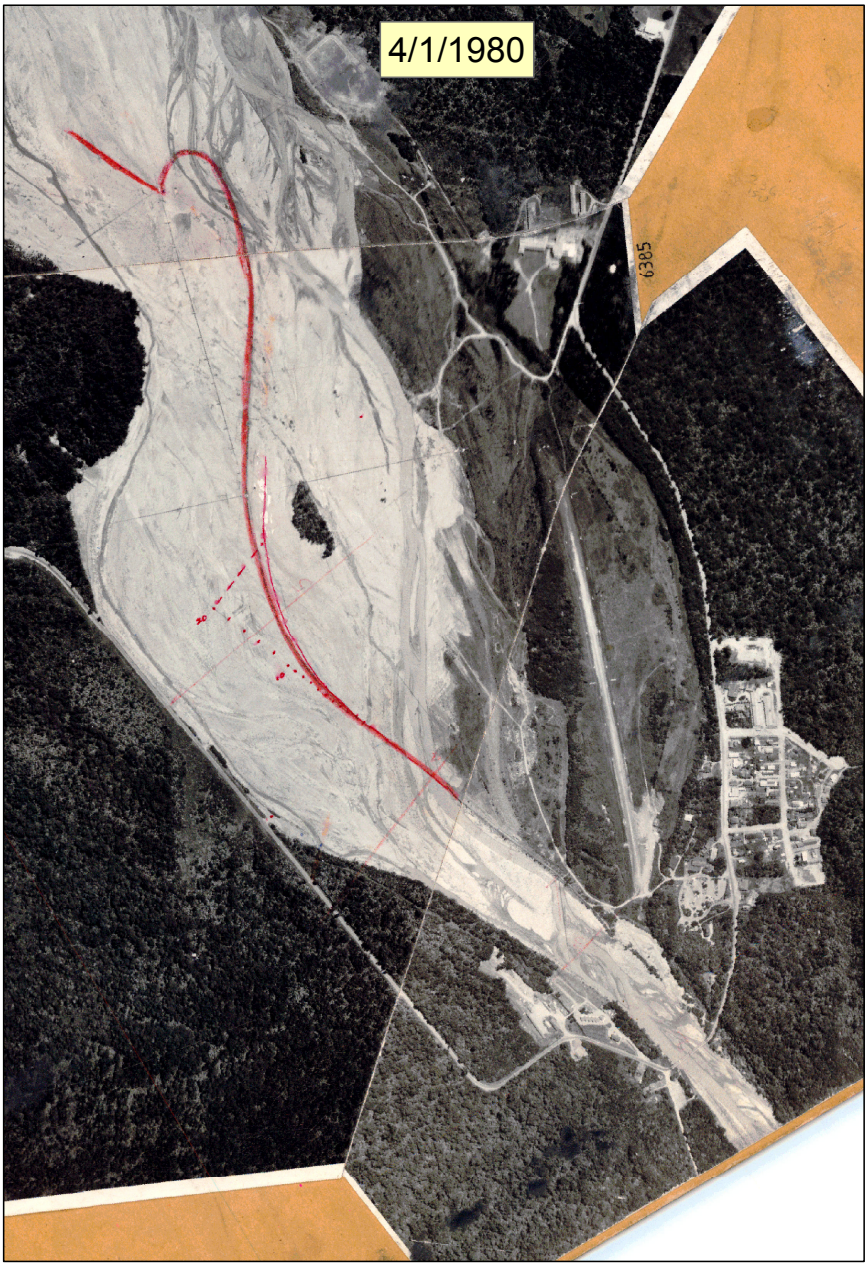

Figure 5: 1980 aerial imagery

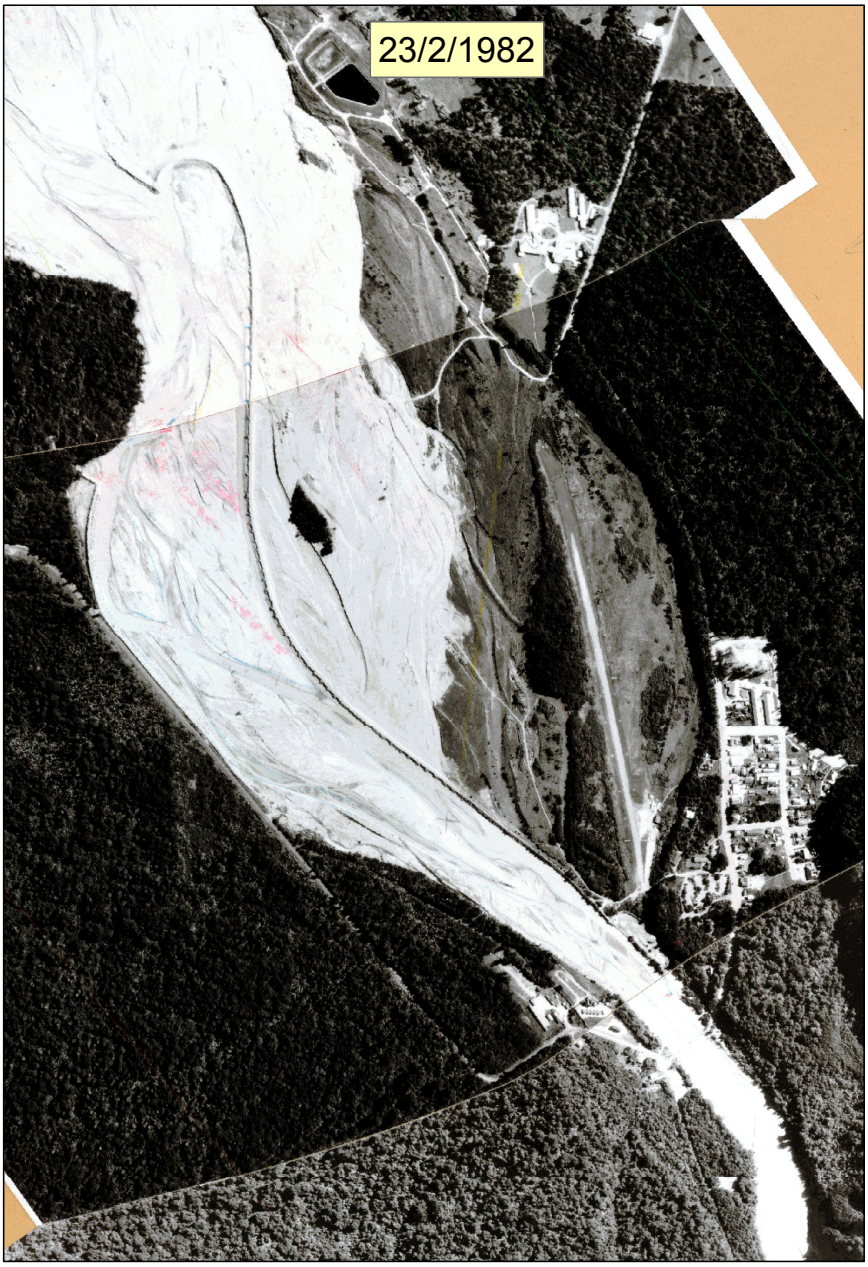

Figure 6: 1982 aerial imagery

Figure 7: 1985 aerial imagery

Figure 8: 1990 aerial imagery

Figure 9: 1994 aerial imagery

Figure 10: 2002 aerial imagery

Figure 11: 2004 aerial imagery

Figure 12: 2011 aerial imagery

Figure 13: 2013 aerial imagery

Appendix B: digital vernier calliper elevation data

Digital vernier calliper elevation data for the intial steady input experiment (S1).

Table 1: Point measurements from the INITIAL NATURAL SCENARIO. Points were taken in the upper, middle and lower sections of the fan at set intervals. Pink represents aggradation, green degradation, and blue no net change (values +/-1 around 0mm). EC stands for elevation change, and was calculated by substracting the previous elevation from the most recent elevation.

Point	Nrth	East	Initial (Hr33)	Hr35	EC (2hrs)	Hr36	EC (1hr)	Hr37	EC (1hr)	Hr38	EC (1hr)	Hr39	EC (1hr)	Hr40	EC (1hr)
1	30	20	35.49	35.46	0.03	31.78	3.68	30.16	1.62	30.18	-0.02	30.13	0.05	29.88	0.25
2	30	40	26.33	23	3.33	20.64	2.36	21.4	-0.76	20.04	1.36	18.47	1.57	15.84	2.63
3	30	60	17.45	12.62	4.83	13.85	-1.23	12.06	1.79	9.74	2.32	9.08	0.66	7.7	1.38
4	45	20	35.31	33.35	1.96	31.4	1.95	32.07	-0.67	31.52	0.55	30.34	1.18	29.67	0.67
5	45	40	29.32	25.05	4.27	23.97	1.08	24.1	-0.13	24.52	-0.42	22.22	2.3	20.54	1.68
6	45	60	22.01	17.47	4.54	17.5	-0.03	16.11	1.39	15.04	1.07	13.63	1.41	13.83	-0.2
7	60	20	38.56	35.58	2.98	34.44	1.14	39.33	-4.89	34.47	4.86	32.32	2.15	31.77	0.55
8	60	40	31.04	28.49	2.55	24.86	3.63	25.72	-0.86	25.23	0.49	25.37	-0.14	25.21	0.16
9	60	60	25	21.22	3.78	20.55	0.67	20.54	0.01	19.64	0.9	18.7	0.94	17.05	1.65
10	105	90	51.32	49.57	1.75	49.37	0.2	48.94	0.43	49.52	-0.58	49.11	0.41	48.63	0.48
11	105	120	43.59	40.34	3.25	39.99	0.35	40.01	-0.02	38.11	1.9	38.7	-0.59	37.78	0.92
12	105	150	34.1	32.36	1.74	31.61	0.75	29.93	1.68	28.84	1.09	28.07	0.77	28.21	-0.14
13	165	65	51.79	51.86	-0.07	51.66	0.2	51.38	0.28	51.36	0.02	51.9	-0.54	51.73	0.17
14	165	90	54.12	52.98	1.14	52.97	0.01	53.9	-0.93	52.68	1.22	52.01	0.67	51.43	0.58
15	165	115	47.02	46.41	0.61	45.32	1.09	46.33	-1.01	46.13	0.2	48.95	-2.82	47.93	1.02

Table 2: Digital Vernier Calliper elevation data for the current confinement alignment stage

Point	Nrth	East	Hr40	Hr41	EC	Hr42	EC	Hr43	EC	Hr44	EC	Hr45	EC
2	30	65	31.13	29.22	1.91	27.57	1.65	23.36	4.21	22.6	0.76	20.03	2.57
3	30	75	31.06	30.12	0.94	27.8	2.32	24.95	2.85	25	-0.05	22.41	2.59
4	40	55	41.06	35.92	5.14	32.35	3.57	30.62	1.73	28.48	2.14	23.91	4.57
5	40	65	39.26	35.61	3.65	31.79	3.82	29.52	2.27	28.78	0.74	24.68	4.1
6	40	75	33.13	32.87	0.26	29.69	3.18	26.06	3.63	24.94	1.12	23.17	1.77
7	60	55	45.47	39.97	5.5	39.79	0.18	36.71	3.08	32.95	3.76	32.64	0.31
8	60	65	43.17	41.43	1.74	38.33	3.1	34.5	3.83	34.92	-0.42	33.45	1.47
9	60	75	37.82	36.6	1.22	35.54	1.06	33.62	1.92	30.95	2.67	29.17	1.78
10	80	55	49.99	47.6	2.39	45.39	2.21	43.34	2.05	42.24	1.1	38.99	3.25
11	80	65	47.94	44.75	3.19	43.38	1.37	40.61	2.77	39.9	0.71	38.52	1.38
12	80	75	43.29	41.55	1.74	41.33	0.22	40.59	0.74	39.04	1.55	36.23	2.81
13	100	55	54.64	50.5	4.14	49.52	0.98	47.67	1.85	47.12	0.55	44.98	2.14
14	100	65	48.96	48.38	0.58	46.52	1.86	45.71	0.81	45.96	-0.25	43.81	2.15
15	100	75	42.23	43.26	-1.03	42.58	0.68	41.34	1.24	39.92	1.42	37.51	2.41
16	120	55	53.56	52.96	0.6	52.85	0.11	53.64	-0.79	48.8	4.84	51.5	-2.7
17	120	65	46.76	47.99	-1.23	47.88	0.11	45.45	2.43	48.08	-2.63	43.24	4.84
18	120	75	45.72	45.04	0.68	45.16	-0.12	43.6	1.56	43.32	0.28	41.45	1.87

Table 3: Digital Vernier Calliper elevation data for the current confinement alignment stage continued...

Point	Nrth	East	Hr46	EC	Hr47	EC	Hr48	EC	Hr49	EC	Hr50	EC
2	30	65	17.95	2.08	14.81	3.14	11.87	2.94	9.95	1.92	9.15	0.8
3	30	75	19.35	3.06	16.36	2.99	14.26	2.1	10.09	4.17	10.19	-0.1
4	40	55	24.26	-0.35	22.02	2.24	20.41	1.61	18.87	1.54	16.17	2.7
5	40	65	24.54	0.14	21.47	3.07	18.4	3.07	14.37	4.03	13.35	1.02
6	40	75	20.98	2.19	18.89	2.09	15.3	3.59	14.72	0.58	14.98	-0.26
7	60	55	27.48	5.16	26.67	0.81	26.13	0.54	21.43	4.7	19.73	1.7
8	60	65	30.39	3.06	27.72	2.67	25.71	2.01	22.8	2.91	19.43	3.37
9	60	75	29.24	-0.07	26.65	2.59	24.38	2.27	21.77	2.61	22.29	-0.52
10	80	55	37.53	1.46	36.36	1.17	36.71	-0.35	33.51	3.2	30.79	2.72
11	80	65	35.62	2.9	34.62	1	32.35	2.27	29.51	2.84	27.91	1.6
12	80	75	35.44	0.79	34.54	0.9	32.44	2.1	31	1.44	28.63	2.37
13	100	55	42.77	2.21	42.83	-0.06	42.51	0.32	39.14	3.37	37.61	1.53
14	100	65	39.64	4.17	39.59	0.05	38.72	0.87	36.51	2.21	35.43	1.08
15	100	75	37.42	0.09	37.13	0.29	35.3	1.83	34.64	0.66	32.19	2.45
16	120	55	48.16	3.34	47.64	0.52	49.13	-1.49	44.21	4.92	42.88	1.33
17	120	65	44.35	-1.11	43.18	1.17	39.35	3.83	39.41	-0.06	38.49	0.92
18	120	75	39.84	1.61	38.79	1.05	38.66	0.13	38.26	0.4	35.78	2.48

Table 4: Digital Vernier Calliper elevation data for the intermediate stopbank alignment

Point	Nrth	East	Hr50	Hr51	EC	Hr52	EC	Hr53	EC	Hr54	EC	Hr55	EC
1	20	45	40.68	32.31	8.37	29.52	2.79	28.21	1.31	23.88	4.33	22.16	1.72
2	20	55	29.38	25.25	4.13	22.5	2.75	20.16	2.34	17.29	2.87	15.84	1.45
3	20	65	6.39	19.85	-13.46	18.31	1.54	14.84	3.47	13.36	1.48	11.29	2.07
4	40	30	45.69	45.12	0.57	41.37	3.75	39.88	1.49	36.1	3.78	31.39	4.71
5	40	45	41.13	35.59	5.54	32.48	3.11	30.79	1.69	27.35	3.44	26.81	0.54
6	40	60	13.7	26.36	-12.66	25.16	1.2	23.34	1.82	20.61	2.73	20.03	0.58
7	40	75	11.91	13.06	-1.15	11.93	1.13	11.89	0.04	11.74	0.15	14.6	-2.86
8	60	15	57.37	57.7	-0.33	52.3	5.4	50.45	1.85	49.97	0.48	45.28	4.69
9	60	30	51.33	46.43	4.9	46.04	0.39	44.09	1.95	40.91	3.18	41.21	-0.3
10	60	45	45.15	37.17	7.98	36.81	0.36	36.36	0.45	33.41	2.95	32.2	1.21
11	60	60	16.56	16.25	0.31	15.55	0.7	16.12	-0.57	16.7	-0.58	16.03	0.67
12	60	75	18.31	18.16	0.15	18.7	-0.54	18.42	0.28	18.21	0.21	17.82	0.39
13	80	20	60.41	54.16	6.25	51.82	2.34	51.92	-0.1	50.09	1.83	50.88	-0.79
14	80	70	21.81	23.83	-2.02	24.1	-0.27	24.55	-0.45	24.46	0.09	24.06	0.4
15	100	20	61.25	59.2	2.05	57.72	1.48	55.28	2.44	55.17	0.11	53.73	1.44
16	100	35	63.4	61.42	1.98	59.51	1.91	58.45	1.06	57.49	0.96	55.4	2.09
17	100	60	32.8	32.93	-0.13	32.96	-0.03	32.73	0.23	33.06	-0.33	32.42	0.64
18	100	70	31.28	31.44	-0.16	31.81	-0.37	31.44	0.37	30.83	0.61	30.74	0.09
19	120	15	68.23	65.65	2.58	66.05	-0.4	63.49	2.56	63.69	-0.2	64.15	-0.46
20	120	35	62.69	61.53	1.16	62.35	-0.82	64.77	-2.42	63.86	0.91	63.96	-0.1
21	120	55	40.51	40.21	0.3	39.53	0.68	40.41	-0.88	40.03	0.38	40.63	-0.6
22	120	75	33.48	33.91	-0.43	34.21	-0.3	34.24	-0.03	34.04	0.2	34.15	-0.11

Table 5: Digital Vernier Calliper elevation data for the intermediate stopbank alignment continued...

Point	Nrth	East	Hr56	EC	Hr57	EC	Hr58	EC	Hr59	EC	Hr60	EC
1	20	45	20.23	1.93	19.21	1.02	18.18	1.03	17.43	0.75	14.6	2.83
2	20	55	14.7	1.14	14.73	-0.03	12.49	2.24	10.23	2.26	8.7	1.53
3	20	65	10.43	0.86	8.9	1.53	7.46	1.44	6.24	1.22	3.69	2.55
4	40	30	30.31	1.08	28.36	1.95	28.37	-0.01	28.21	0.16	26.95	1.26
5	40	45	26.89	-0.08	25.87	1.02	24.46	1.41	22.69	1.77	20.98	1.71
6	40	60	20.26	-0.23	18.65	1.61	16.1	2.55	15.85	0.25	15.3	0.55
7	40	75	13.9	0.7	11.75	2.15	12.95	-1.2	12.79	0.16	9.18	3.61
8	60	15	41.84	3.44	41.43	0.41	41.49	-0.06	41.88	-0.39	41.13	0.75
9	60	30	37.65	3.56	37.89	-0.24	36.99	0.9	34.82	2.17	33.59	1.23
10	60	45	33.28	-1.08	33.11	0.17	30.82	2.29	32.93	-2.11	28.83	4.1
11	60	60	20.47	-4.44	21.03	-0.56	20.7	0.33	20.29	0.41	20.18	0.11
12	60	75	17.47	0.35	15.67	1.8	16.16	-0.49	16.06	0.1	15.05	1.01
13	80	20	50.19	0.69	49.29	0.9	46.12	3.17	46.61	-0.49	45.82	0.79
14	80	70	23.92	0.14	23.54	0.38	23.67	-0.13	24.12	-0.45	24.65	-0.53
15	100	20	53.84	-0.11	52.02	1.82	51.5	0.52	50.01	1.49	47.3	2.71
16	100	35	55.45	-0.05	55.38	0.07	55.95	-0.57	55.03	0.92	54.06	0.97
17	100	60	32.84	-0.42	33.15	-0.31	33.49	-0.34	33.75	-0.26	33.5	0.25
18	100	70	30.43	0.31	30.31	0.12	31.13	-0.82	30.32	0.81	31.03	-0.71
19	120	15	59.47	4.68	59.07	0.4	57.91	1.16	54.87	3.04	56.4	-1.53
20	120	35	64.04	-0.08	63.55	0.49	61.45	2.1	55.79	5.66	59.26	-3.47
21	120	55	39.99	0.64	40.01	-0.02	40.75	-0.74	39.81	0.94	41.42	-1.61
22	120	75	33.77	0.38	33.69	0.08	33.99	-0.3	33.41	0.58	33.6	-0.19

Table 6: Digital Vernier Calliper elevation data for the extreme stopbank alignment

Point	Nrth	East	Hr60	Hr61	EC	Hr62	EC	Hr63	EC	Hr64	EC	Hr65	EC
1	25	115	59.82	51.68	8.14	47.17	4.51	47.11	0.06	46.54	0.57	46.1	0.44
2	25	135	24.07	32.66	-8.59	28.85	3.81	28.41	0.44	26.67	1.74	25.74	0.93
3	25	150	13.74	20.89	-7.15	15.93	4.96	17.8	-1.87	17.92	-0.12	16.87	1.05
4	25	165	6.48	6.21	0.27	11.71	-5.5	12.08	-0.37	10.09	1.99	9.06	1.03
5	40	105	62.65	55.78	6.87	51.76	4.02	51.5	0.26	50.53	0.97	50.59	-0.06
6	40	130	27.47	27.22	0.25	26.9	0.32	30.68	-3.78	30.54	0.14	30.79	-0.25
7	40	150	15.06	17.98	-2.92	23.07	-5.09	21.49	1.58	19.09	2.4	18.4	0.69
8	40	170	9.54	9.91	-0.37	10.12	-0.21	9.8	0.32	11.23	-1.43	12.96	-1.73
9	55	85	73.72	66.27	7.45	64.82	1.45	65.21	-0.39	65.65	-0.44	64.39	1.26
10	55	105	63.28	57.1	6.18	54.68	2.42	51.4	3.28	50.63	0.77	50.62	0.01
11	55	125	34.5	34.41	0.09	33.83	0.58	33.3	0.53	34.2	-0.9	33.12	1.08
12	55	145	25.83	25.77	0.06	30.25	-4.48	28.03	2.22	26.35	1.68	24.87	1.48
13	55	165	18.18	18.08	0.1	18.07	0.01	17.66	0.41	18.98	-1.32	20.57	-1.59
14	55	180	14.51	14.78	-0.27	14.45	0.33	14.5	-0.05	14.25	0.25	16.35	-2.1
15	75	75	72.24	74.08	-1.84	73.55	0.53	71.83	1.72	71.95	-0.12	71.63	0.32
16	75	100	68.68	67.22	1.46	63.36	3.86	61.17	2.19	61.48	-0.31	61.23	0.25
17	75	125	41.17	41.48	-0.31	42.62	-1.14	44	-1.38	43.9	0.1	39.49	4.41
18	75	170	23.01	22.45	0.56	22.37	0.08	22.65	-0.28	22.79	-0.14	21.62	1.17
19	100	75	76.09	77.49	-1.4	76.99	0.5	75.39	1.6	75.85	-0.46	74.56	1.29
20	100	95	72.16	71.72	0.44	65.14	6.58	62.05	3.09	61.15	0.9	59.9	1.25
21	100	120	49.58	48.27	1.31	48.64	-0.37	48.81	-0.17	47.54	1.27	47.68	-0.14
22	100	150	40.23	40.55	-0.32	40.36	0.19	40.08	0.28	40.19	-0.11	38.73	1.46
23	100	170	31.68	31.11	0.57	31.1	0.01	31.3	-0.2	30.11	1.19	30.89	-0.78
24	125	70	80.1	78.02	2.08	77.44	0.58	77.47	-0.03	76.86	0.61	76.61	0.25
25	125	95	74.11	73.66	0.45	71.27	2.39	66.66	4.61	64.02	2.64	62.89	1.13
26	125	120	58.93	58.57	0.36	58.92	-0.35	59.04	-0.12	58.26	0.78	59.18	-0.92
27	125	145	49.38	49.08	0.3	48.74	0.34	48.53	0.21	49.01	-0.48	48.56	0.45
28	125	165	39.05	39.05	0	38.69	0.36	39.06	-0.37	38.91	0.15	37.48	1.43
29	150	60	78.56	76.01	2.55	75.86	0.15	76.92	-1.06	76.33	0.59	78.04	-1.71
30	150	80	77.17	76.46	0.71	75.66	0.8	74.36	1.3	72.92	1.44	72.79	0.13
31	150	105	76.3	76.43	-0.13	72.39	4.04	69.96	2.43	69.4	0.56	68.7	0.7
32	150	125	66.69	69.48	-2.79	66.14	3.34	66.01	0.13	67.71	-1.7	63.05	4.66

Table 7: Digital Vernier Calliper elevation data for the extreme stopbank alignment continued...

Point	Nrth	East	Hr66	EC	Hr67	EC	Hr68	EC	Hr69	EC	Hr70	EC
1	25	115	45.91	0.19	44.04	1.87	45.04	-1	44.65	0.39	42.5	2.15
2	25	135	26.92	-1.18	22.8	4.12	23.24	-0.44	24.85	-1.61	22.26	2.59
3	25	150	15.03	1.84	14.04	0.99	14.88	-0.84	13.15	1.73	13.69	-0.54
4	25	165	8.05	1.01	8.09	-0.04	9.32	-1.23	6.97	2.35	6.12	0.85
5	40	105	49.7	0.89	48.89	0.81	50.08	-1.19	47.94	2.14	46.8	1.14
6	40	130	31.03	-0.24	29.28	1.75	30.23	-0.95	29.6	0.63	28.69	0.91
7	40	150	18.04	0.36	18.22	-0.18	17.57	0.65	16.9	0.67	16.14	0.76
8	40	170	12.99	-0.03	11.99	1	12.81	-0.82	12.02	0.79	11.15	0.87
9	55	85	64.68	-0.29	64.07	0.61	64.48	-0.41	64.07	0.41	62.9	1.17
10	55	105	47.85	2.77	47.2	0.65	47.8	-0.6	47.57	0.23	48.05	-0.48
11	55	125	34.03	-0.91	34.43	-0.4	35.89	-1.46	35.47	0.42	34.87	0.6
12	55	145	24.66	0.21	25.03	-0.37	22.92	2.11	24.79	-1.87	24.04	0.75
13	55	165	19.61	0.96	20.08	-0.47	18.74	1.34	17.46	1.28	17.91	-0.45
14	55	180	14.76	1.59	14.96	-0.2	15.04	-0.08	13.93	1.11	13.31	0.62
15	75	75	72.16	-0.53	71.17	0.99	71.28	-0.11	71.42	-0.14	71.81	-0.39
16	75	100	56.5	4.73	56.25	0.25	56.81	-0.56	55.12	1.69	54.08	1.04
17	75	125	40.07	-0.58	40.05	0.02	37.7	2.35	39.51	-1.81	39.04	0.47
18	75	170	21.88	-0.26	20.81	1.07	23.07	-2.26	22.3	0.77	20.29	2.01
19	100	75	74.22	0.34	73.38	0.84	73.62	-0.24	73.77	-0.15	71.54	2.23
20	100	95	60.38	-0.48	60.2	0.18	59.47	0.73	59.55	-0.08	58.87	0.68
21	100	120	47.53	0.15	47	0.53	46.86	0.14	47.09	-0.23	46.62	0.47
22	100	150	38.9	-0.17	37.86	1.04	37.06	0.8	37.76	-0.7	37.06	0.7
23	100	170	29.95	0.94	29.36	0.59	28.04	1.32	27.2	0.84	26.48	0.72
24	125	70	77.19	-0.58	76.96	0.23	76.08	0.88	75.81	0.27	78.63	-2.82
25	125	95	63.02	-0.13	62.78	0.24	63.05	-0.27	63.08	-0.03	63.38	-0.3
26	125	120	59.85	-0.67	60.87	-1.02	58.52	2.35	58.93	-0.41	59.38	-0.45
27	125	145	47.92	0.64	46.92	1	45.69	1.23	46.66	-0.97	45.3	1.36
28	125	165	37.4	0.08	35.49	1.91	34.6	0.89	32.66	1.94	32.94	-0.28
29	150	60	77.92	0.12	77.2	0.72	78.55	-1.35	76.26	2.29	76.99	-0.73
30	150	80	73.33	-0.54	72.72	0.61	73.59	-0.87	74.18	-0.59	73.66	0.52
31	150	105	68.93	-0.23	69.36	-0.43	69.32	0.04	70.07	-0.75	66.76	3.31
32	150	125	63.17	-0.12	62.03	1.14	60.68	1.35	59.41	1.27	58.91	0.5